Assessing the influence of phosphine substituents on the catalytic properties of self-stabilised digold(I) complexes with supporting ferrocene phosphinonitrile ligands

Ondřej Bárta, Ivana Císařová, Jiří Schulz, and Petr Štěpnička*

Department of Inorganic Chemistry, Faculty of Science, Charles University,

Hlavova 2030, 128 40 Prague, Czech Republic

Supporting Information

Contents

Materials and methods

All syntheses were performed under an argon atmosphere using standard Schlenk techniques. Compounds **1c**,[1] **6c**,[2] [AuCl(tht)],[3] [Au(PPh_3)(MeCN)][SbF_6],[4] and [Au(PPh_3)(OTf)][5] were prepared as previously described. Other chemicals were purchased from commercial suppliers (Sigma-Aldrich and Alfa-Aesar) and were used as received. Dichloromethane, THF and methanol were dried using a PureSolv MD5 solvent purification system (Innovative Technology, USA). Acetone was dried over potassium carbonate and distilled under an argon atmosphere. Other solvents (Lach-Ner, Czech Republic) were of reagent grade and were used without further purification.

NMR spectra were recorded at 25°C on a Varian INOVA 400 (^{1}H, 399.95; ^{13}C, 100.58; and ^{31}P, 161.90 MHz; and ^{19}F, 376.29 MHz) or on a Bruker Avance III HD 400 (^{1}H, 400.13; and ^{13}C, 100.62 MHz) spectrometer at 25°C. ^{1}H NMR spectra measured as a part of the kinetic measurement were recorded on a Varian INOVA 300 spectrometer operating at 299.94 MHz. Chemical shifts (δ in ppm) are given relative to internal tetramethylsilane (^{1}H and ^{13}C) or, alternatively, to neat $CFCl_3$ (^{19}F) and to 85% aqueous H_3PO_4 (^{31}P) as external references. In addition to the usual representation of signal multiplicity (s = single, d = doublet, t = triplet, q = quartet and br = broad, among others),[6] vt and vq are used to denote virtual multiplets due to magnetically non-equivalent protons at cyclopentadienyl rings (spin systems AA′BB′ and AA′BB′X for the cyano- and phosphine-substituted rings, respectively, where A, B = ^{1}H, and X = ^{31}P); fc = ferrocene-1,1′-diyl, Cy = cyclohexyl, Fur = 2-furyl. IR spectra were recorded in Nujol mulls, in the range of 400-4000 cm^{-1} using a Nicolet 6700 FTIR spectrometer. ESI mass spectra were recorded on a Compact QTOF-MS spectrometer (Bruker Daltonics) using samples dissolved in HPLC-grade methanol. Elemental analyses were performed using a Perkin–Elmer 2400 Series II CHNS/O analyser. The presence of clathrated solvent (if any) was confirmed by NMR analysis.

Syntheses and catalytic tests

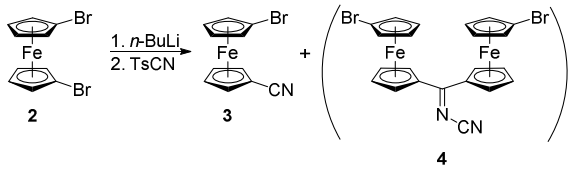

Preparation of 1-bromo-1′-cyanoferrocene (3) and isolation of N-(bis(1′-bromoferrocenyl)-methylene)cyanamide (4). In an oven-dried flask, 1,1′-dibromoferrocene (**2**; 7.91 g, 23.0 mmol) was dissolved in dry THF (100 mL) under an argon atmosphere, and the red solution was cooled to –78°C using a dry ice-ethanol bath. *n*-Butyllithium (9.2 mL of 2.5 M in hexanes, 23.0 mmol) was slowly added, and the resulting orange suspension was stirred at –78°C for 1 h, subsequently adding dropwise a solution of tosyl cyanide (5.0 g, 27.6 mmol) in dry THF (40 mL), pre-cooled to –78°C. The orange colour of the reaction mixture slowly changed to dark red, and the solids dissolved. The reaction mixture was stirred for another 2 hours at –78°C and then at room temperature overnight before quenching by saturated aqueous $NaHCO_3$ (50 mL). The organic phase was separated, and the aqueous layer was back-extracted with diethyl ether (2× 30 mL). The combined organic layers were washed with brine and dried over $MgSO_4$. The crude product was pre-absorbed onto silica gel by evaporation and purified by chromatography over a silica gel column, eluting with hexane/ethyl acetate (3:1). The chromatography resulted in three main bands. The first orange band, which contained ferrocene and bromoferrocene, resulting from unwanted protonolysis, was discarded. Evaporation of the major second orange band provided the target product, which was further crystallised from hot hexane/ethyl acetate. The crystals were filtered off, washed with cold pentane and dried under vacuum. Yield of **3**: 4.98 g (75%), red prisms. Lastly, the third, minor band of intense purple colour was evaporated to give a dark purple oily residue, which was identified as cyanamide **4** (0.53 g). The compound was further purified by dissolution in chloroform and precipitation with hexane. Crystals suitable for structure determination were obtained by liquid-phase diffusion of hexane into a chloroform solution of this compound.

*Analytical data for 1-bromo-1′-cyanoferrocene (**3**).* ^{1}H NMR (299.94 MHz, $CDCl_3$): δ = 4.30 (vt, J' = 1.9 Hz, 2 H, CH of fc), 4.44 (vt, J' = 1.9 Hz, 2 H, CH of fc), 4.57 (vt, J' = 1.9 Hz, 2 H, CH of fc), 4.68 (vt, J' = 1.9 Hz, 2 H, CH of fc) ppm. The data are in accordance with previously published values.[7]

*Analytical data for N-(bis(1′-bromoferrocenyl)methylene)cyanamide (**4**).* ^{1}H NMR (399.95 MHz, $CDCl_3$, 25°C): δ = 4.19 (br s, 2 H, CH of fc), 4.33 (br s, 2 H, CH of fc), 4.46 (br s, 2 H, CH of fc), 4.56 (br s, 2 H, CH of fc), 4.69 (vt, J' = 2.0 Hz, 4 H, CH of fc), 5.07 (br s, 2 H, CH of fc), 5.35 (br s, 2 H, CH of fc) ppm. ^{1}H NMR (399.95 MHz, $CDCl_3$, 50°C): δ = 4.25 (br s, 4 H, CH of fc), 4.50 (br s, 4 H,

CH of fc), 4.67 (vt, J' = 2.0 Hz, 4 H, CH of fc), 5.20 (br s, 4 H, CH of fc) ppm. $^{13}C\{^1H\}$ NMR (100.58 MHz, $CDCl_3$, 25°C): δ = 70.03 (br s, fc), 70.58 (br s, fc), 72.60 (s, fc), 72.98 (br s, fc), 73.66 (br s, fc), 75.70 (br s, fc), 116.13 (s, C≡N), 191.20 (s, C=N) ppm. ESI– MS: *m/z* = 379 ($[Cp(CNCN)fcBr]^-$). IR (Nujol): ν_{max} = 2161 s, 1537 s, 1409 m, 1400 w, 1350 m, 1323 w, 1302 s, 1230 w, 1216 w, 1152 m, 1067 m, 1049 m, 1038 m, 1023 m, 1003 w, 962 w, 897 w, 877 w, 868 m, 843 w, 822 s, 738 w, 663 w, 540 m, 518 m, 495 s, 482 s, 459 m, 423 w cm^{-1}. Anal. Calc. for $C_{22}H_{16}Br_2Fe_2N_2$ (579.9): C 45.57, H 2.78, N 4.83%. Found: C 45.24, H 2.70, N 4.76%.

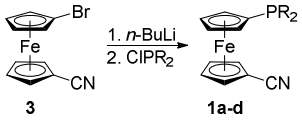

3 **1a-d**

General procedure for the preparation of phosphinonitriles R₂PfcC≡N (1). Under an argon atmosphere, compound **3** (1.45 g, 5.0 mmol) was dissolved in dry THF (40 mL), and the resulting red solution was cooled to –78°C in a dry ice-ethanol bath. An *n*-butyllithium solution (2.0 mL of 2.5 M in hexanes, 5.0 mmol) was added in small portions. The mixture was stirred at –78°C for 1 hour, subsequently adding dropwise the respective chlorophosphine (6.0 mmol). After stirring for an additional hour, the cooling bath was removed, and the reaction mixture was stirred at room temperature for 2 hours (overnight for chloro-di(2-furyl)phosphine). Then, the reaction was quenched by adding saturated aqueous $NaHCO_3$ (10 mL), the organic phase was separated, and the aqueous layer was extracted with diethyl ether (2× 10 mL). The combined organic layers were washed with brine, dried over $MgSO_4$ and evaporated with chromatographic silica gel. The pre-adsorbed crude product was purified by column chromatography on silica gel using a hexane/ethyl acetate (3:1) mixture as the eluent. The first yellow (minor) band, predominantly containing cyanoferrocene, was discarded. The second orange band was collected and evaporated to afford the product, which was further crystallised.

*Preparation of iPr₂PfcC≡N (**1a**)*. The general procedure was used, and the product was crystallised by dissolving in hot heptane and cooling the saturated solution slowly to –18°C. Yield: 1.47 g (90%), red needles. ^1H NMR (399.95 MHz, $CDCl_3$): δ = 1.07 (dd, $^3J_{HH}$ = 7.0 Hz, $^3J_{HP}$ = 7.0 Hz, 6 H, CHMe_2), 1.10 (dd, $^3J_{HH}$ = 7.1 Hz, $^3J_{HP}$ = 9.0 Hz, 6 H, CHMe_2), 1.93 (sept of d, $^3J_{HH}$ = 7.0 Hz, $^2J_{HH}$ = 2.0 Hz, 2 H, C*H*Me_2), 4.34 (vq, J' = 1.6 Hz, 2 H, CH of fc), 4.37 (vt, J' = 1.9 Hz, 2 H, CH of fc), 4.50 (vt, J' = 1.8 Hz, 2 H, CH of fc), 4.63 (vt, J' = 1.9 Hz, 2 H, CH of fc) ppm. $^{13}C\{^1H\}$ NMR (100.58 MHz, $CDCl_3$): δ = 19.82 (d, $^2J_{CP}$ = 10 Hz, CH*C*H_3), 20.03 (d, $^2J_{CP}$ = 15 Hz, CH*C*H_3), 23.38 (d, $^1J_{CP}$ = 11 Hz, *C*HCH$_3$), 52.45 (s, *C*–CN of fc), 72.46 (d, J_{CP} = 2 Hz, CH of fc), 72.52 (s, CH of fc), 72.68 (s, CH of fc), 73.25 (d, J_{CP} = 10 Hz, CH of fc), 79.36 (d, $^1J_{CP}$ = 21 Hz, *C*–P(*i*Pr)$_2$ of fc), 120.00 (s, C≡N) ppm. $^{31}P\{^1H\}$ NMR (161.90 MHz, $CDCl_3$): δ = 0.1 (s, P(*i*Pr)$_2$) ppm. ESI+ MS: *m/z* = 328 ($[M + H]^+$), 350 ($[M + Na]^+$), 366 ($[M + K]^+$). IR (Nujol): ν_{max} = 2224 s, 1364 m. 1307 w, 1233 s, 1197 w, 1156

m, 1055 m, 1040 m, 1030 s, 913 w, 881 w, 859 w, 845 m, 821 s, 655 w, 637 w, 607 w, 558 m, 508 m, 492 s, 476 m, 466 s cm^{-1}. Anal. Calc. for $C_{17}H_{22}FeNP$ (327.2): C 62.41, H 6.78, N 4.28%. Found: C 62.00, H 6.48, N 4.16%.

*Preparation of Cy₂PfcC≡N (**1b**).* This compound was prepared according to the general procedure. The product was crystallised from hot ethyl acetate/heptane. Yield: 1.44 g (71%), orange-red needles. ^{1}H NMR (399.95 MHz, $CDCl_3$): δ = 1.00-1.38 (m, 10 H, Cy), 1.64-1.94 (m, 12 H, Cy), 4.31 (vq, J' = 1.6 Hz, 2 H, CH of fc), 4.36 (vt, J' = 1.9 Hz, 2 H, CH of fc), 4.48 (vt, J' = 1.8 Hz, 2 H, CH of fc), 4.61 (vt, J' = 1.9 Hz, 2 H, CH of fc) ppm. $^{13}C\{^{1}H\}$ NMR (100.58 MHz, $CDCl_3$): δ = 26.78 (s, CH_2 of Cy), 27.62 (d, J_{CP} = 8 Hz, CH_2 of Cy), 27.72 (d, J_{CP} = 11 Hz, CH_2 of Cy), 30.57 (d, J_{CP} = 13 Hz, CH_2 of Cy), 30.67 (d, J_{CP} = 10 Hz, CH_2 of Cy), 33.76 (d, J_{CP} = 11 Hz, CH of Cy), 52.92 (s, *C*–CN of fc), 72.77 (d, J_{CP} = 2 Hz, CH of fc), 72.85 (s, CH of fc), 73.16 (s, CH of fc), 73.96 (d, J_{CP} = 10 Hz, CH of fc), 80.10 (d, $^{1}J_{CP}$ = 20 Hz, *C*–PCy_2 of fc), 120.47 (s, C≡N) ppm. $^{31}P\{^{1}H\}$ NMR (161.90 MHz, $CDCl_3$): δ = –8.0 (s, PCy_2) ppm. ESI+ MS: *m/z* = 408 ($[M + H]^+$), 430 ($[M + Na]^+$), 446 ($[M + K]^+$). IR (Nujol): ν_{max} = 2225 s, 1343 m, 1263 w, 1232 m, 1192 m, 1176 w, 1154 m, 1030 s, 1000 m, 914 m, 884 w, 845 s, 821 s, 556 m, 507 m, 488 s, 462 s, 441 m cm^{-1}. Anal. Calc. for $C_{23}H_{30}FeNP$ (407.3): C 67.82, H 7.42, N 3.44%. Found: C 67.77, H 7.42, N 3.36%.

*Preparation of Fur₂PfcC≡N (**1d**)*. The general procedure described was followed, and the compound was purified by crystallization from hot hexane. Yield: 1.61g (86%), orange needles. ^{1}H NMR (399.95 MHz, $CDCl_3$): δ = 4.24 (vt, J' = 2.0 Hz, 2 H, CH of fc), 4.51 (vt, J' = 2.0 Hz, 2 H, CH of fc), 4.53 (vt of d, J' = 1.8 Hz, J = 0.6 Hz, 2 H, CH of fc), 4.56 (vq, J' = 1.9 Hz, 2 H, CH of fc), 6.41 (dt, J = 3.3 Hz, J = 1.7 Hz, 2 H, CH of Fur), 6.72 (ddd, J = 3.3 Hz, J = 2.0 Hz, J = 0.7 Hz, 2 H, CH of Fur), 7.67 (m, 2 H, CH of Fur) ppm. $^{13}C\{^{1}H\}$ NMR (100.58 MHz, $CDCl_3$): δ = 52.80 (s, *C*–CN of fc), 71.89 (d, J = 1 Hz, CH of fc), 72.60 (s, CH of fc), 73.59 (d, J_{CP} = 5 Hz, CH of fc), 75.68 (d, J_{CP} = 17 Hz, CH of fc), 110.67 (d, J_{CP} = 6 Hz, CH of Fur), 119.58 (s, C≡N), 120.40 (d, J_{CP} = 25 Hz, CH of Fur), 147.06 (d, J_{CP} = 2 Hz, CH of Fur), 151.21 (d, J_{CP} = 8 Hz, C^{ipso} of Fur) ppm. Note: The ^{13}C NMR signal due to *C*–P of fc overlaps with one of the CH resonances. $^{31}P\{^{1}H\}$ NMR (161.90 MHz, $CDCl_3$): δ = –66.1 (s, $PFur_2$) ppm. ESI+ MS: *m/z* = 398 ($[M + Na]^+$). IR (Nujol): ν_{max} = 2228 s, 1552 m, 1312 w, 1231 m, 1220 m, 1210 m, 1163 m, 1155 m, 1123 m, 1108 w, 1059 w, 1028 s, 1015 sh, 1005 s, 912 sh, 903 s, 883 m, 848 m, 834 s, 746 s, 656 m, 646 w, 635 w, 627 w, 596 m, 555 m, 516 w, 502 m, 491 m, 479 s, 471 s, 450 s cm^{-1}. Anal. Calc. for $C_{19}H_{14}FeNO_2P$ (375.1): C 60.83, H 3.76, N 3.73%. Found: C 60.57, H 3.70, N 3.52%.

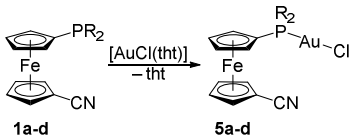

1a-d 5a-d

General procedure for the preparation of complexes [AuCl(R$_2$PfcC≡N-κP)] (5). Solid [AuCl(tht)] (160 mg, 0.50 mmol) and the respective phosphinonitrile (0.50 mmol) were dissolved in dry dichloromethane (5 mL) under an argon atmosphere, and the orange solution was stirred at room temperature for 60 minutes. The product was obtained after evaporating the solvent under reduced pressure.

*Preparation of [AuCl(iPr$_2$PfcC≡N-κP)] (**5a**).* The product was prepared according to the general procedure. The crude product was dissolved in dichloromethane (1 mL), and the solution was poured into an excess of cold pentane. The precipitated solid was filtered off, washed with pentane (to remove residual tetrahydrothiophene) and dried under vacuum. Yield: 267 mg (95%), orange powder. The crystals suitable for structure determination were grown by liquid-phase diffusion of hexane into an acetone solution of the complex.

^{1}H NMR (399.95 MHz, $CDCl_3$): δ = 1.24 (dd, $^3J_{HH}$ = 7.0 Hz, $^3J_{HP}$ = 10.8 Hz, 6 H, CH*Me*$_2$), 1.29 (dd, $^3J_{HH}$ = 7.0 Hz, $^3J_{HP}$ = 9.8 Hz, 6 H, CH*Me*$_2$), 2.32 (d of sept, $^2J_{HP}$ = 8.7 Hz, $^3J_{HH}$ = 7.0 Hz, 2 H, C*H*Me$_2$), 4.55 (vq, J' = 2.0 Hz, 2 H, CH of fc), 4.64 (vt, J' = 2.0 Hz, 2 H, CH of fc), 4.72 (vtd, J' = 1.9 Hz, J' = 1.0 Hz, 2 H, CH of fc), 4.80 (vt, J' = 2.0 Hz, 2 H, CH of fc) ppm. ^{13}C{^{1}H} NMR (100.58 MHz, $CDCl_3$): δ = 19.36 (d, $^2J_{CP}$ = 9 Hz, CH*C*H$_3$), 19.38 (d, $^2J_{CP}$ = 12 Hz, CH*C*H$_3$), 25.34 (d, $^1J_{CP}$ = 36 Hz, *C*HCH$_3$), 53.64 (s, *C*–CN of fc), 70.17 (d, $^1J_{CP}$ = 57 Hz, *C*–P*i*Pr$_2$ of fc), 73.61 (s, CH of fc), 73.98 (s, CH of fc), 73.99 (d, J_{CP} = 10 Hz, CH of fc), 74.30 (d, J_{CP} = 7 Hz, CH of fc), 118.98 (s, C≡N) ppm. ^{31}P{^{1}H} NMR (161.90 MHz, $CDCl_3$): δ = 49.8 (s, P*i*Pr$_2$) ppm. ESI+ MS: *m/z* = 662 ([M + Na]$^+$). IR (Nujol): ν_{max} = 2228 s, 1252 m, 1231 m, 1201 w, 1169 m, 1036 s, 915 w, 889 w, 838 s, 828 s, 679 m, 652 m, 631 w, 547 m, 509 w, 499 m, 486 m, 468 m, 415 m cm^{-1}. Anal. Calc. for $C_{17}H_{23}AuClFeNP$ (559.6): C 36.49, H 3.96, N 2.50%. Found: C 36.84, H 3.89, N 2.53%.

*Preparation of [AuCl(Cy$_2$PfcC≡N-κP)] (**5b**).* The compound was prepared and isolated similarly to the isopropyl analogue. Yield: 316 mg (98%), orange powder. Crystals used for structure determination were grown by liquid-phase diffusion of hexane into an acetone solution of the complex.

^{1}H NMR (399.95 MHz, $CDCl_3$): δ = 1.13-1.52 (m, 10 H, Cy), 1.67-1.78 (m, 2 H, Cy), 1.80-1.94 (m, 4 H, Cy), 1.96-2.15 (m, 6 H, Cy), 4.51 (vq, J' = 2.0 Hz, 2 H, CH of fc), 4.62 (vt, J' = 2.0 Hz, 2 H, CH of fc), 4.70 (vtd, J' = 2.0 Hz, J' = 1.0 Hz, 2 H, CH of fc), 4.77 (vt, J' = 2.0 Hz, 2 H, CH of fc) ppm. ^{13}C{^{1}H} NMR (100.58 MHz, $CDCl_3$): δ = 25.61 (d, J_{CP} = 2 Hz, CH_2 of Cy), 26.45 (d, J_{CP} = 2 Hz, CH_2 of Cy), 26.58 (s, CH_2 of Cy), 29.72 (d, J_{CP} = 2 Hz, CH_2 of Cy), 29.98 (s, CH_2 of Cy), 34.69 (d, J_{CP} = 35 Hz, CH of Cy), 53.70 (s, *C*–CN of fc), 70.84 (d, J_{CP} = 57 Hz, *C*–PCy$_2$ of fc), 73.70 (s, CH of fc), 73.77 (s, CH of fc), 73.98 (d, J_{CP} = 7 Hz, CH of fc), 74.41 (d, J_{CP} = 10 Hz, CH of fc), 119.04 (s, C≡N) ppm. ^{31}P{^{1}H}

NMR (161.90 MHz, $CDCl_3$): δ = 41.4 (s, PCy_2) ppm. ESI+ MS: *m/z* = 662 ($[M + Na]^+$), 678 ($[M + K]^+$). IR (Nujol): ν_{max} = 2224 s, 1347 w, 1310 w, 1267 w, 1231 m, 1201 m, 1181 m, 1170 m, 1111 w, 1038 m, 1005 w, 911 w, 894 w, 848 m, 828 s, 755 w, 736 m, 630 m, 555 m, 542 m, 525 m, 511 w, 493 s, 470 s, 446 m, 433 m cm^{-1}. Anal. Calc. for $C_{23}H_{30}AuClFeNP$ (639.7): C 43.18, H 4.73, N 2.19%. Found: C 43.21, H 4.57, N 2.09%.

*Preparation of [AuCl(Fur₂PfcC≡N-κP)] (**5d**).* The orange oily crude product obtained using the general procedure was dissolved in acetone, and the solution was layered with hexane. Crystallisation over several days afforded orange crystals (used also for structure determination), which were filtered off, washed with pentane and dried under vacuum. Yield: 240 mg (79%), orange needles.

^1H NMR (399.95 MHz, $CDCl_3$): δ = 4.50 (vt, J' = 2.0 Hz, 2 H, CH of fc), 4.62 (vt, J' = 2.0 Hz, 2 H, CH of fc), 4.75 (vq, J' = 1.7 Hz, 2 H, CH of fc), 4.79 (apparent p, J' = 1.8 Hz, 2 H, CH of fc), 6.56 (dt, J = 3.5 Hz, J = 1.7 Hz, 2 H, CH of Fur), 7.11 (ddd, J = 3.5 Hz, J = 3.0 Hz, J = 0.7 Hz, 2 H, CH of Fur), 7.81 (td, J = 1.8 Hz, J = 0.7 Hz, 2 H, CH of Fur) ppm. $^{13}C\{^1H\}$ NMR (100.58 MHz, $CDCl_3$): δ = 53.96 (s, *C*–CN of fc), 69.86 (d, J_{CP} = 83 Hz, *C*–$PFur_2$ of fc), 72.95 (s, CH of fc), 73.49 (s, CH of fc), 75.14 (d, J_{CP} = 10 Hz, CH of fc), 75.93 (d, J_{CP} = 16 Hz, CH of fc), 111.45 (d, J_{CP} = 9 Hz, CH of Fur), 118.54 (s, C≡N), 124.25 (d, J_{CP} = 26 Hz, CH of Fur), 143.22 (d, J_{CP} = 94 Hz, C^{ipso} of Fur), 149.65 (d, J_{CP} = 6 Hz, CH of Fur) ppm. $^{31}P\{^1H\}$ NMR (161.90 MHz, $CDCl_3$): δ = –14.4 (s, $PFur_2$) ppm. ESI+ MS: *m/z* = 630 ($[M + Na]^+$). IR (Nujol): ν_{max} = 2230 s, 1721 w, 1551 m, 1410 w, 1387 m, 1311 w, 1234 w, 1218 m, 1196 m, 1186 m, 1177 m, 1126 s, 1060 w, 1031 m, 1019 s, 1012 sh, 911 m, 892 w, 882 m, 849 m, 836 m, 826 m, 775 s, 763 s, 647 m, 638 m, 626 m, 593 m, 552 s, 540 s, 524 m, 512 m, 476 s, 466 sh cm^{-1}. Anal. Calc. for $C_{19}H_{14}AuClFeNO_2P$ (607.7): C 37.56, H 2.32, N 2.31%. Found: C 37.50, H 2.23, N 2.15%.

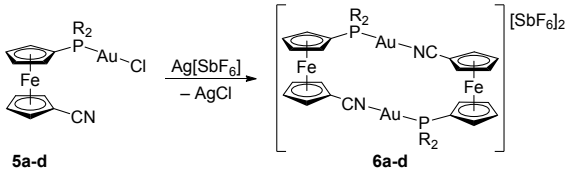

5a-d 6a-d

General procedure for the preparation of dimers [Au₂(μ(P,N)-R₂PfcC≡N)₂][SbF₆]₂ (6). Under an argon atmosphere, $Ag[SbF_6]$ (34.5 mg, 0.10 mmol) and the respective complex **5** (0.10 mmol) were dissolved in dry acetone (3 mL). The orange solution containing a white precipitate (AgCl) was stirred at room temperature, in the dark, for 60 minutes, and subsequently filtered through a PTFE syringe filter (0.45 μm pore size) directly into an excess of cold pentane. Sonication of the resulting orange cloudy mixture induced precipitation of the product, which was completed by allowing the suspension to stand at 5°C for 2 hours. The precipitate was collected, washed with pentane and dried under vacuum.

*Preparation of [Au₂(μ(P,N)-iPr₂PfcC≡N)₂][SbF₆]₂ (**6a**).* The compound was prepared according to the general method. Yield: 62 mg (82%), yellow powder.

^{1}H NMR (399.95 MHz, acetone-d$_6$): δ = 1.35 (dd, $^{3}J_{HH}$ = 7.0 Hz, $^{3}J_{HP}$ = 4.5 Hz, 6 H, CH*Me*$_2$), 1.39 (dd, $^{3}J_{HH}$ = 7.0 Hz, $^{3}J_{HP}$ = 5.7 Hz, 6 H, CH*Me*$_2$), 2.72 (d of sept, $^{2}J_{HP}$ = 8.5 Hz, $^{3}J_{HH}$ = 7.0 Hz, 2 H, C*H*Me$_2$), 4.89 (vq, J' = 2.0 Hz, 2 H, CH of fc), 5.06 (br s, 4 H, CH of fc), 5.35 (br s, 2 H, CH of fc) ppm. ^{31}P{^{1}H} NMR (161.90 MHz, acetone-d$_6$): δ = 49.0 (s, P*i*Pr$_2$) ppm. ESI+ MS: *m/z* = 583 ([Au(*i*Pr$_2$PfcCN)(MeOH)HCN]$^+$). IR (Nujol): ν_{max} = 2263 s, 1312 w, 1247 m, 1206 w, 1184 m, 1173 m, 1087 w, 1040 m, 917 m, 881 w, 850 m, 830 m, 686 w, 657 vs, 554 w, 514 m, 490 m, 471 m cm^{-1}. Anal. Calc. for $C_{34}H_{44}Au_2F_{12}Fe_2N_2P_2Sb_2$ (1519.8): C 26.87, H 2.92, N 1.84%. Found: C 26.66, H 2.75, N 1.69%.

*Preparation of [Au₂(μ(P,N)-Cy₂PfcC≡N)₂][SbF₆]₂ (**6b**)*. The general procedure was used. Yield: 74 mg (88%), orange powder. Crystals suitable for structure determination were obtained by liquid-phase diffusion of hexane into an acetone solution of the complex.

^{1}H NMR (399.95 MHz, acetone-d$_6$): δ = 1.16-1.62 (m, 10 H, Cy), 1.66-1.76 (m, 2 H, Cy), 1.82-1.96 (m, 4 H, Cy), 2.12-2.32 (m, 4 H, Cy), 2.46-2.60 (m, 2 H, Cy), 4.87 (vq, J' = 2.0 Hz, 2 H, CH of fc), 5.06 (br s, 4 H, CH of fc), 5.35 (br s, 2 H, CH of fc) ppm. ^{31}P{^{1}H} NMR (161.90 MHz, acetone-d$_6$): δ = 40.2 (s, PCy$_2$) ppm. ESI+ MS: *m/z* = 631 ([Au(Cy$_2$PfcCN)HCN]$^+$), 689 ([Au(Cy$_2$PfcCN)-(Me$_2$CO)HCN]$^+$). IR (Nujol): ν_{max} = 2256 s, 1711 m, 1294 w, 1272 w, 1243 w, 1243 w, 1220 m, 1202 m, 1174 m, 1113 w, 1058 w, 1041 m, 1004 w, 918 m, 897 w, 851 m, 838 m, 750 w, 657 vs, 609 w, 553 w, 515 m, 497 m, 472 m, 445 w cm^{-1}. Anal. Calc. for $C_{46}H_{60}Au_2F_{12}Fe_2N_2P_2Sb_2$ (1680.1): C 32.89, H 3.60, N 1.67%. Found: C 33.08, H 3.21, N 1.25%.

*Preparation of [Au₂(μ(P,N)-Fur₂PfcC≡N)₂][SbF₆]₂ (**6d**)*. The general procedure was followed. Yield: 71 mg (88%), orange powder. Crystals suitable for structure determination were obtained by liquid phase diffusion of hexane into an acetone solution of the complex.

^{1}H NMR (399.95 MHz, acetone-d$_6$): δ = 4.78 (vt, J' = 2.0 Hz, 2 H, CH of fc), 5.04 (m, 2 H, CH of fc), 5.08 (vq, J' = 1.8 Hz, 2 H, CH of fc), 5.17 (vt, J' = 1.9 Hz, 2 H, CH of fc), 6.80 (dt, J = 3.5 Hz, J = 1.7 Hz, 2 H, CH of Fur), 7.43 (ddd, J = 3.5 Hz, J = 2.8 Hz, J = 0.7 Hz, 2 H, CH of Fur), 8.18 (td, J = 1.9 Hz, J = 0.7 Hz, 2 H, CH of Fur) ppm. ^{31}P{^{1}H} NMR (161.90 MHz, acetone-d$_6$): δ = –16.7 (s, PFur$_2$) ppm. ESI+ MS: *m/z* = 599 ([Au(Fur$_2$PfcCN)HCN]$^+$), 802 ([Au(Fur$_2$PfcCN)(Fur$_2$PC$_5$H$_6$)]$^+$). IR (Nujol): ν_{max} = 2288 sh, 2274 s, 1553 w, 1395 w, 1309 w, 1246 w, 1221 w, 1202 w, 1188 m, 1178 w, 1132 m, 1065 w, 1038 m, 1012 s, 917 sh, 910 m, 885 w, 855 w, 833 m, 772 s, 755 s, 661 vs, 620 w, 609 w, 589 w, 575 m, 561 w, 538 w, 527 m, 514 m, 478 s, 466 s cm^{-1}. Anal. Calc. for $C_{38}H_{28}Au_2F_{12}Fe_2N_2O_4P_2Sb_2$ (1615.7): C 28.25, H 1.75, N 1.73%. Found: C 28.37, H 1.69, N 1.33%.

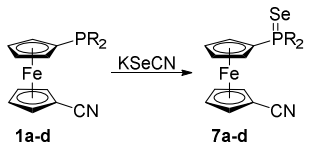

General procedure for the preparation of selenides R_2(Se)PfcC≡N (7).[8] Potassium selenocyanate (39.6 mg, 0.275 mmol) and the respective phosphinonitrile (0.250 mmol) were dissolved in a mixture of dry methanol (4 mL) and dry dichloromethane (1 mL), and the resulting mixture was stirred at room temperature overnight. Following evaporation with chromatography-grade silica gel, the pre-absorbed crude product was purified by column chromatography over silica gel, as specified in detail below.

*Preparation of iPr_2(Se)PfcC≡N (**7a**).* The crude product, prepared according to the general procedure, was purified by column chromatography on silica gel using hexane/ethyl acetate (3:1) as the eluent. Evaporation of the major orange band provided analytically pure product. Yield: 65 mg (64%), orange microcrystalline solid. ^{1}H NMR (399.95 MHz, $CDCl_3$): δ = 1.19 (dd, $^3J_{HH}$ = 7.0 Hz, $^3J_{HP}$ = 3.3 Hz, 6 H, CH*Me*$_2$), 1.23 (dd, $^3J_{HH}$ = 7.0 Hz, $^3J_{HP}$ = 3.6 Hz, 6 H, CH*Me*$_2$), 2.30 (d of sept, $^2J_{HP}$ = 8.4 Hz, $^3J_{HH}$ = 7.0 Hz, 2 H, C*H*Me$_2$), 4.60 (vq, J' = 1.8 Hz, 2 H, CH of fc), 4.64 (vq, J' = 1.7 Hz, 2 H, CH of fc), 4.68 (vt, J' = 2.0 Hz, 2 H, CH of fc), 4.80 (vt, J' = 2.0 Hz, 2 H, CH of fc) ppm. ^{13}C{^{1}H} NMR (100.58 MHz, $CDCl_3$): δ = 16.72 (d, $^2J_{CP}$ = 1 Hz, CH*C*H$_3$), 17.49 (d, $^2J_{CP}$ = 2 Hz, CH*C*H$_3$), 27.64 (d, $^1J_{CP}$ = 45 Hz, *C*HCH$_3$), 53.41 (s, *C*–CN of fc), 73.48 (d, J_{CP} = 8 Hz, CH of fc), 73.66 (s, CH of fc), 73.88 (d, J_{CP} = 9 Hz, CH of fc), 74.05 (s, CH of fc), 75.09 (d, $^1J_{CP}$ = 67 Hz, *C*–P*i*Pr$_2$ of fc), 119.35 (s, C≡N) ppm. ^{31}P{^{1}H} NMR (161.90 MHz, $CDCl_3$): δ = 57.8 (s with ^{77}Se satellites, $^1J_{PSe}$ = 715 Hz, P*i*Pr$_2$) ppm. ESI+ MS: *m/z* = 408 ([M + H]$^+$). IR (Nujol): ν_{max} = 2225 s, 1417 w, 1364 m, 1310 w, 1253 w, 1243 m, 1233 m, 1202 m, 1169 s, 1100 w, 1081 w, 1062 w, 1052 w, 1043 m, 1034 s, 935 w, 911 w, 891 m, 882 m, 859 w, 844 m, 828 s, 818 m, 676 s, 652 s, 629 m, 562 s, 554 s, 510 m, 498 s, 481 m, 470 s, 435 m cm^{-1}. Anal. Calc. for $C_{17}H_{22}FeNPSe$ (406.2): C 50.27, H 5.46, N 3.45%. Found: C 50.26, H 5.10, N 3.44%.

*Preparation of Cy_2(Se)PfcC≡N (**7b**).* The crude product was purified by chromatography on silica gel using hexane/ethyl acetate (1:1). The major orange band was collected and evaporated to afford analytically pure product. Yield: 85 mg (70%), yellow-orange solid. ^{1}H NMR (399.95 MHz, $CDCl_3$): δ = 1.10-1.46 (m, 10 H, Cy), 1.66-1.75 (m, 2 H, Cy), 1.78-1.92 (m, 4 H, Cy), 1.94-2.10 (m, 6 H, Cy), 4.57 (vq, J' = 1.8 Hz, 2 H, CH of fc), 4.63 (vq, J' = 1.7 Hz, 2 H, CH of fc), 4.65 (vt, J' = 2.0 Hz, 2 H, CH of fc), 4.79 (vt, J' = 2.0 Hz, 2 H, CH of fc) ppm. ^{13}C{^{1}H} NMR (100.58 MHz, $CDCl_3$): δ = 25.72 (d, J_{CP} = 2 Hz, CH_2 of Cy), 26.28 (d, J_{CP} = 2 Hz, CH_2 of Cy), 26.34 (d, J_{CP} = 4 Hz, CH_2 of Cy), 26.47 (d, J_{CP} = 3 Hz, CH_2 of Cy), 27.31 (d, J_{CP} = 4 Hz, CH_2 of Cy), 37.05 (d, J_{CP} = 45 Hz, CH of Cy), 53.48 (s, *C*–CN of fc), 73.22 (d, J_{CP} = 8 Hz, CH of fc), 73.81 (s, CH of fc), 73.89 (s, CH of fc), 74.08 (d, J_{CP} = 9 Hz, CH of fc), 75.72 (d, J_{CP} = 67 Hz, *C*–PCy_2 of fc), 119.42 (s, C≡N) ppm. ^{31}P{^{1}H} NMR (161.90 MHz, $CDCl_3$): δ = 49.5 (s with ^{77}Se satellites, $^1J_{PSe}$ = 708 Hz, PCy_2) ppm. ESI+ MS:

m/z = 488 ([M + H]$^+$). IR (Nujol): ν_{max} = 2229 s, 1346 m, 1311 w, 1297 m, 1273 w, 1231 m, 1215 w, 1200 m, 1181 m, 1169 s, 1115 w, 1084 w, 1063 w, 1038 s, 1027 m, 1002 m, 919 m, 896 m, 877 w, 851 m, 841 s, 825 m, 816 s, 748 m, 738 m, 633 m, 553 s, 547 s, 528 m, 512 m, 497 s, 486 m, 462 s, 444 m, 432 m cm^{-1}. Anal. Calc. for $C_{23}H_{30}FeNPSe$ (486.3): C 56.81, H 6.22, N 2.88%. Found: C 56.53, H 6.00, N 2.90%.

*Preparation of Ph$_2$(Se)PfcC≡N (**7c**).* The crude product was prepared as described above and further purified by column chromatography on silica gel with hexane/ethyl acetate (3:1). Only the major orange band was collected. Analytically pure product was obtained after evaporation. Yield: 104 mg (88%), orange solid. ^{1}H NMR (399.95 MHz, $CDCl_3$): δ = 4.52 (vt, *J*′ = 2.0 Hz, 2 H, CH of fc), 4.60 (vt, *J*′ = 2.0 Hz, 2 H, CH of fc), 4.62 (vq, *J*′ = 2.1 Hz, 2 H, CH of fc), 4.71 (vq, *J*′ = 1.8 Hz, 2 H, CH of fc), 7.41-7.52 (m, 6 H, Ph), 7.67-7.74 (m, 4 H, Ph) ppm. ^{13}C{^{1}H} NMR (100.58 MHz, $CDCl_3$): δ = 53.32 (s, *C*–CN of fc), 73.37 (s, CH of fc), 73.61 (s, CH of fc), 74.79 (d, J_{CP} = 9 Hz, CH of fc), 75.28 (d, J_{CP} = 12 Hz, CH of fc), 77.21 (d, J_{CP} = 86 Hz, *C*–PPh$_2$ of fc), 118.88 (s, C≡N), 128.46 (d, J_{CP} = 13 Hz, CH of Ph), 131.65 (d, J_{CP} = 3 Hz, CH of Ph), 131.95 (d, J_{CP} = 11 Hz, CH of Ph), 132.59 (d, J_{CP} = 79 Hz, C^{ipso} of Ph) ppm. ^{31}P{^{1}H} NMR (161.90 MHz, $CDCl_3$): *δ* 31.1 (s with ^{77}Se satellites, $^1J_{PSe}$ = 741 Hz, PPh$_2$) ppm. ESI+ MS: *m/z* 476 ([M + H]$^+$). IR (Nujol): ν_{max} = 2224 s, 1308 m, 1230 m, 1199 w, 1191 w, 1171 s, 1155 m, 1098 s, 1069 w, 1032 s, 997 w, 912 m, 840 s, 827 m, 755 s, 712 m, 702 m, 694 s, 638 m, 575 s, 554 m, 531 s, 490 m, 483 s, 469 m, 452 m, 437 w cm^{-1}. Anal. Calc. for $C_{23}H_{18}FeNPSe$ (474.2): C 58.26, H 3.83, N 2.95%. Found: C 58.00, H 3.65, N 2.90%.

*Preparation of Fur$_2$P(Se)PfcC≡N (**7d**).* The general procedure was followed to synthesize the crude product, which was purified by chromatography on silica gel in hexane/ethyl acetate (1:1). The orange viscous oil, obtained after evaporation of the major orange band, was crystallised from hot hexane. Cooling the solution to –18°C resulted in the formation of orange crystals, which were collected, washed with pentane and dried under vacuum. Yield: 79 mg (70%), orange needles. ^{1}H NMR (399.95 MHz, $CDCl_3$): δ = 4.49 (vt, *J*′ = 2.0 Hz, 2 H, CH of fc), 4.65 (vt, *J*′ = 2.0 Hz, 2 H, CH of fc), 4.70 (vq, *J*′ = 1.8 Hz, 2 H, CH of fc), 4.87 (d of vt, *J* = 2.9 Hz, *J*′ = 1.9 Hz, 2 H, CH of fc), 6.52 (dt, *J* = 3.5 Hz, *J* = 1.7 Hz, 2 H, CH of Fur), 7.13 (ddd, *J* = 3.4 Hz, *J* = 2.5 Hz, *J* = 0.8 Hz, 2 H, CH of Fur), 7.75 (ddd, *J* = 2.2 Hz, *J* = 1.7 Hz, *J* = 0.8 Hz, 2 H, CH of Fur) ppm. ^{13}C{^{1}H} NMR (100.58 MHz, $CDCl_3$): δ = 53.66 (s, *C*–CN of fc), 73.31 (s, CH of fc), 73.57 (s, CH of fc), 74.52 (d, J_{CP} = 11 Hz, CH of fc), 74.59 (d, J_{CP} = 98 Hz, *C*–PFur$_2$) of fc), 75.09 (d, J_{CP} = 14 Hz, CH of fc), 111.21 (d, J_{CP} = 9 Hz, CH of Fur), 119.01 (s, C≡N), 122.68 (d, J_{CP} = 22 Hz, CH of Fur), 146.27 (d, J_{CP} = 116 Hz, C^{ipso} of Fur), 148.78 (d, J_{CP} = 7 Hz, CH of Fur) ppm. ^{31}P{^{1}H} NMR (161.90 MHz, $CDCl_3$): δ = –6.4 (s with ^{77}Se satellites, $^1J_{PSe}$ = 777 Hz, PFur$_2$) ppm. ESI+ MS: *m/z* 456 ([M + H]$^+$). IR (Nujol): ν_{max} = 2226 s, 1548 m, 1388 m, 1361 m, 1311 w, 1232 w, 1208 m, 1200 m, 1175 m, 1126 s, 1061 w, 1054 w, 1035 m, 1004 s, 909 m, 883 w, 840 m, 827 m, 783 m, 774 sh, 768 s, 649 m, 630 m, 593

m, 578 s, 557 m, 536 s, 524 m, 512 m, 483 s, 464 s cm^{-1}. Anal. Calc. for $C_{19}H_{14}FeNO_2PSe$ (454.1): C 50.25, H 3.11, N 3.08%. Found: C 50.20, H 3.05, N 2.92%.

General procedure for the synthesis of propargyl amides 8. Under an argon atmosphere, 4-(dimethylamino)pyridine (61 mg, 0.5 mmol) was dissolved in dry dichloromethane (15 mL), and propargylamine (0.35 mL, 5.5 mmol) and dry triethylamine (0.77 mL, 5.5 mmol) were successively added. The resulting pale yellow solution was cooled in an ice bath, and the appropriate acyl chloride (5.0 mmol) was added dropwise. The reaction mixture was stirred at 0°C for 15 minutes and then at room temperature overnight. After quenching with water (10 mL), the organic layer was separated, and the aqueous layer was extracted with dichloromethane (2× 5 mL). The combined organic layers were washed with brine, dried over anhydrous $MgSO_4$ and evaporated. The crude product was dissolved in hot ethyl acetate/heptane mixture in the presence of charcoal and a small amount of silica gel, which were filtered off, and the colourless filtrate was allowed to cool slowly to 5°C to provide the target amide as a crystalline product.

*N-(Prop-2-yn-1-yl)benzamide (**8a**).*[9] The general procedure was used to prepare **8a**, yielding 0.49 g (62%) of a colourless crystalline solid. ^{1}H NMR (400.13 MHz, $CDCl_3$): δ = 2.28 (t, $^4J_{HH}$ = 2.6 Hz, 1H, C≡CH), 4.25 (dd, J_{HH} = 5.2 Hz, $^4J_{HH}$ = 2.6 Hz, 2 H, CH_2), 6.48 (br s, 1 H, NH), 7.40-7.46 (m, 2 H, Ph), 7.48-7.54 (m, 1 H, Ph), 7.76-7.82 (m, 2 H, Ph) ppm. ^{13}C{^{1}H} NMR (100.62 MHz, $CDCl_3$): δ = 29.78 (s, CH_2), 71.85 (s, C≡*C*H), 79.50 (s, *C*≡CH), 127.04 (s, CH of Ph), 128.61 (s, CH of Ph), 131.78 (s, CH of Ph), 133.73 (s, C^{ipso} of Ph), 167.13 (s, C=O) ppm.

*4-Methyl-N-(prop-2-yn-1-yl)benzamide (**8b**).*[10] The general procedure was used to prepare **8b**, yielding 0.60 g (69%) of a colourless crystalline solid. ^{1}H NMR (400.1g MHz, $CDCl_3$): δ = 2.27 (t, $^4J_{HH}$ = 2.6 Hz, 1 H, C≡CH), 2.39 (s, 3 H, CH_3), 4.24 (dd, J_{HH} = 5.2 Hz, $^4J_{HH}$ = 2.6 Hz, 2 H, CH_2), 6.42 (br s, 1 H, NH), 7.23 (apparent d, J_{HH} = 7.9 Hz, 2 H, CH of C_6H_4), 7.69 (apparent d, J_{HH} = 8.2 Hz, 2 H, CH of C_6H_4) ppm. ^{13}C{^{1}H} NMR (100.62 MHz, $CDCl_3$): δ = 21.47 (s, CH_3), 29.72 (s, CH_2), 71.76 (s, C≡*C*H), 79.64 (s, *C*≡CH), 127.04 (s, CH of C_6H_4), 129.25 (s, CH of C_6H_4), 130.88 (s, C^{ipso} of C_6H_4), 142.24 (s, C^{ipso} of C_6H_4), 167.06 (s, C=O) ppm.

*4-Methoxy-N-(prop-2-yn-1-yl)benzamide (**8c**).*[9] The general procedure was used to prepare **8c**, yielding 0.73 g (77%) of a colourless crystalline solid. ^{1}H NMR (400.13 MHz, $CDCl_3$): δ = 2.27 (t, $^4J_{HH}$ = 2.6 Hz, 1 H, C≡CH), 3.84 (s, 3 H, OCH_3), 4.24 (dd, J_{HH} = 5.2 Hz, $^4J_{HH}$ = 2.6 Hz, 2 H, CH_2), 6.39 (br s, 1 H, NH), 6.92 (apparent d, J_{HH} = 8.9 Hz, 2 H, CH of C_6H_4), 7.76 (apparent d, J_{HH} = 8.9 Hz, 2 H, CH of C_6H_4) ppm. ^{13}C{^{1}H} NMR (100.62 MHz, $CDCl_3$): δ = 29.71 (s, CH_2), 55.41 (s, OCH_3), 71.70 (s, C≡*C*H), 79.74 (s, *C*≡CH), 113.79 (s, CH of C_6H_4), 126.01 (s, C^{ipso} of C_6H_4), 128.89 (s, CH of C_6H_4), 162.39 (s, C^{ipso} of C_6H_4), 166.65 (s, C=O) ppm.

*4-Chloro-N-(prop-2-yn-1-yl)benzamide (**8d**).*[11] The general procedure was used to prepare **8d**, yielding 0.71 g (73%) of a colourless crystalline solid. ^{1}H NMR (400.13 MHz, $CDCl_3$): δ = 2.29 (t, $^{4}J_{HH}$ = 2.6 Hz, 1 H, C≡CH), 4.24 (dd, J_{HH} = 5.2 Hz, $^{4}J_{HH}$ = 2.6 Hz, 2 H, CH_2), 6.45 (br s, 1 H, NH), 7.41 (apparent d, J_{HH} = 8.7 Hz, 2 H, CH of C_6H_4), 7.73 (apparent d, J_{HH} = 8.7 Hz, 2 H, CH of C_6H_4) ppm. ^{13}C{^{1}H} NMR (100.62 MHz, $CDCl_3$): δ = 29.87 (s, CH_2), 72.04 (s, C≡*C*H), 79.26 (s, *C*≡CH), 128.49 (s, CH of C_6H_4), 128.89 (s, CH of C_6H_4), 132.08 (s, C^{ipso} of C_6H_4), 138.10 (s, C^{ipso} of C_6H_4), 166.09 (s, C=O) ppm.

*4-(Trifluoromethyl)-N-(prop-2-yn-1-yl)benzamide (**8e**).*[12] The general procedure was used to prepare **8e**, yielding 0.86 g (76%) of a colourless crystalline solid. ^{1}H NMR (399.95 MHz, $CDCl_3$): δ = 2.30 (t, $^{4}J_{HH}$ = 2.6 Hz, 1 H, C≡CH), 4.27 (dd, J_{HH} = 5.3 Hz, $^{4}J_{HH}$ = 2.6 Hz, 2 H, CH_2), 6.53 (br s, 1 H, NH), 7.68-7.73 (m, 2 H, CH of C_6H_4), 7.88-7.93 (m, 2 H, CH of C_6H_4) ppm. ^{13}C{^{1}H} NMR (100.58 MHz, $CDCl_3$): δ = 29.97 (s, CH_2), 72.23 (s, C≡*C*H), 79.05 (s, *C*≡CH), 123.59 (q, $^{1}J_{CF}$ = 273 Hz, CF_3), 125.70 (q, $^{3}J_{CF}$ = 4 Hz, CH of C_6H_4), 127.55 (s, CH of C_6H_4), 133.55 (q, $^{2}J_{CF}$ = 33 Hz, C^{ipso} of C_6H_4), 136.99 (s, C^{ipso} of C_6H_4), 165.91 (s, C=O) ppm. ^{19}F NMR (376.29 MHz, $CDCl_3$): δ = –63.3 (s, CF_3) ppm.

*N-(Prop-2-yn-1-yl)cyclohexanecarboxamide (**8f**).*[13] The general procedure was used to prepare **8f**, yielding 0.73 g (88%) of a colourless crystalline solid. ^{1}H NMR (400.13 MHz, $CDCl_3$): δ = 1.15-1.33 (m, 3 H, CH_2 of Cy), 1.37-1.51 (m, 2 H, CH_2 of Cy), 1.63-1.71 (m, 1 H, CH_2 of Cy), 1.74-1.92 (m, 4 H, CH_2 of Cy), 2.11 (tt, J_{HH} = 11.7 Hz, J_{HH} = 3.5 Hz, 1 H, CH of Cy), 2.22 (t, $^{4}J_{HH}$ = 2.6 Hz, 1 H, C≡CH), 4.05 (dd, J_{HH} = 5.2 Hz, $^{4}J_{HH}$ = 2.6 Hz, 2 H, CH_2), 5.77 (br s, 1 H, NH) ppm. ^{13}C{^{1}H} NMR (100.62 MHz, $CDCl_3$): δ = 25.68 (s, CH_2 of Cy), 25.70 (s, CH_2 of Cy), 29.09 (s, CH_2), 29.52 (s, CH_2 of Cy), 45.22 (s, CH of Cy), 71.49 (s, C≡*C*H), 79.81 (s, *C*≡CH), 175.65 (s, C=O) ppm.

Kinetic study of gold(I)-catalysed cyclization of propargyl amides 8. *Method A*. The respective amide **8** (typically 0.2 mmol or 0.1 mmol) was dissolved in 0.8 mL of CD_2Cl_2, and the solution was added to a solid catalyst (**6** or [Au(MeCN)(PPh_3)][SbF_6], typically 1 mol.% of Au), which immediately dissolved, forming a yellow solution (colourless when using [Au(MeCN)(PPh_3)]-[SbF_6] as the catalyst), and the reaction mixture was transferred to the NMR tube. NMR spectra were recorded every 10 minutes for 3 hours. Conversion was determined by comparing the integral intensities of the signals due to the methylene group of the starting amide and to product **9**.

Method B (for low catalyst loadings). A stock solution (containing 0.6 mM "Au") was freshly prepared by dissolving **6d** (2.42 mg, 1.5 μmol) in CD_2Cl_2 in a 5-mL volumetric flask. An appropriate amount of stock solution was mixed with a solution of the appropriate *N*-propargylamide **8** (0.2 mmol) in CD_2Cl_2, in a total volume of 0.8 mL. The yellow reaction mixture

was transferred to the NMR tube. NMR spectra were recorded every 10 minutes for 90 min. Conversion was determined as specified above.

Catalyst poisoning experiment. The solution of amide **8a** (31.8 mg, 0.2 mmol) and ($PhCH_2NEt_3$)Cl (0.6 mg, 2.6 μmol) in CD_2Cl_2 (0.8 mL) was added onto the solid **6d** (1.61 mg, 1.0 μmol), which immediately dissolved. The resulting yellow solution was transferred to an NMR tube. ^{1}H NMR spectra were collected every 10 minutes for the period of 30 minutes.

Catalytic experiments with isolation of the product. A solution of the appropriate amide **8** (0.2 mmol) in dry dichloromethane (0.8 mL) was added to a vial loaded with catalyst **6d** (1.61 mg, 1.0 μmol), and the mixture was stirred at room temperature for 3 hours. The product was then isolated by chromatography on a silica gel column using hexane/ethyl acetate (5:1) as the eluent. The evaporation of the eluate provided the product in sufficient purity. Note: Prolonged storage of the product in the presence of oxygen leads to its degradation to peroxo-compounds, as previously described.[12]

*5-Methylene-2-phenyl-4,5-dihydrooxazole (**9a**)*.[9] Colourless liquid. ^{1}H NMR (400.13 MHz, $CDCl_3$): δ = 4.36 (q, $^2J_{HH} \approx {}^4J_{HH} \approx 2.7$ Hz, 1 H, C=C*H*H), 4.65 (t, $^4J_{HH} \approx 2.9$ Hz, 2 H, NCH_2), 4.81 (q, $^2J_{HH} \approx {}^4J_{HH} \approx 3.0$ Hz, 1 H, C=CH*H*), 7.40-7.47 (m, 2 H, CH of C_6H_5), 7.47-7.54 (m, 1 H, CH of C_6H_5), 7.94-8.01 (m, 2 H, CH of C_6H_5) ppm. ^{13}C{^{1}H} NMR (100.62 MHz, $CDCl_3$): δ = 57.77 (s, NCH_2), 83.74 (s, C=*C*H_2), 126.77 (s, C^{ipso} of C_6H_5), 127.99 (s, CH of C_6H_5), 128.48 (s, CH of C_6H_5), 131.79 (s, CH of C_6H_5), 158.85 (s, *C*=CH_2), 163.70 (s, C=N) ppm.

*5-Methylene-2-(4-methylphenyl)-4,5-dihydrooxazole (**9b**)*.[14] Colourless liquid. ^{1}H NMR (400.13 MHz, $CDCl_3$): δ = 2.40 (s, 3 H, CH_3), 4.34 (q, $^2J_{HH} \approx {}^4J_{HH} \approx 2.7$ Hz, 1 H, C=C*H*H), 4.63 (t, $^4J_{HH} \approx 2.9$ Hz, 2 H, NCH_2), 4.80 (q, $^2J_{HH} \approx {}^4J_{HH} \approx 3.0$ Hz, 1 H, C=CH*H*), 7.24 (apparent d, $J_{HH} = 7.6$ Hz, 2 H, CH of C_6H_4), 7.86 (apparent d, $J_{HH} = 8.2$ Hz, 2 H, CH of C_6H_4) ppm. ^{13}C{^{1}H} NMR (100.62 MHz, $CDCl_3$): δ = 21.61 (s, CH_3), 57.72 (s, NCH_2), 83.52 (s, C=*C*H_2), 123.98 (s, C^{ipso} of C_6H_4), 127.95 (s, CH of C_6H_4), 129.21 (s, CH of C_6H_4), 142.26 (s, C^{ipso} of C_6H_4), 158.94 (s, *C*=CH_2), 163.78 (s, C=N) ppm.

*2-(4-Methoxyphenyl)-5-methylene-4,5-dihydrooxazole (**9c**)*.[9] Colourless solid. ^{1}H NMR (400.13 MHz, $CDCl_3$): δ = 3.85 (s, 3 H, CH_3), 4.34 (q, $^2J_{HH} \approx {}^4J_{HH} \approx 2.7$ Hz, 1 H, C=C*H*H), 4.62 (t, $^4J_{HH} \approx 2.8$ Hz, 2 H, NCH_2), 4.78 (q, $^2J_{HH} \approx {}^4J_{HH} \approx 2.9$ Hz, 1 H, C=CH*H*), 6.94 (apparent d, $J_{HH} = 8.9$ Hz, 2 H, CH of C_6H_4), 7.92 (apparent d, $J_{HH} = 8.9$ Hz, 2 H, CH of C_6H_4) ppm. ^{13}C{^{1}H} NMR (100.62 MHz, $CDCl_3$): δ = 55.38 (s, CH_3), 57.70 (s, NCH_2), 83.37 (s, C=*C*H_2), 113.87 (s, CH of C_6H_4), 119.24 (s, C^{ipso} of C_6H_4), 129.75 (s, CH of C_6H_4), 159.01 (s, *C*=CH_2), 162.41 (s, C^{ipso} of C_6H_4), 163.45 (s, C=N) ppm.

*2-(4-Chlorophenyl)-5-methylene-4,5-dihydrooxazole (**9d**)*. Colourless solid. ^{1}H NMR (400.13 MHz, $CDCl_3$): δ = 4.37 (q, $^{2}J_{HH} \approx {}^{4}J_{HH} \approx 2.7$ Hz, 1 H, C=C*H*H), 4.64 (t, $^{4}J_{HH} \approx 2.9$ Hz, 2 H, NCH_2), 4.81 (q, $^{2}J_{HH} \approx {}^{4}J_{HH} \approx 3.0$ Hz, 1 H, C=CH*H*), 7.42 (apparent d, $J_{HH} = 8.7$ Hz, 2 H, CH of C_6H_4), 7.91 (apparent d, $J_{HH} = 8.6$ Hz, 2 H, CH of C_6H_4) ppm. ^{13}C{^{1}H} NMR (100.62 MHz, $CDCl_3$): δ = 57.80 (s, NCH_2), 84.07 (s, C=*C*H_2), 125.26 (s, C^{ipso} of C_6H_4), 128.85 (s, CH of C_6H_4), 129.32 (s, CH of C_6H_4), 138.06 (s, C^{ipso} of C_6H_4), 158.67 (s, *C*=CH_2), 162.85 (s, C=N) ppm. Anal. Calc. for $C_{10}H_8ClNO$ (193.6): C 32.03, H 4.16, N 7.23%. Found: C 62.35, H 4.32, N 6.96%.

*5-Methylene-2-(4-(trifluoromethyl)phenyl)-4,5-dihydrooxazole (**9e**)*.[14] White solid. ^{1}H NMR (399.95 MHz, $CDCl_3$): δ = 4.41 (q, $^{2}J_{HH} \approx {}^{4}J_{HH} \approx 2.8$ Hz, 1 H, C=C*H*H), 4.68 (t, $^{4}J_{HH} \approx 2.9$ Hz, 2 H, NCH_2), 4.85 (q, $^{2}J_{HH} \approx {}^{4}J_{HH} \approx 3.1$ Hz, 1 H, C=CH*H*), 7.71 (apparent d, $J_{HH} = 8.1$ Hz, 2 H, CH of C_6H_4), 8.10 (apparent d, $J_{HH} = 8.0$ Hz, 2 H, CH of C_6H_4) ppm. ^{13}C{^{1}H} NMR (100.58 MHz, $CDCl_3$): δ = 57.89 (s, NCH_2), 84.45 (s, C=*C*H_2), 123.70 (q, $^{1}J_{CF} = 273$ Hz, CF_3), 125.51 (q, $^{3}J_{CF} = 4$ Hz, CH of C_6H_4), 128.39 (s, CH of C_6H_4), 130.12 (s, C^{ipso} of C_6H_4), 133.42 (q, $^{2}J_{CF} = 33$ Hz, C^{ipso} of C_6H_4), 158.54 (s, *C*=CH_2), 162.60 (s, C=N) ppm. ^{19}F NMR (376.29 MHz, $CDCl_3$): δ = –63.3 (s, CF_3) ppm.

*2-Cyclohexyl-5-methylene-4,5-dihydrooxazole (**9f**)*.[15] Colourless liquid. ^{1}H NMR (400.13 MHz, $CDCl_3$): δ = 1.17-1.37 (m, 3 H, CH_2 of Cy), 1.39-1.52 (m, 2 H, CH_2 of Cy), 1.63-1.72 (m, 1 H, CH_2 of Cy), 1.74-1.84 (m, 2 H, CH_2 of Cy), 1.92-2.01 (m, 2 H, CH_2 of Cy), 2.36 (tm, $J_{HH} = 11.3$ Hz, 1 H, CH of Cy), 4.23 (q, $^{2}J_{HH} \approx {}^{4}J_{HH} \approx 2.6$ Hz, 1 H, C=C*H*H), 4.40 (td, $^{4}J_{HH} = 2.9$ Hz, $^{5}J_{HH} = 1.4$ Hz, 2 H, NCH_2), 4.63 (q, $^{2}J_{HH} \approx {}^{4}J_{HH} \approx 2.9$ Hz, 1 H, C=CH*H*) ppm. ^{13}C{^{1}H} NMR (100.62 MHz, $CDCl_3$): δ = 25.53 (s, CH_2 of Cy), 25.80 (s, CH_2 of Cy), 29.38 (s, CH_2 of Cy), 37.38 (s, CH of Cy), 57.13 (s, NCH_2), 82.73 (s, C=*C*H_2), 159.15 (s, *C*=CH_2), 170.67 (s, C=N) ppm.

X-Ray crystallography

Full-set diffraction data ($\pm h \pm k \pm l$, θ_{max} = 26.0 or 27.5°) were collected using a Bruker D8 VENTURE Kappa Duo instrument equipped with a PHOTON100 detector, a IμS micro-focus X-ray tube (Mo Kα radiation, λ = 0.71073 Å) and a Cryostream cooler (Oxford Cryosystems). The structures were solved using direct methods (SHELXT-2014)[16] and subsequently refined by full-matrix least-squares based on F^2 using SHELXL-2014 or SHELXL-2017.[17] All non-hydrogen atoms were refined with anisotropic displacement parameters. The hydrogen atoms were included in their theoretical positions and refined as riding atoms with U_{iso}(H) set to a 1.2U_{eq} of their bonding carbon atom. The cyano group in the structure of **5a** was disordered over two positions. The refined occupancies were 47:53. A recent version of the PLATON program[18] was used to perform geometric calculations and to prepare all structural diagrams. Selected crystallographic data, data collection and structure refinement parameters are outlined in Table S1. The individual structures are discussed below.

CCDC 1909789 (**1d**), 1909790 (**4**), 1909791 (**5a**), 1909792 (**5b**), 1909793 (**5d**), 1909794 (**6b**·Me_2CO), and 1909795 (**6d**), contain the supplementary crystallographic data for this paper. These data are available free of charge from The Cambridge Crystallographic Data Centre.

Table S1. Selected crystallographic data and structure refinement parameters

Compound	**1d**	**4**
Formula	$C_{19}H_{14}FeNO_2P$	$C_{22}H_{16}Br_2Fe_2N_2$
M/g mol^{-1}	375.13	579.89
Crystal system	monoclinic	monoclinic
Space group	$P2_1/c$ (No. 14)	$P2_1/n$ (No. 14)
T/K	150(2)	120(2)
a/Å	10.7290(4)	13.7570(4)
b/Å	19.7011(8)	10.0313(3)
c/Å	7.6835(3)	14.6288(4)
α/deg	90	90
β/deg	93.613(1)	110.809(1)
γ/deg	90	90
V/Å^3	1620.9(1)	1887.10(9)
Z	4	4
μ(Mo Kα)/mm^{-1}	1.039	5.783
F(000)	768	1136
Diffrns collected	16586	27109
Independent diffrns	3704	4317
Observed diffrns[a]	3430	4005
R_{int}[b]/%	2.17	3.48
No. of parameters	217	253
R[c] obsd diffrns/%	2.37	1.93
R, wR[c] all data /%	2.67, 5.97	2.20, 4.57
Δρ/e Å^{-3}	0.33, −0.34	0.39, −0.64

[a] Diffractions with $I > 2\sigma(I)$. [b] Definitions: $R_{int} = \Sigma|F_o^2 - F_o^2(\text{mean})|/\Sigma F_o^2$, where F_o^2(mean) denotes the average intensity of symmetry-equivalent diffractions. [c] $R = \Sigma||F_o| - |F_c||/\Sigma|F_o|$, w$R = [\Sigma\{w(F_o^2 - F_c^2)^2\}/\Sigma w(F_o^2)^2]^{½}$.

Table S1 continued

Compound	**5a**	**5b**	**5d**
Formula	$C_{17}H_{22}AuClFeNP$	$C_{23}H_{30}AuClFeNP$	$C_{19}H_{14}AuClFeNO_2P$
M/g mol^{-1}	559.59	639.71	607.55
Crystal system	monoclinic	monoclinic	monoclinic
Space group	$P2_1/n$ (No. 14)	$P2_1/c$ (No. 14)	$P2_1/c$ (No. 14)
T/K	120(2)	120(2)	150(2)
a/Å	10.3726(5)	9.0034(5)	10.8892(4)
b/Å	9.1257(5)	14.2805(8)	8.6369(3)
c/Å	19.301(1)	17.7023(11)	20.4246(7)
α/deg	90	90	90
β/deg	94.845(2)	99.915(2)	97.231(1)
γ/deg	90	90	90
V/Å^3	1820.5(2)	2242.0(2)	1905.6(1)
Z	4	4	4
μ(Mo Kα)/mm^{-1}	9.076	7.383	8.688
F(000)	1072	1248	1152
Diffrns collected	22513	15883	23652
Independent diffrns	4180	5157	4365
Observed diffrns[a]	3945	4604	4125
R_{int}[b]/%	2.15	2.18	2.29
No. of parameters	211	253	236
R[c] obsd diffrns/%	1.30	1.82	1.43
R, wR[c] all data /%	1.47, 2.66	2.29, 3.59	1.63, 3.10
Δρ/e Å^{-3}	0.49, –0.51	0.48, –0.61	0.41, –0.68

Table S1 continued

Compound	**6b**·Me_2CO	**6d**
Formula	$C_{49}H_{66}Au_2F_{12}Fe_2N_2OP_2Sb_2$	$C_{38}H_{28}Au_2F_{12}Fe_2N_2O_4P_2Sb_2$
M/g mol^{-1}	1738.11	1615.70
Crystal system	triclinic	monoclinic
Space group	$P\bar{1}$ (No. 2)	$P2_1/n$ (No. 14)
T/K	120(2)	120(2)
a/Å	11.534(1)	9.1821(3)
b/Å	12.008(1)	20.4012(6)
c/Å	39.793(5)	12.1762(4)
α/deg	87.710(4)	90
β/deg	85.000(4)	105.018(1)
γ/deg	86.529(4)	90
V/Å^3	54777(1)	2203.0(1)
Z	4	2
μ(Mo Kα)/mm^{-1}	6.963	8.650
F(000)	3328	1504
Diffrns collected	108326	39498
Independent diffrns	23907	5069
Observed diffrns[a]	21388	4704
R_{int}[b]/%	3.65	3.07
No. of parameters	1301	290
R[c] obsd diffrns/%	4.15	1.74
R, wR[c] all data /%	4.86, 8.03	2.07, 3.54
Δρ/e Å^{-3}	2.08, −2.23	1.46, −1.39

Solid-state structure of ***4***

Compound **4** crystallises with the symmetry of the monoclinic space group $P2_1/n$ and with one molecule in the asymmetric unit. The molecular structure of **4** (Figure S1) consists of the central C=N−C≡N moiety doubly substituted by two mutually rotated, chemically equivalent 1′-bromoferrocen-1-yl units. The angle subtended by the cyclopentadienyl planes C(1-5) and C(21-25) is 42.9(1)°. The cyclopentadienyls in both substituents are slightly tilted (the dihedral angles of the cyclopentadienyl planes are 5.4(1)° and 2.0(1)° for the ferrocene units comprising Fe1 and Fe2, respectively). Although the cyclopentadienyl rings at both ferrocene units are eclipsed, their substituents assume different positions. While they are located above each other (τ = 0.6(1)°; τ is the torsion angle C1-Cg1-Cg2-C6, where Cg1 and Cg2 are the centroids of the cyclopentadienyl rings C(1-5) and C(6-10), respectively) in the Fe1 ferrocene unit, they occupy more distant, anticlinal positions (τ = −146.5(1)°) in the Fe2 ferrocene moiety.[19] The ranges of the individual Fe-C bonds were 2.039(2)-2.060(2) Å and 2.022(2)-2.067(2) Å for Fe1 and Fe2, respectively.

The geometric parameters of the cyanoimine moiety of **4** are similar to those in other structurally characterised 1,4-quinonediimines.[20] The three chemically different C-N bonds of **4** are clearly distinguishable by their lengths (C11-N1 = 1.311(2) Å, C12-N1 = 1.336(2) Å, C12-N2 = 1.157(2) Å) and the cyanomine fragment is bent at C11 (C1-C11-C21 = 119.2(1)°). A slight bending is also observed at the terminal C−CN fragment (N1-C12-N2 = 170.7(2)°).

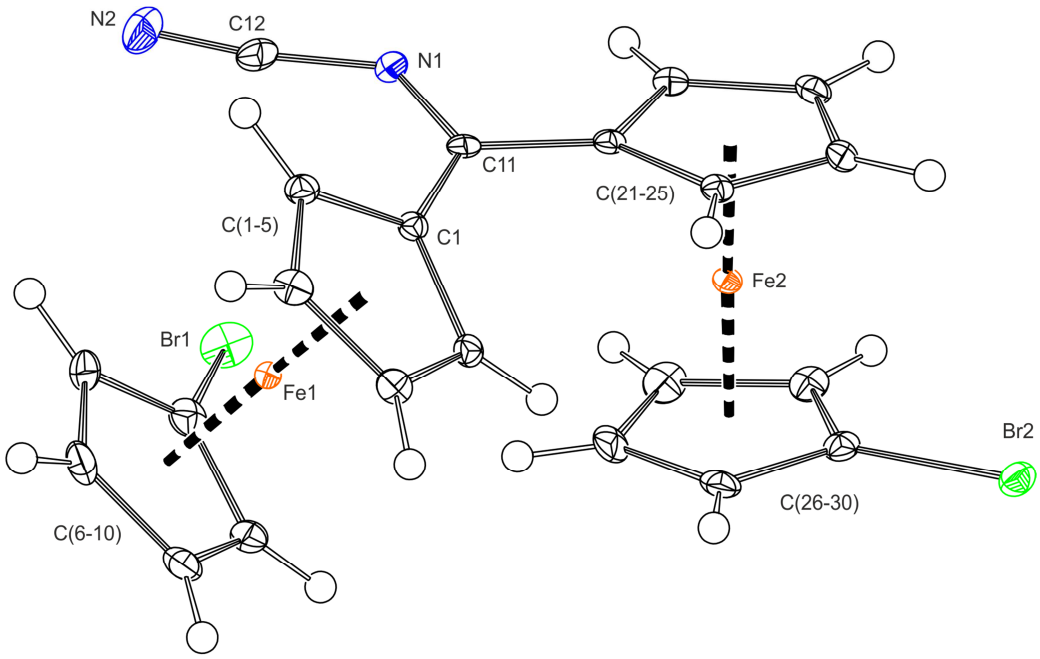

Figure S1. PLATON plot of the molecular structure of cyanoimine **4** showing atom labelling and displacement ellipsoids at the 50% probability level

*Crystal structure of **1d***

Compound **1d** (Figure S2) crystallises with the symmetry of the monoclinic space group $P2_1/c$ and with one molecule in the asymmetric unit. The molecule of **1d** contains an undistorted ferrocene moiety with Fe-C distances in the range of 2.029(1)-2.066(1) Å and with parallel cyclopentadienyl rings (tilt angle 1.82(8)°). The substituents of the central ferrocene unit in positions 1 and 1′ adopt a conformation near anticlinal eclipsed, as evidenced by the τ angle of −148.1(1)° (τ is the torsion angle C1-Cg1-Cg2-C6, where Cg1 and Cg2 are the centroids of the cyclopentadienyl rings C(1-5) and C(6-10), respectively). The nitrile moiety is linear (C11-N = 1.144(2) Å, C1-C11-N = 178.3(2)°) and lies in the plane of its parent cyclopentadienyl ring (the angle subtended by the C11-N bond and by the least-squares cyclopentadienyl plane C(6-10) is 2.5(1)°). Similarly, the vector of the pivotal P-C6 bond departs from the plane of its parent cyclopentadienyl ring C(1-5) by only 3.21(7)°, and the furyl substituents are oriented above the ferrocene unit and to its side; the dihedral angles between the furane rings and the C(1-5) planes are 75.70(9)° and 81.67(9)° for the rings comprising O1 and O2, respectively. The dihedral angle between the planes of the furane rings is 55.83(9)°. The P-C bonds are 1.814(1) Å (C6), 1.803(1) Å (C12), and 1.810(1) Å (C16), and the furane rings show partly localised character (cf. the individual C-C bond lengths C12-C13 1.360(2), C13-C14 1.425(2), C14-C15 1.341(2) Å; C16-C17 1.349(2), C17-C18 1.424(2), C18-C19 1.328(3) Å; the C-O distances in the furane rings are ≈1.37 Å).

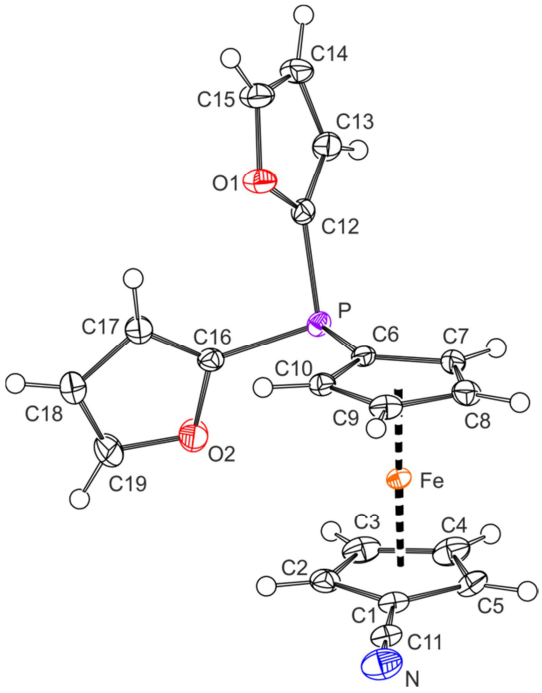

Figure S2. PLATON plot of the molecular structure of phosphine **1d** with atom labelling and displacement ellipsoids at the 50% probability level

*Crystal structures of the chloridogold(I) complexes **5***

Molecular structures of **5a**, **5b** and **5d** are presented in Figure S3, and the selected structural parameters are outlined in Table S2. The coordination environments of the gold(I) ions in these complexes are linear dicoordinate, with Au-donor distances similar to those reported for [AuCl(PPh_3)][21] and [AuCl(**1c**-κ*P*)].[2] The P–Au–Cl arms in **5a**, **5b** and **5d**, extending from the tetrahedral phosphorus atoms, are inclined towards the ferrocene unit. The ferrocene moieties are marginally tilted (up to 5° in **5b**) and assume different conformations in different compounds. In **5a**, the CN-substituted cyclopentadienyl ring is disordered over two positions, corresponding to eclipsed anticlinal and eclipsed synclinal conformations at the ferrocene unit (refined occupancies 53:47). In **5b** and **5d**, the respective conformations are eclipsed synclinal (or 1,2′) and an intermediate conformation near anticlinal eclipsed. When compared to the structure of free ligand **1d**, the structure of **5d** reveals shortened P-C bonds (by 0.01-0.03 Å) due to electron density shift from the substituents to the phosphorus atom and less acute C6-P-C16 and C12-P-C16 angles (the C6-P-C12 angle remains virtually unchanged).

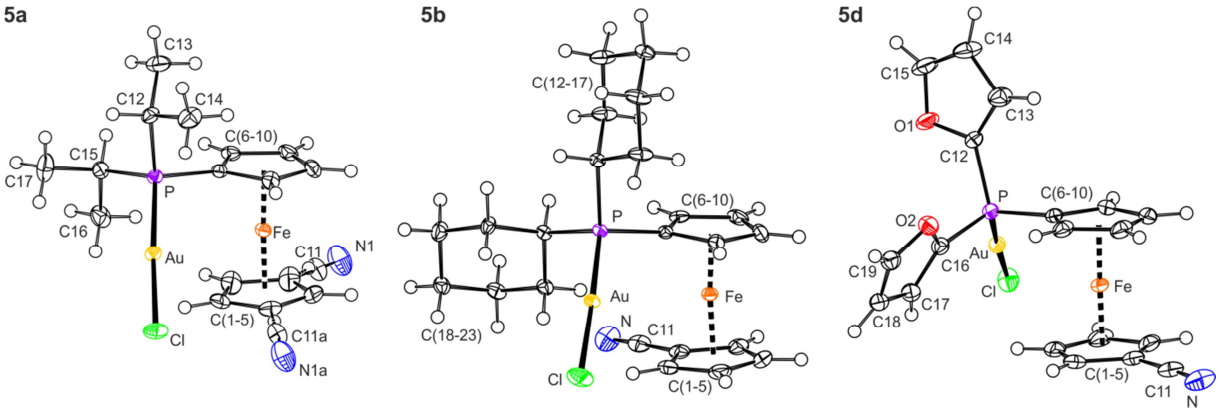

Figure S3. PLATON plots of the molecular structures of **5a**, **5b** and **5d** showing atom labelling and displacement ellipsoids at the 50% probability level. Both orientations of the disordered CN group are shown for **5a**.

Table S2. Selected distances and angles for the chloridogold(I) complexes **5** (in Å and deg)[a]

Parameter	**5a** (*n* = 15)	**5b** (*n* = 1)	**5d** (*n* = 16)
Au-P	2.2361(5)	2.2319(7)	2.2191(6)
Au-Cl	2.2890(5)	2.2850(7)	2.2817(7)
P-Au-Cl	177.17(2)	175.06(3)	176.97(2)
Fe-C (range)	2.030(2)-2.060(2)	2.034(3)-2.054(3)	2.027(2)-2.059(2)
∠Cp1,Cp2	3.2(1)	5.1(2)	1.4(1)
τ	−145.1(2)/71.4(2)[b]	69.5(2)	−155.4(2)
C11-N	1.135(6)	1.143(4)	1.139(4)
P-C6	1.797(2)	1.798(2)	1.788(2)
P-C12	1.844(2)	1.843(2)	1.789(2)
P-C*n*	1.832(2)	1.831(3)	1.779(2)

[a] Parameters Cp1, Cp2 and τ are defined as for the free ligand **1d** (see the previous page). [b] Values pertaining to the two orientations of the disordered nitrile group

*Crystal structures of **6b**·Me$_2$CO and **6d***

Compounds **6b**·Me$_2$CO and **6d** were structurally authenticated by single-crystal X-ray diffraction analysis as cationic digold(I) complexes containing a pair of P,N-bridging phosphinonitrile ligands, whose charge was compensated for by two hexafluoridoantimonate(V) anions. Structure determination of compound **6a** also confirmed the dimeric nature of the complex. However, the structure could not be satisfactorily refined due to extensive disorder. Compound **6d** crystallises with the symmetry of the monoclinic space group $P2_1/n$ with the dimeric unit $[Au_2(\mu(P,N)\text{-}\mathbf{1d})_2]^{2+}$ located around the crystallographic inversion centre which, in turn, renders only half of the complex cation and one $[SbF_6]^-$ anion symmetrically independent. In the case of **6b**·Me$_2$CO, the asymmetric part of the triclinic unit cell (space group *P*–1) contains one complete cationic dimer (Au1 and Au2) and two halves from two additional dimers located at the crystallographic inversion centres (Au3 and Au4), four anions and one acetone molecule. Structural diagrams for **6b**·Me$_2$CO and **6d** are shown in Figures S4-S6, and the relevant structural parameters are outlined in Table S3.

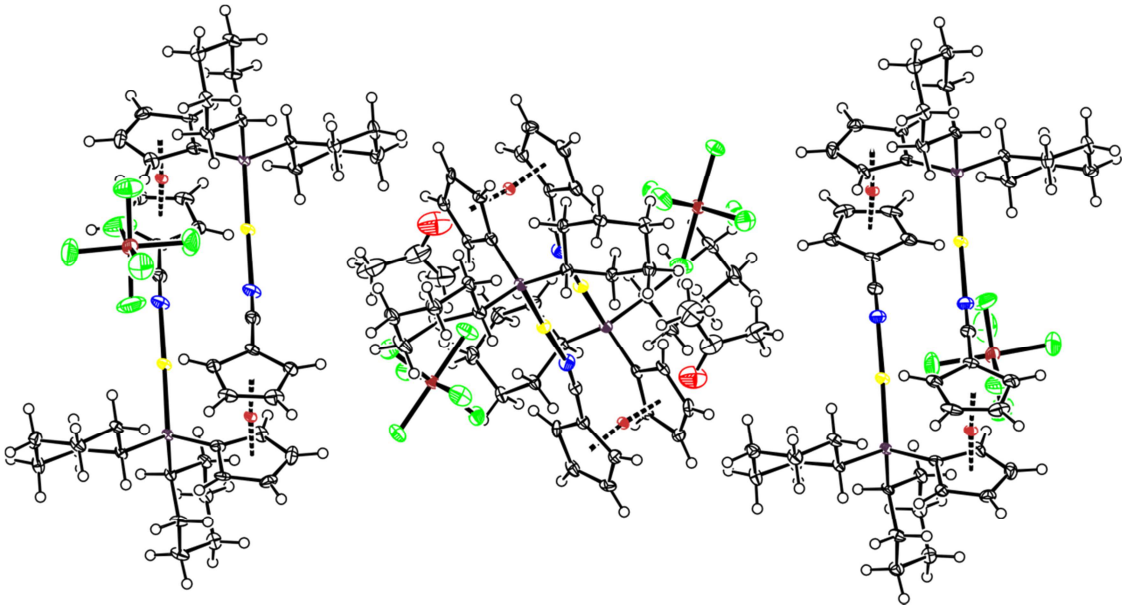

Figure S4. Full PLATON plot of the structure of **6b**·Me_2CO with 50% probability ellipsoids

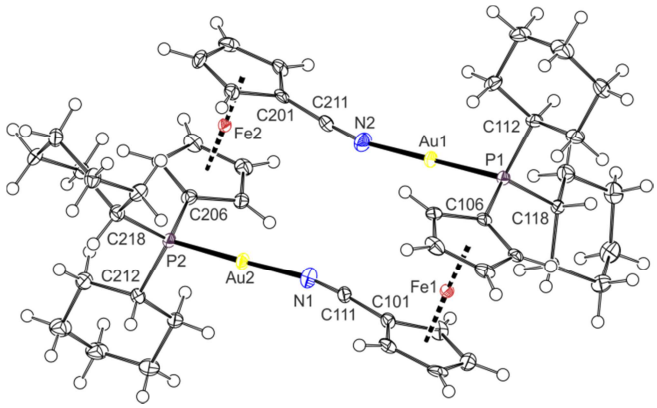

Figure S5. PLATON plot of the complex cation comprising atoms Au1 and Au2 in the structure of **6b**·Me_2CO; displacement ellipsoids are scaled to the 50% probability level.

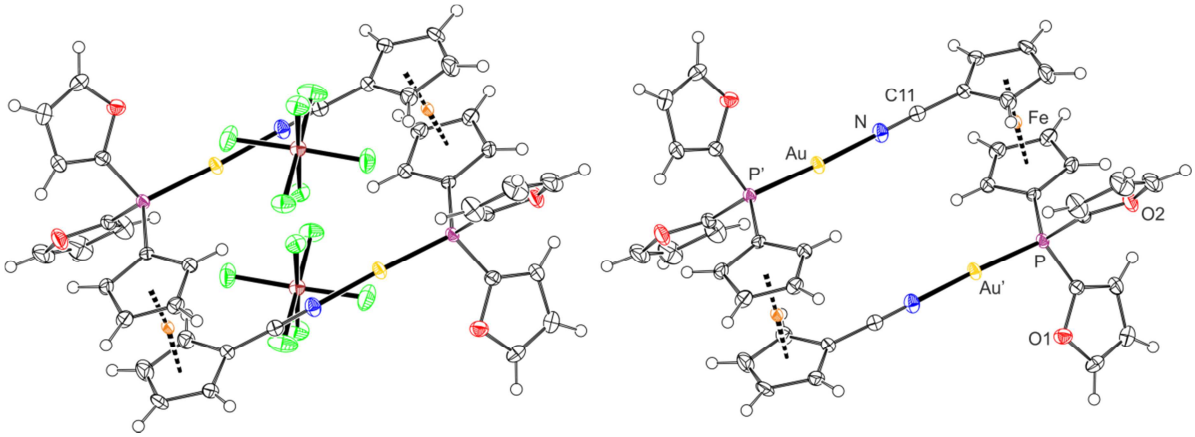

Figure S6. PLATON plot of the molecular structure of **6d** (left); PLATON plot of the complex cation in the structure of **6d** showing atom labelling (right). Displacement ellipsoids enclose 50% probability level. Note: the labelling is strictly analogous to that used for the free ligand **1d**.

The overall geometry of the digold(I) cations in the structures of **6b**·Me_2CO and **6d** is similar to that of the analogous cation resulting from ligand **1d**.[2] Notably, the Au-P and Au-N distances in **6d** are significantly shorter than in **6b**, presumably reflecting the strengthening of these bonds by π-back donation in the complex with the weaker-donating ligand **1d**. Similarly to **5d**, the P-C bonds in **6d** are approximately 0.2 Å shorter than those in the uncoordinated ligand **1d**. By contrast, the C≡N bond lengths remain virtually unaffected by coordination in all cases. The ferrocene moieties assume conformations near synclinal eclipsed (ideal value: τ = 72°), which brings the phosphine moiety to the side of the ferrocene scaffold and thus gives rise to an arrangement in which the P-Au-N moieties are mutually offset. Yet, the variation in the τ parameter among structurally independent but chemically identical fragments in the structure of **6b**·Me_2CO suggests that the coordination of the phosphinonitrile ligands is rather flexible, thus allowing conformational changes within dimeric cations.

Table S3. Selected distances and angles for **6b**·MeCO and **6d** (in Å and deg).[a]

Parameter	**6b**·Me_2CO (Fe1/Au1)	**6b**·Me_2CO (Fe2/Au2)	**6b**·Me_2CO (Fe3/Au3)	**6b**·Me_2CO (Fe4/Au4)	**6d**
Au-P	2.241(2)	2.250(2)	2.237(2)	2.239(2)	2.2139(7)
Au-N	2.048(6)	2.047(6)	2.054(6)	2.050(6)	2.032(2)
P-Au-N	177.7(2)	178.0(2)	174.4(2)	174.4(2)	176.21(7)
Fe-C (range)	2.034(6)-2.064(6)	2.013(6)-2.062(7)	2.021(6)-2.051(7)	2.033(6)-2.058(7)	2.023(3)-2.063(3)
∠Cp1,Cp2	7.5(4)	6.8(4)	3.3(4)	3.3(4)	3.1(2)
τ	–68.2(5)	74.6(4)	–60.5(5)	57.1(5)	–78.4(2)
C11-N	1.137(8)	1.139(9)	1.132(9)	1.140(8)	1.140(3)
P-C6	1.792(6)	1.795(6)	1.797(6)	1.789(6)	1.783(3)
P-C12	1.846(6)	1.841(6)	1.838(6)	1.845(6)	1.792(3)
P-C*n*	1.830(6)	1.846(6)	1.829(6)	1.828(6)	1.785(3)

[a] Parameters Cp1, Cp2 and τ are defined as for the free ligand **1d**; *n* = 18 (**6b**·Me_2CO) or 16 (**6d**).

Additional kinetic plots

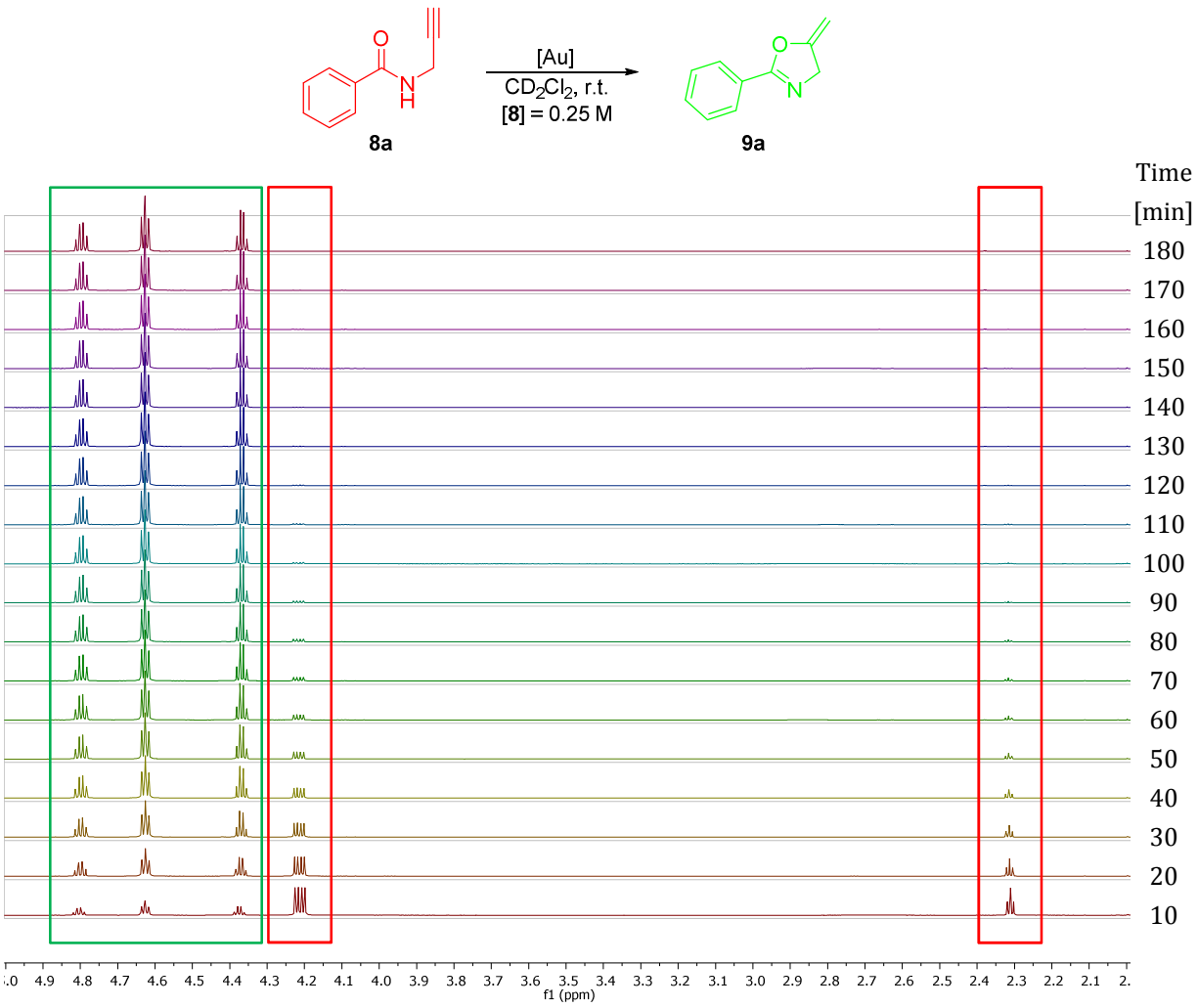

Figure S7. Representative ^{1}H NMR spectra illustrating the conversion of **8a** into **9a** catalysed by complex **6d** (1 mol.% Au, $[\mathbf{8a}]_0$ = 0.25 M) in CD_2Cl_2 at 25°C

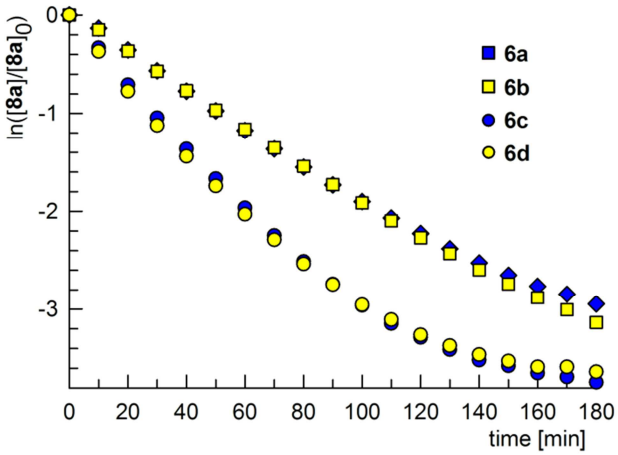

Figure S8. ln([**8a**]/[**8a**]$_0$) vs. time plots of different catalysts illustrating the departure from first-order behaviour at higher conversions (in CD_2Cl_2, [**8a**]$_0$ = 0.25 M, 25°C); the rate constants quoted in the main text were obtained by fitting these curves in the linear range of 10-60 min

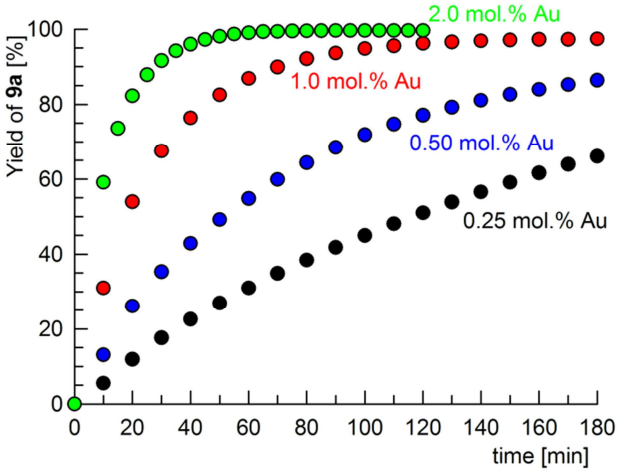

Figure S9. Kinetic profiles for the cyclisation of substrate **8a** catalysed by varying amounts of complex **6d** (in CD_2Cl_2, [**8a**]$_0$ = 0.25 M, 25°C)

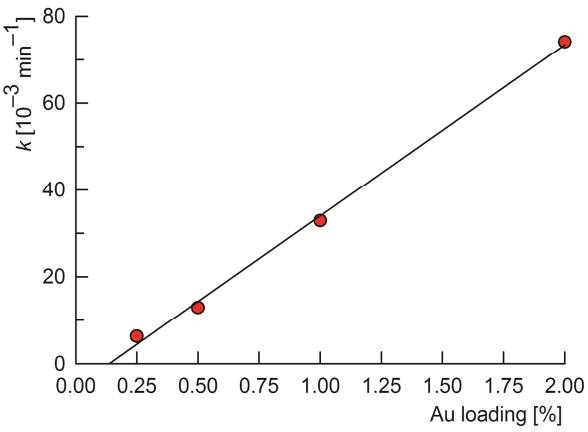

Figure S10. Linear relationship between catalyst concentration and observed reaction rate of the cyclisation of substrate **8a** catalysed by complex **6d** (in CD_2Cl_2, $[\mathbf{8a}]_0$ = 0.25 M, 25°C). Parameters of the linear fit are as follows: k (10^{-3} min^{-1}) = −5(2) + 39(1) c_{Au} (%); R^2 = 0.9975.

DFT computations

DFT calculations have been performed using the PBE0 density functional[22] in conjunction with the SDD (Fe, Au)[23] and cc-pVDZ (C, H, N, O, and P)[24] basis sets, as implemented in the Gaussian 09 program package, revision D.[25] Solvent effects (dichloromethane) have been approximated using the polarised continuum model (PCM).[26] Geometry optimisations were started from geometries determined by crystallographic analysis where possible. Reported energies refer to Gibbs free energies at 298 K. The optimised molecular structures are available in Supporting Information.

References

1 K. Škoch, I. Císařová and P. Štěpnička, *Inorg. Chem.,* 2014, **53**, 568-577.

2 K. Škoch, I. Císařová and P. Štěpnička, *Chem. Eur. J.,* 2015, **21**, 15998-16004.

3 R. Usón, A. Laguna and M. Laguna, *Inorg. Synth.,* 1989, **26**, 85-91.

4 C. Nieto-Oberhuber, M. P. Muñoz, S. López, E. Jiménez-Núñez, C. Nevado, E. Herrero-Gómez, M. Raducan and A. M. Echavarren, *Chem. Eur. J.,* 2006, **12**, 1677-1693.

5 M. Preisenberger, A. Schier and H. Schmidbaur, *J. Chem. Soc., Dalton Trans.,* 1999, 1645-1650.

6 R. M. Silverstein, F. X. Webster and D. J. Kiemle, *Spectrometric Identification of Organic Compounds*, 7th ed., Wiley, Hoboken, 2005.

7 A. Chesney, M. R. Bryce, R. W. J. Chubb, A. S. Batsanov and J. A. K. Howard, *Synthesis,* 1998, 413-416.

8 P. Nicpon and D. W. Meek, *Inorg. Chem.,* 1966, **5**, 1297-1298.

9 X. Meng and S. Kim, *Org. Biomol. Chem.,* 2011, **9**, 4429-4431.

10 R. L. Melen, M. M. Hansmann, A. J. Lough, A. S. K. Hashmi and D. W. Stephan, *Chem. Eur. J.,* 2013, **19**, 11928-11938.

11 N. Willand, M. Desroses, P. Toto, B. Dirié, Z. Lens, V. Villeret, P. Rucktooa, C. Locht, A. Baulard and B. Deprez, *ACS Chem. Biol.,* 2010, ***5***, 1007-1013.

12 A. S. K. Hashmi, M. C. B. Jaimes, A. M. Schuster and F. Rominger, *J. Org. Chem.,* 2012, **77**, 6394-6408.

13 A. Lukin, T. Vedekhina, D. Tovpeko, N. Zhuriloa and M. Krasavin, *RSC Adv.,* 2016, **6**, 57956- 57959.

14 G. C. Senadi, W.-P. Hu, J.-S. Hsiao, J. K. Vandavasi, C.-Y. Chen and J.-J. Wang, *Org. Lett.,* 2012, **14**, 4478-4481.

15 S. Doherty, J. G. Knight, A. S. K. Hashmi, C. H. Smyth, N. A. B. Ward, K. J. Robson, S. Tweedley, R. W. Harrington and W. Clegg, *Organometallics,* 2010, **29**, 4139-4147.

16 G. M. Sheldrick, *Acta Crystallogr., Sect. A: Found. Adv*., 2015, ***71***, 3-8.

17 G. M. Sheldrick, *Acta Crystallogr., Sect. C, Struct. Chem*., 2015, 71, 3-8.

18 A. L. Spek, *J. Appl. Crystallogr*., 2003, 36, 7-13.

19 K.-S. Gan, T. S. A. Hor in *Ferrocenes: Homogeneous Catalysis, Organic Synthesis, Materials Science* (Eds. A. Togni, T. Hayashi), Wiley-VCH, Weinheim, 1995; ch. 1, pp. 3-104

20 Selected examples: a) *N*,*N*′-dicyano-1,4-benzoquinonediimine: G. D. Andreetti, S. Bradamante, P. C. Bizzarri and G. A. Pagani, *Mol. Cryst. Liq. Cryst.,* 1985, **120**, 309-314; b) 2,5-dimethyl-*N*,*N*′-dicyano-1,4-benzoquinonediimine: A. Aumüllerz, P. Erk, S. Hünig, E. Hadicke, K. Peters and H. G. von Schnering, *Chem. Ber.,* 1991, **124**, 2001-2004; c) *N*,*N*′-

dicyano-1,4-indaquinonediimine: E. Tillmanns and F. Schvabenlander, *Acta Crystallogr., Sect. C: Cryst. Struct. Commun*., 1994, **50**, 715-717.

21] S. P. C. Dunstan, P. C. Healy, A. N. Sobolev, E. R. T. Tiekink, A. H. White and M. L. Williams, *J. Mol. Struct.,* 2014, **1072**, 253-259.

22 a) C. Adamo and V. Barone, *J. Chem. Phys.,* 1999, **110**, 6158-6170; b) M. Ernzerhof and G. E. Scuseria, *J. Chem. Phys.,* 1999, **110**, 5029-5036.

23 a) M. Dolg, U. Wedig, H. Stoll and H. J. Preuss, *J. Chem. Phys.,* 1987, **86**, 866-872; b) D. Andrae, U. Haussermann, M. Dolg, H. Stoll and H. Preuss, *Theor. Chim. Acta,* 1990, **77**, 123-141.

24 a) T. H. Dunning, Jr., *J. Chem. Phys.,* 1989, **90**, 1007-1023; b) D. E. Woon and T. H. Dunning, Jr., *J. Chem. Phys.,* 1993, **98**, 1358-1371.

25 Gaussian 09, Revision D.01, M. J. Frisch, G. W. Trucks, H. B. Schlegel, G. E. Scuseria, M. A. Robb, J. R. Cheeseman, G. Scalmani, V. Barone, B. Mennucci, G. A. Petersson, H. Nakatsuji, M. Caricato, X. Li, H. P. Hratchian, A. F. Izmaylov, J. Bloino, G. Zheng, J. L. Sonnenberg, M. Hada, M. Ehara, K. Toyota, R. Fukuda, J. Hasegawa, M. Ishida, T. Nakajima, Y. Honda, O. Kitao, H. Nakai, T. Vreven, J. A. Montgomery, Jr., J. E. Peralta, F. Ogliaro, M. Bearpark, J. J. Heyd, E. Brothers, K. N. Kudin, V. N. Staroverov, R. Kobayashi, J. Normand, K. Raghavachari, A. Rendell, J. C. Burant, S. S. Iyengar, J. Tomasi, M. Cossi, N. Rega, J. M. Millam, M. Klene, J. E. Knox, J. B. Cross, V. Bakken, C. Adamo, J. Jaramillo, R. Gomperts, R. E. Stratmann, O. Yazyev, A. J. Austin, R. Cammi, C. Pomelli, J. W. Ochterski, R. L. Martin, K. Morokuma, V. G. Zakrzewski, G. A. Voth, P. Salvador, J. J. Dannenberg, S. Dapprich, A. D. Daniels, Ö. Farkas, J. B. Foresman, J. V. Ortiz, J. Cioslowski and D. J. Fox, Gaussian, Inc., Wallingford CT, 2009.

26 a) J. Tomasi, B. Mennucci and R. Cammi, *Chem. Rev.,* 2005, **105**, 2999-3093; b) G. Scalmani and M. J. Frisch, *J. Chem. Phys.,* 2010, **132**, 114110-114115.

Copies of the NMR spectra

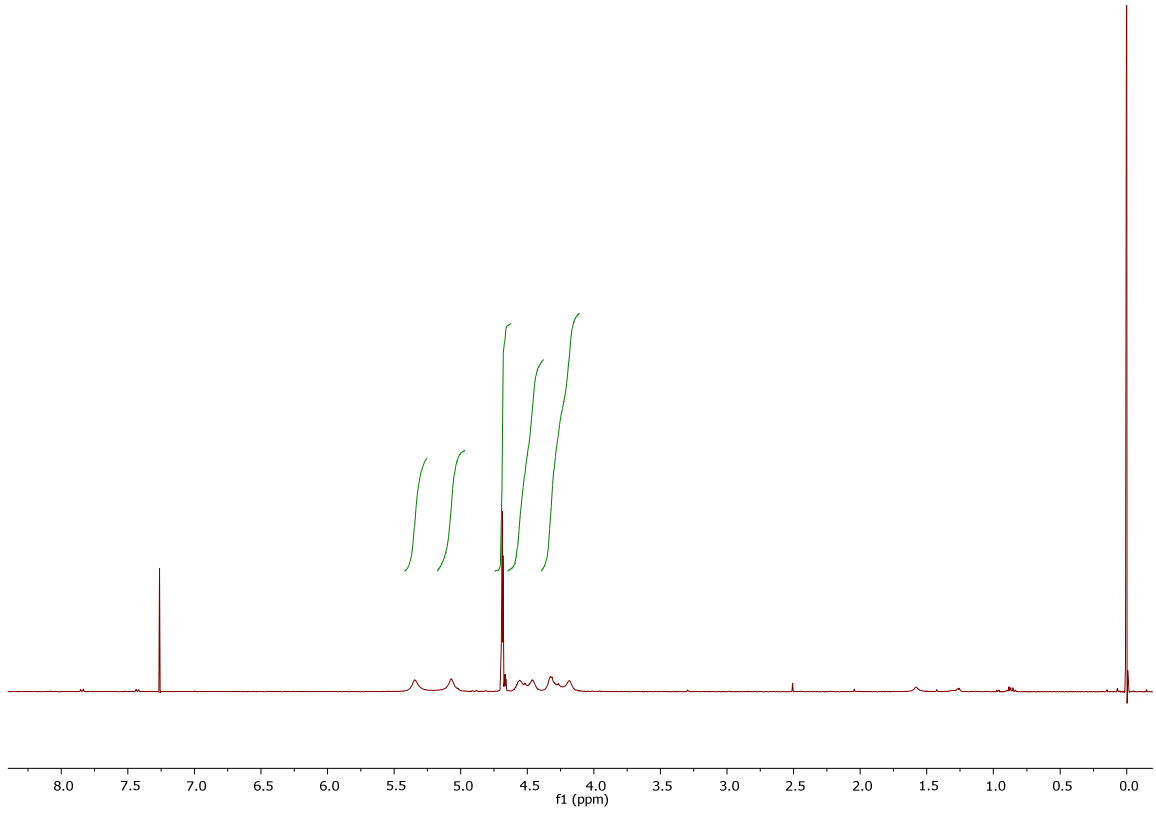

Figure S11. ^{1}H NMR spectrum (400 MHz, $CDCl_3$) of **4**

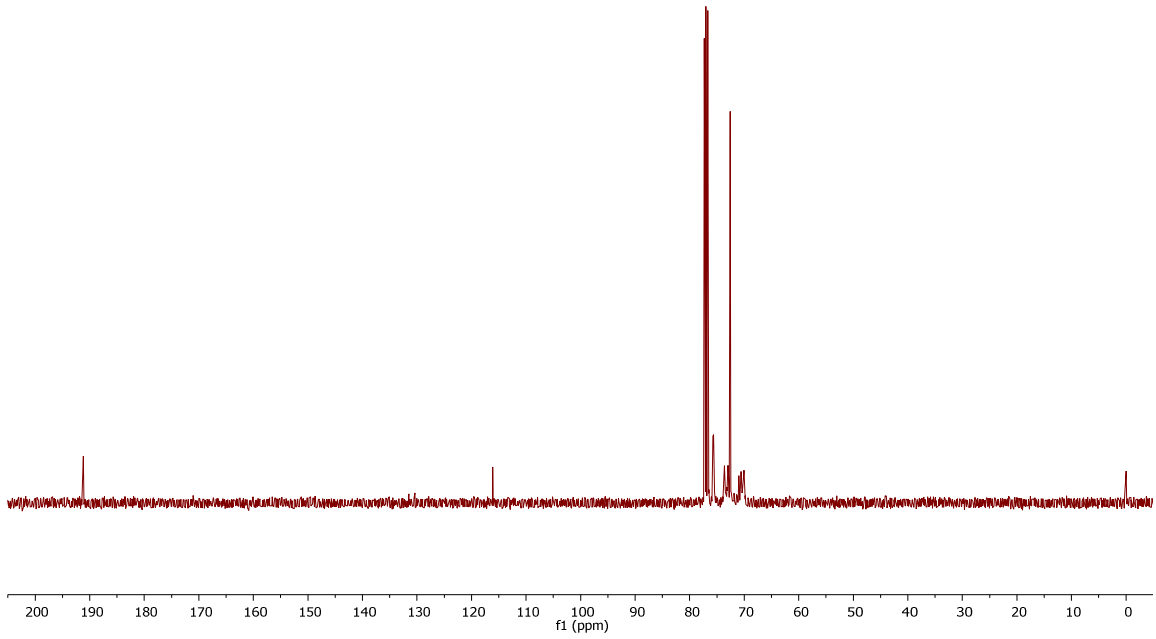

Figure S12. $^{13}C\{^{1}H\}$ NMR spectrum (101 MHz, $CDCl_3$) of **4**

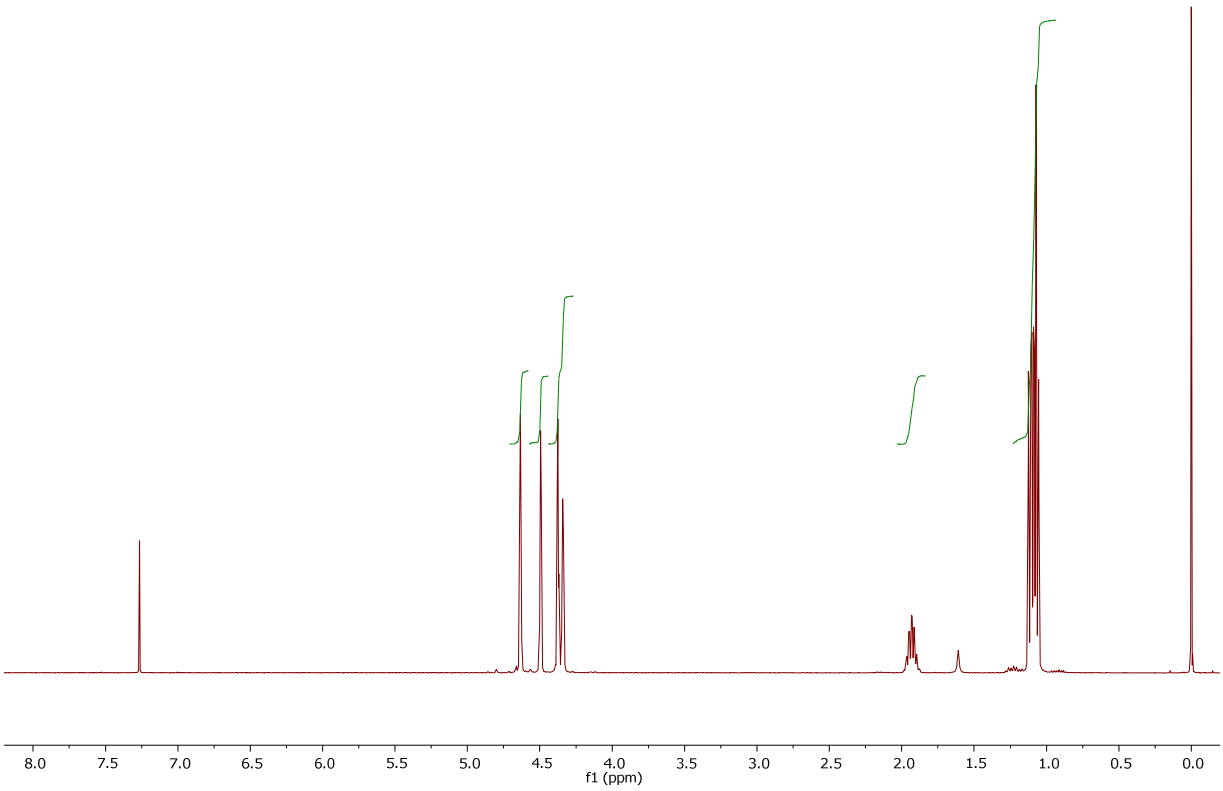

Figure S13. ^{1}H NMR spectrum (400 MHz, $CDCl_3$) of **1a**

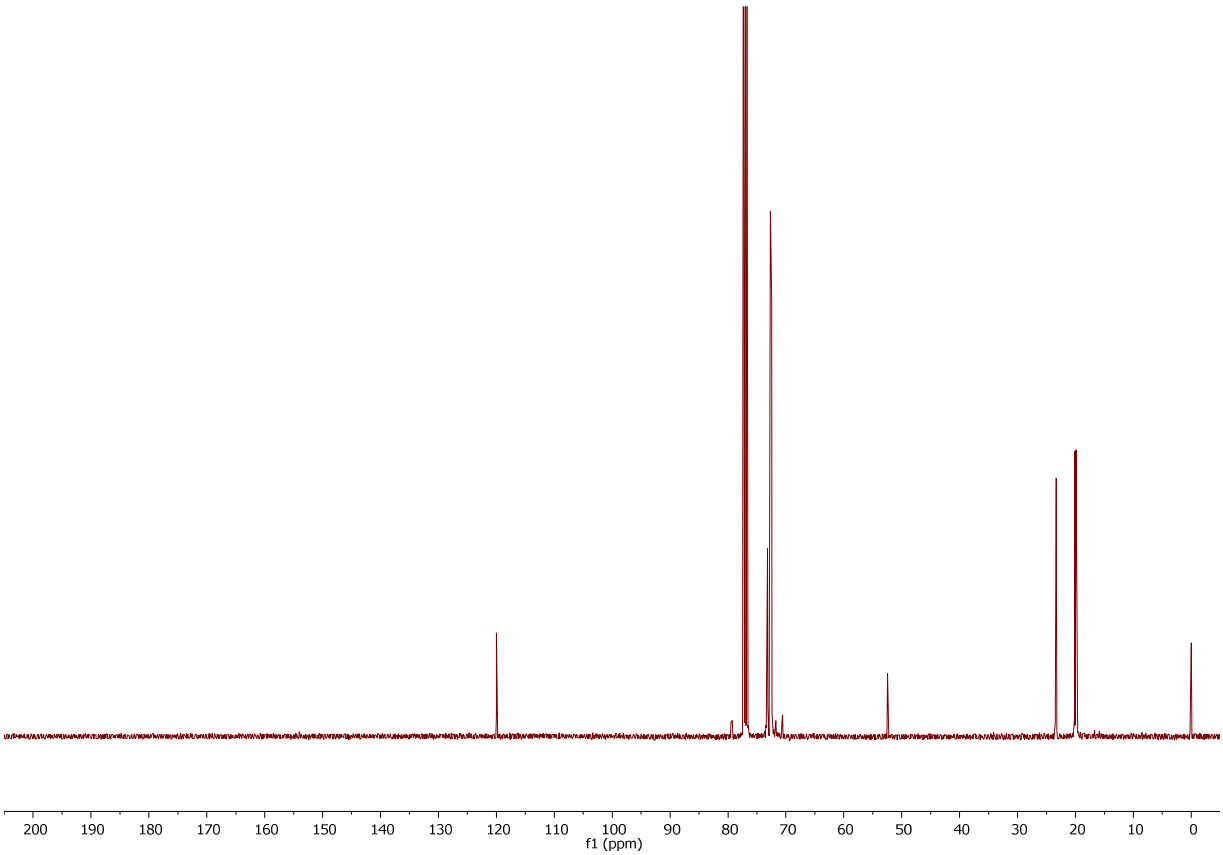

Figure S14. $^{13}C\{^{1}H\}$ NMR spectrum (101 MHz, $CDCl_3$) of **1a**

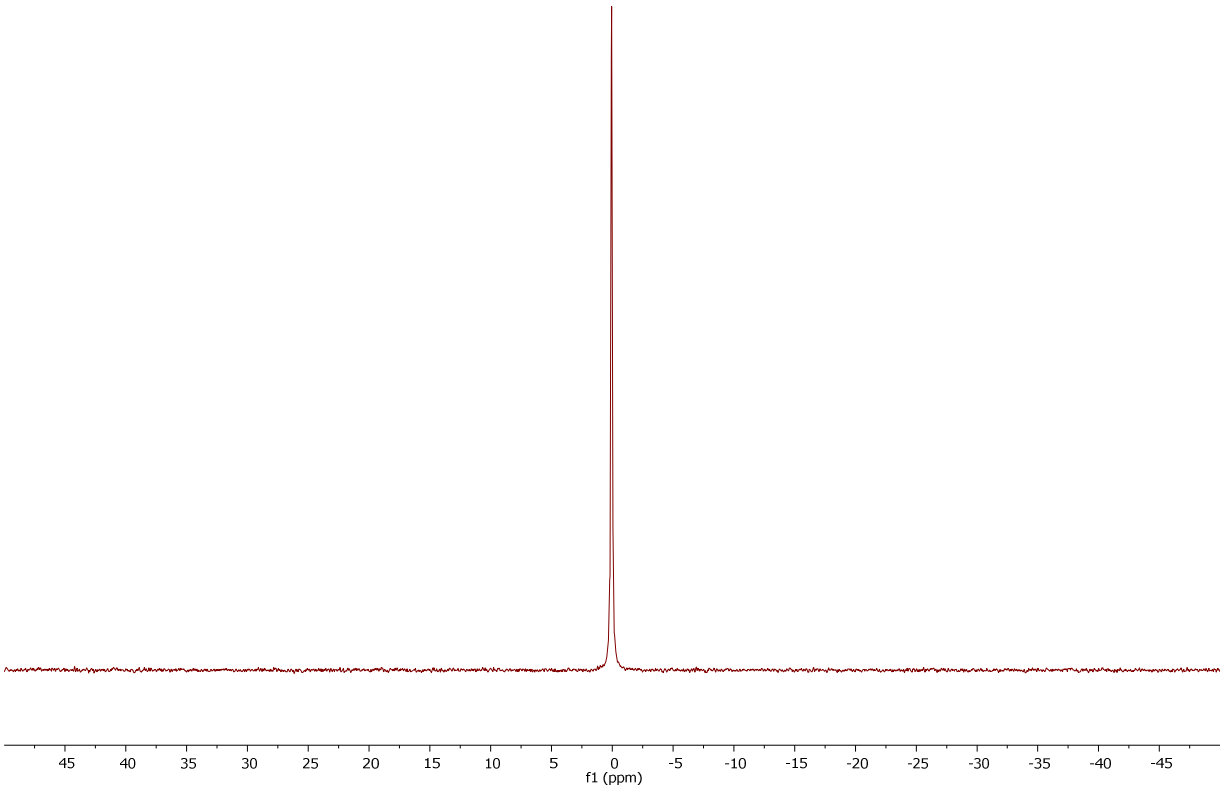

Figure S15. $^{31}P\{^{1}H\}$ NMR spectrum (162 MHz, $CDCl_3$) of **1a**

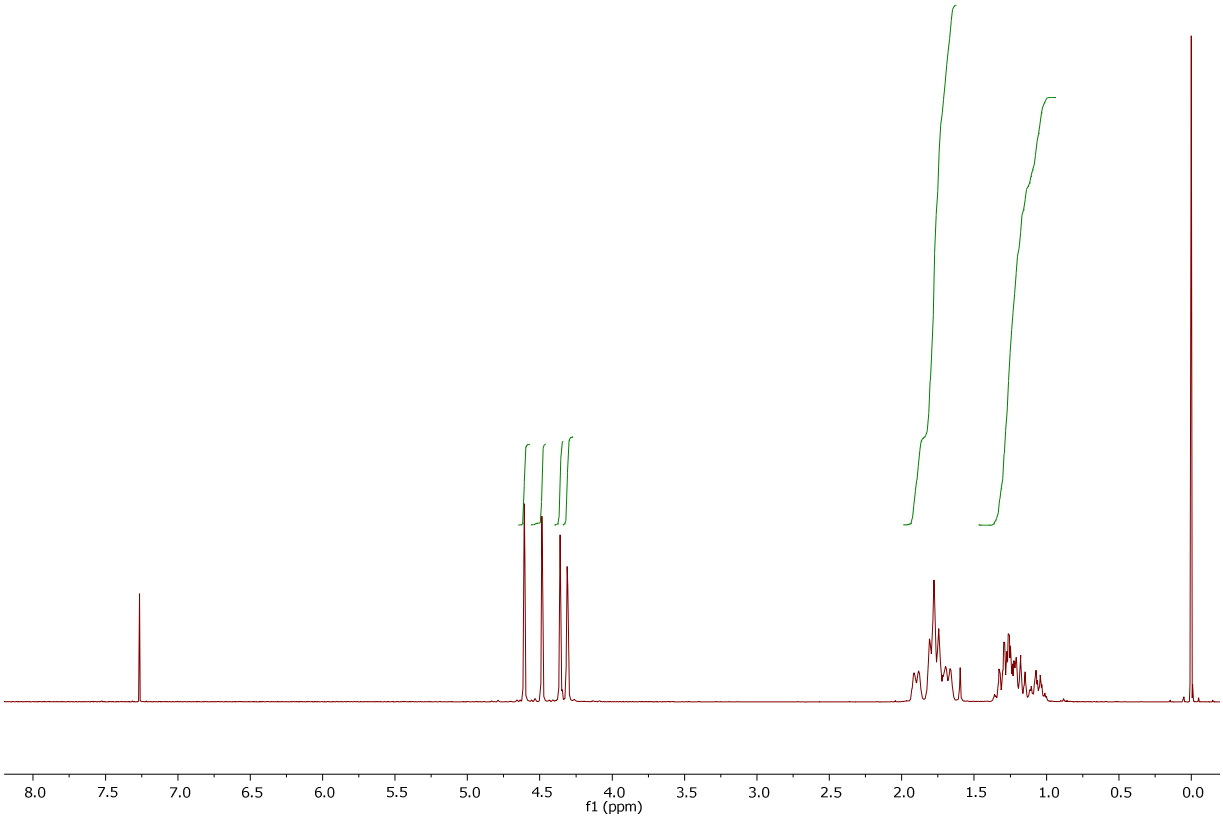

Figure S16. ^{1}H NMR spectrum (400 MHz, $CDCl_3$) of **1b**

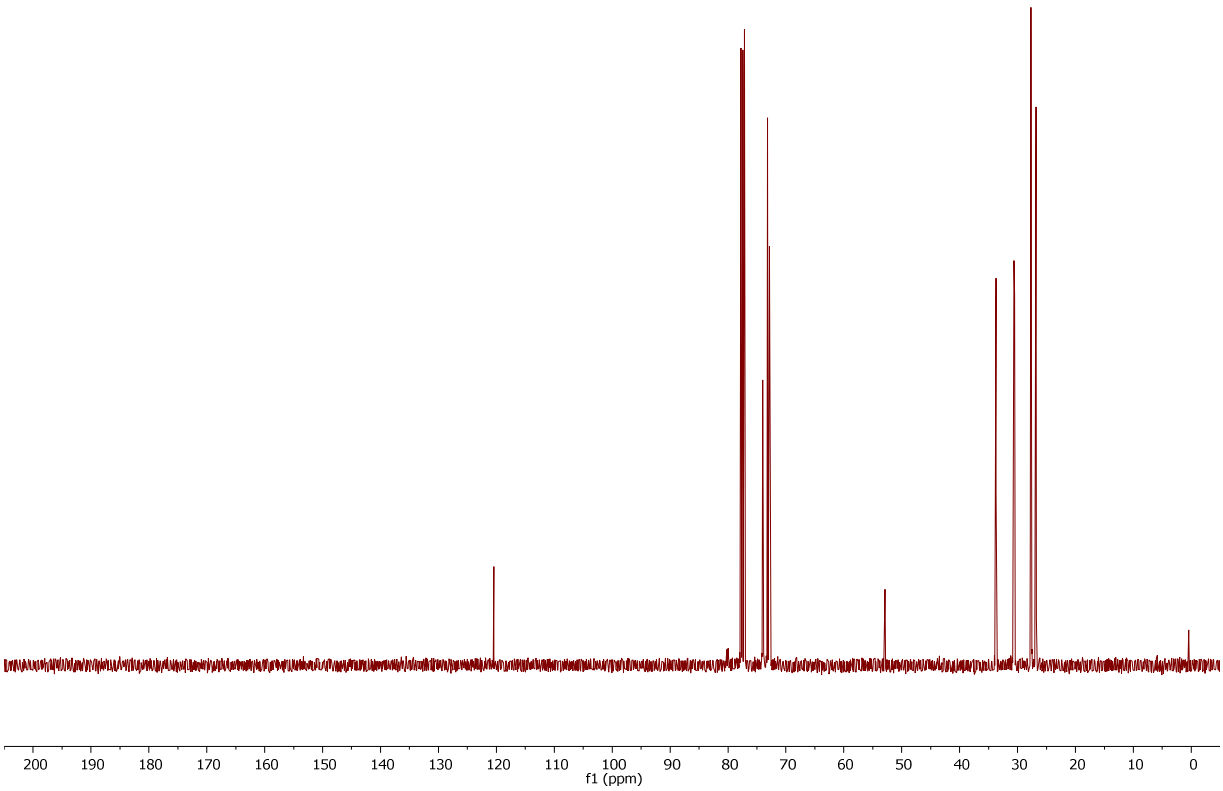

Figure S17. $^{13}C\{^{1}H\}$ NMR spectrum (101 MHz, $CDCl_3$) of **1b**

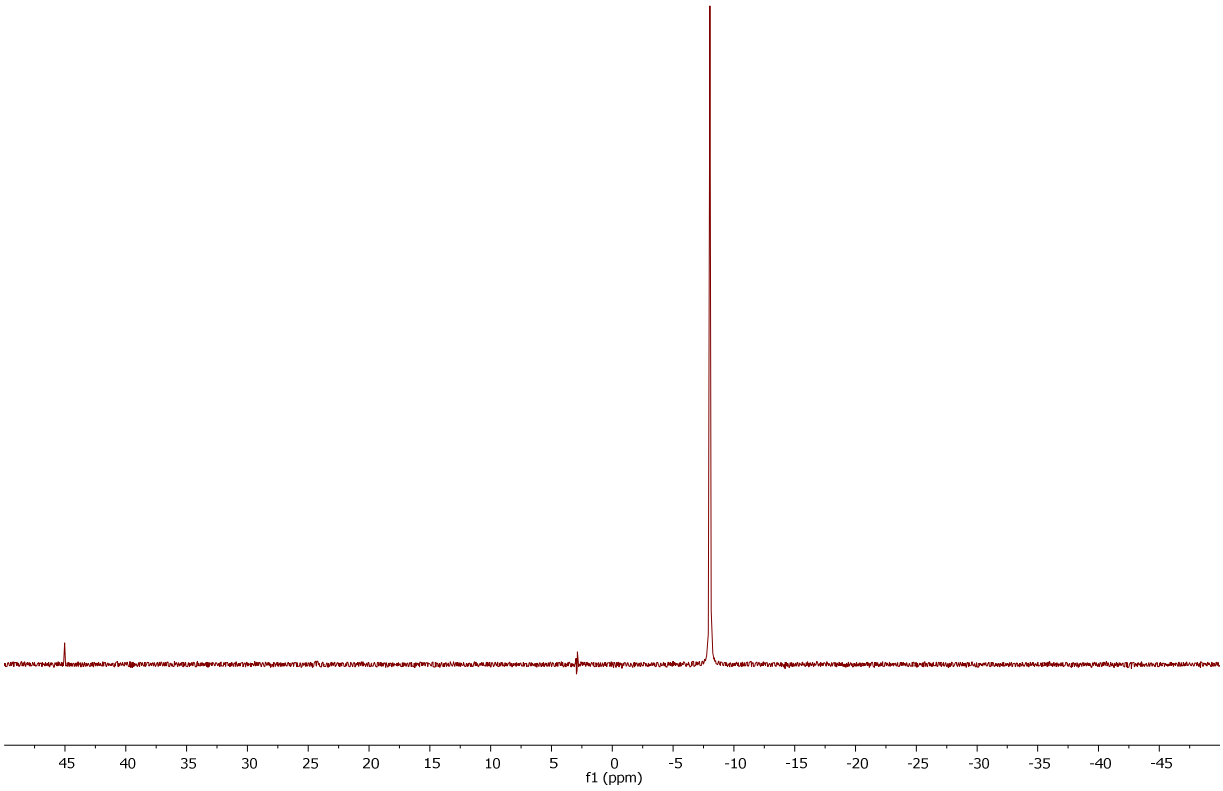

Figure S18. $^{31}P\{^{1}H\}$ NMR spectrum (162 MHz, $CDCl_3$) of **1b**

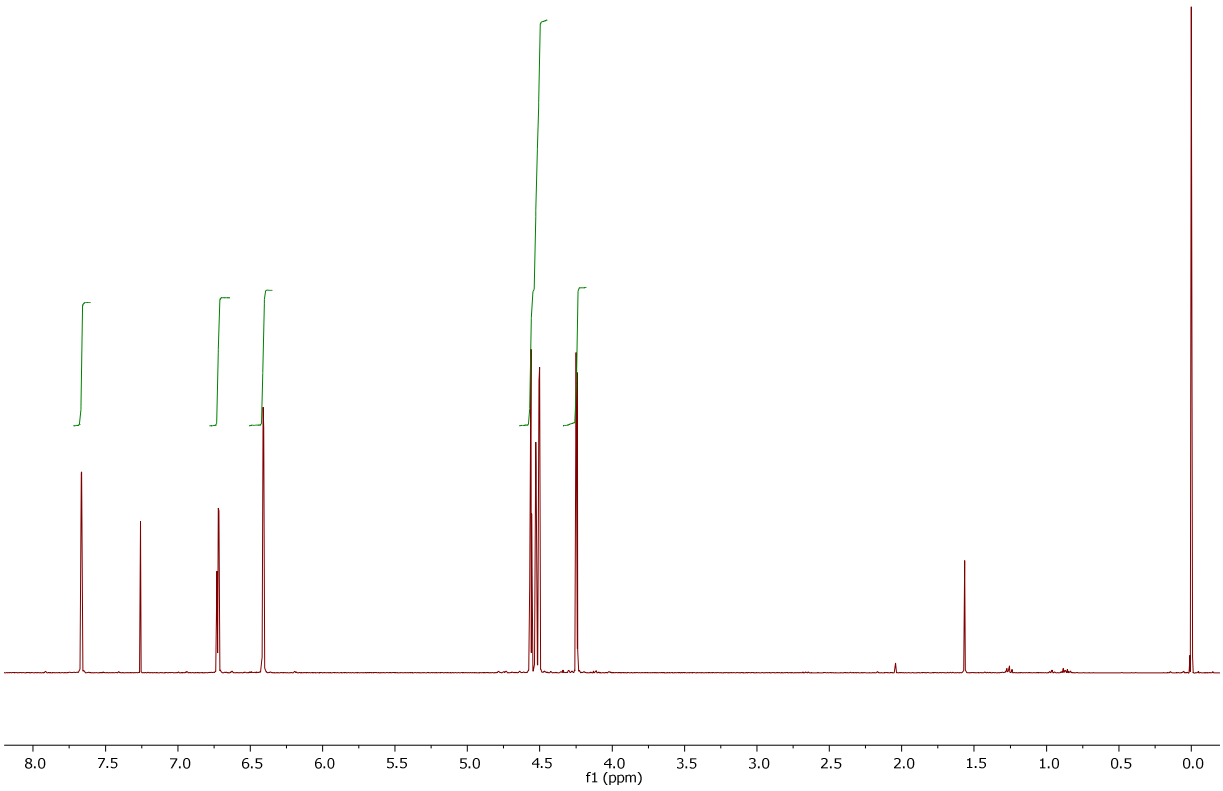

Figure S19. ^{1}H NMR spectrum (400 MHz, $CDCl_3$) of **1d**

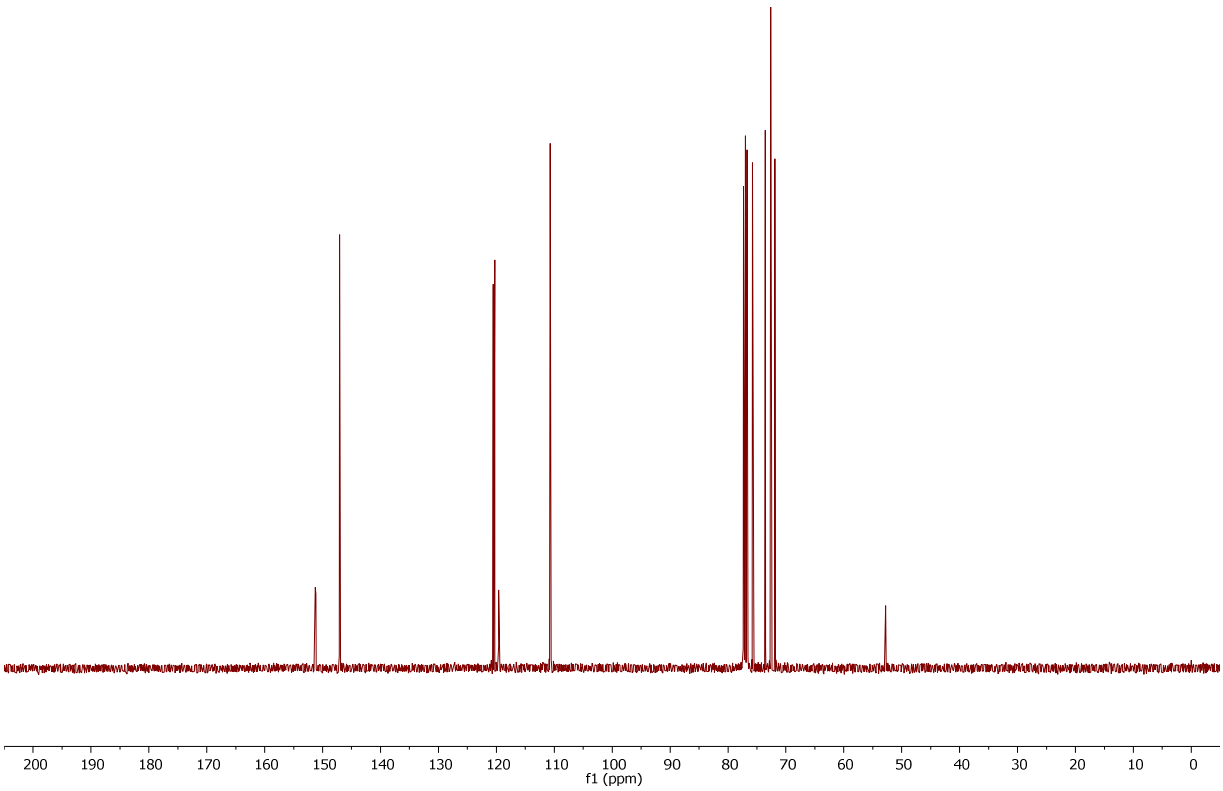

Figure S20. $^{13}C\{^{1}H\}$ NMR spectrum (101 MHz, $CDCl_3$) of **1d**

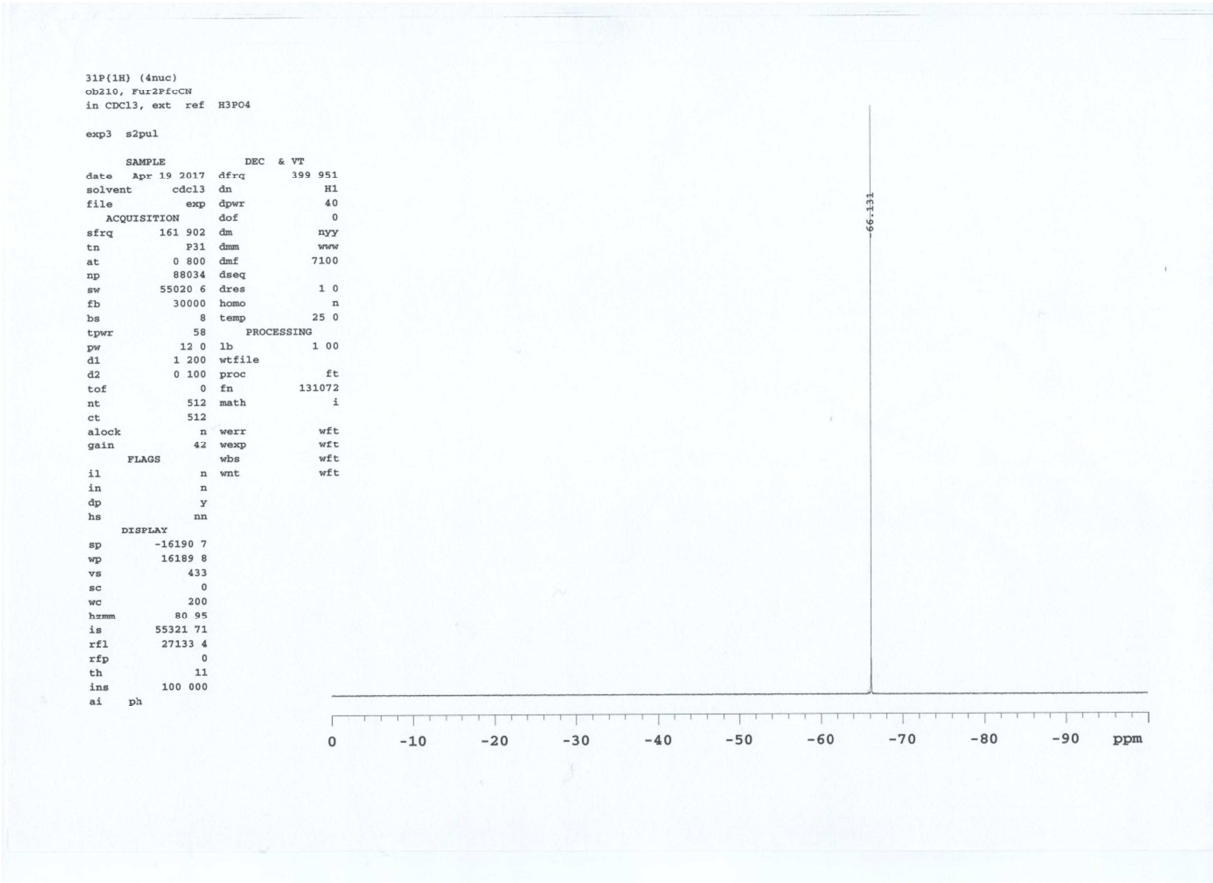

Figure S21. $^{31}P\{^{1}H\}$ NMR spectrum (162 MHz, $CDCl_3$) of **1d**

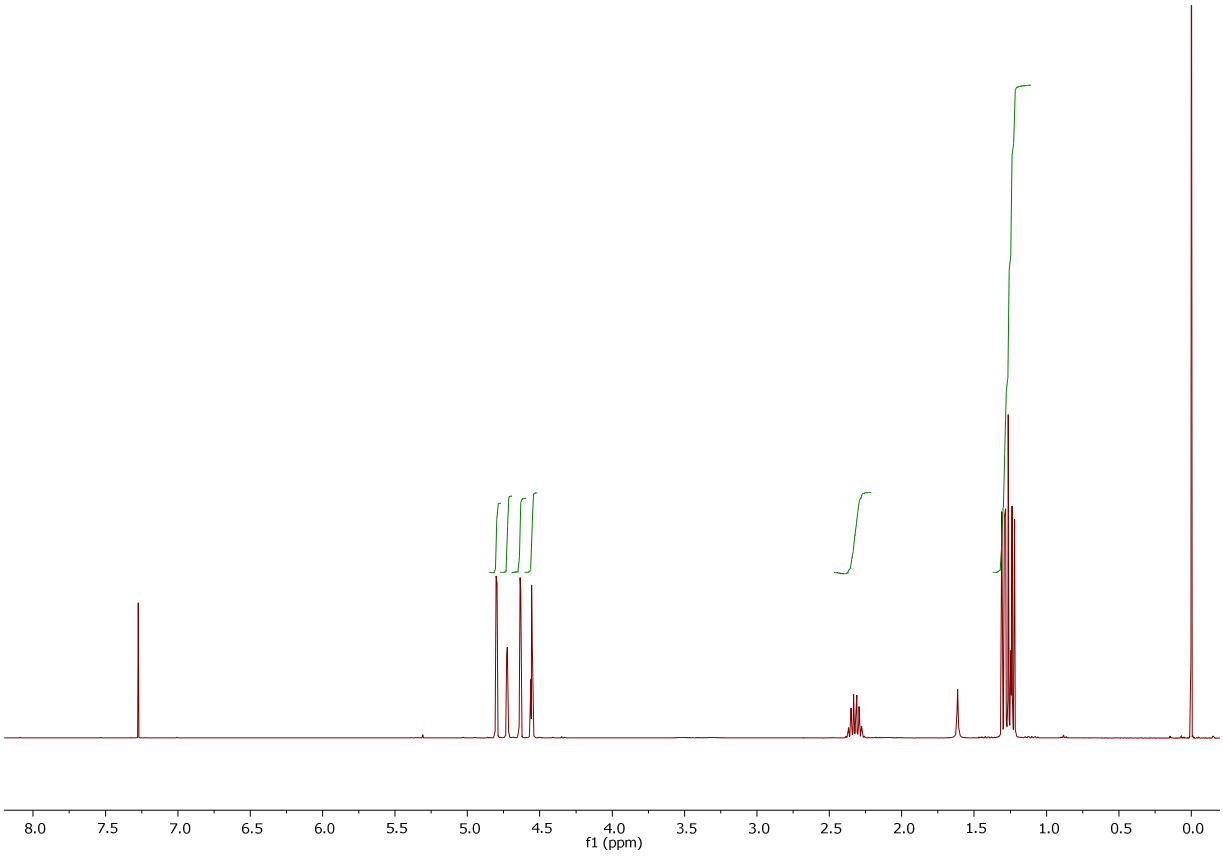

Figure S22. ^{1}H NMR spectrum (400 MHz, $CDCl_3$) of **5a**

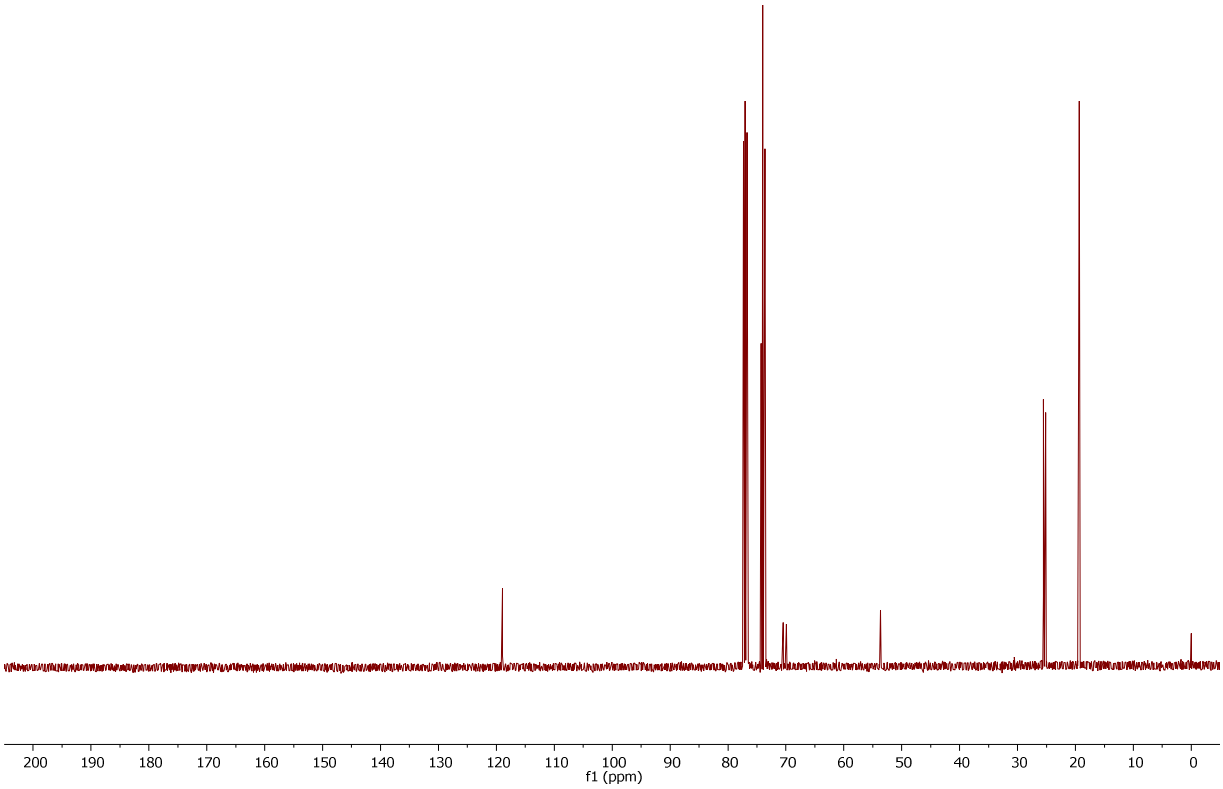

Figure S23. $^{13}C\{^{1}H\}$ NMR spectrum (101 MHz, $CDCl_3$) of **5a**

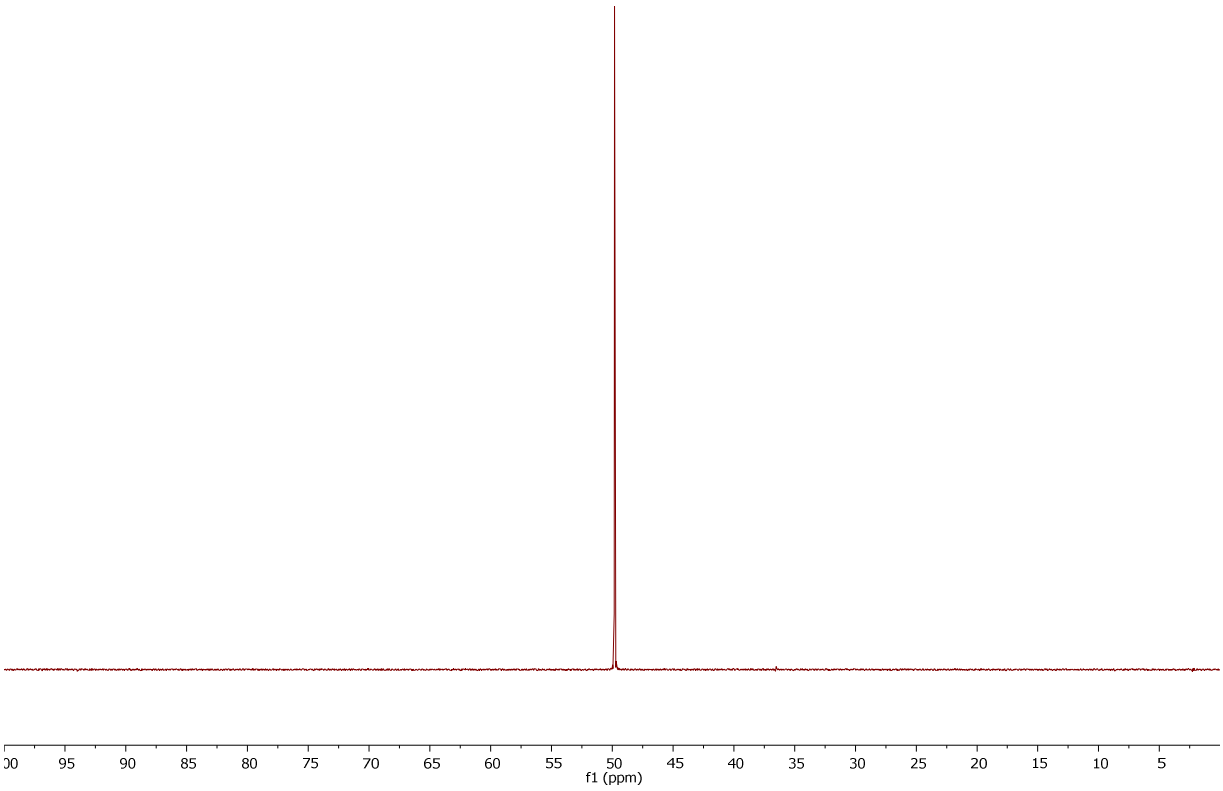

Figure S24. $^{31}P\{^{1}H\}$ NMR spectrum (162 MHz, $CDCl_3$) of **5a**

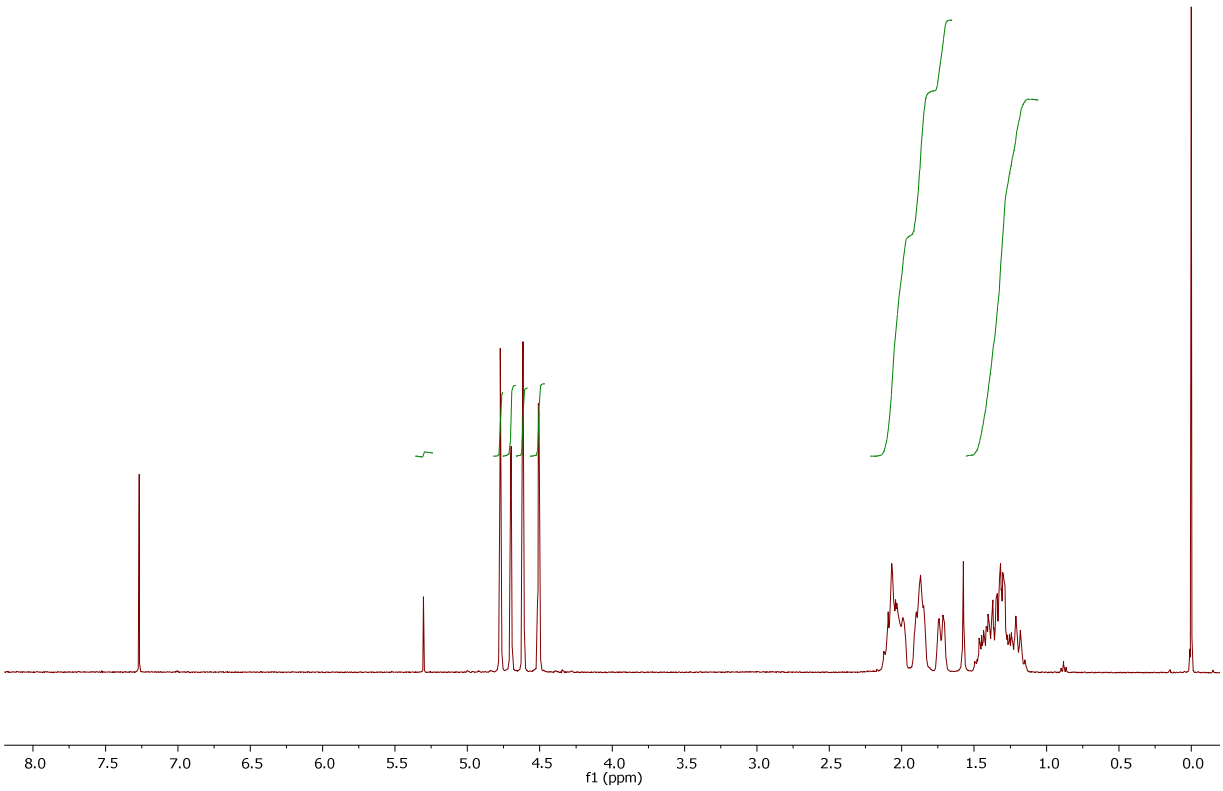

Figure S25. ^{1}H NMR spectrum (400 MHz, $CDCl_3$) of **5b**

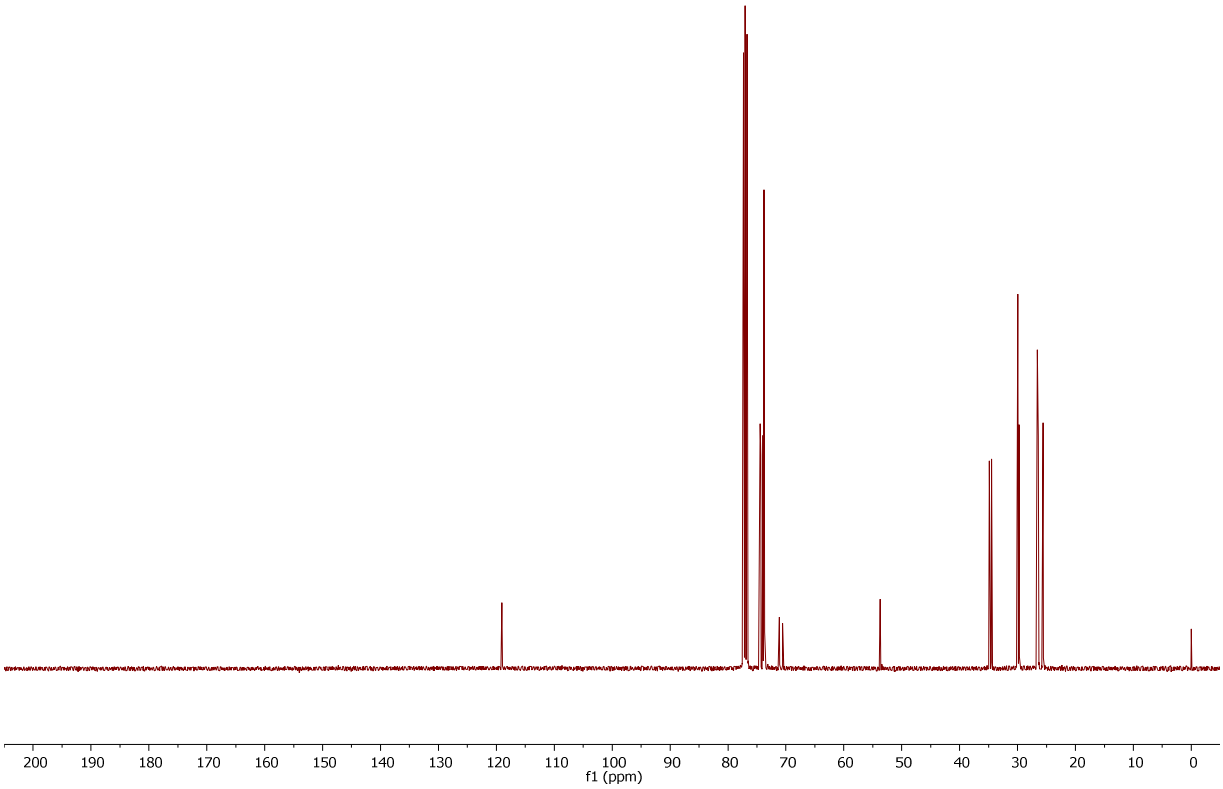

Figure S26. $^{13}C\{^{1}H\}$ NMR spectrum (101 MHz, $CDCl_3$) of **5b**

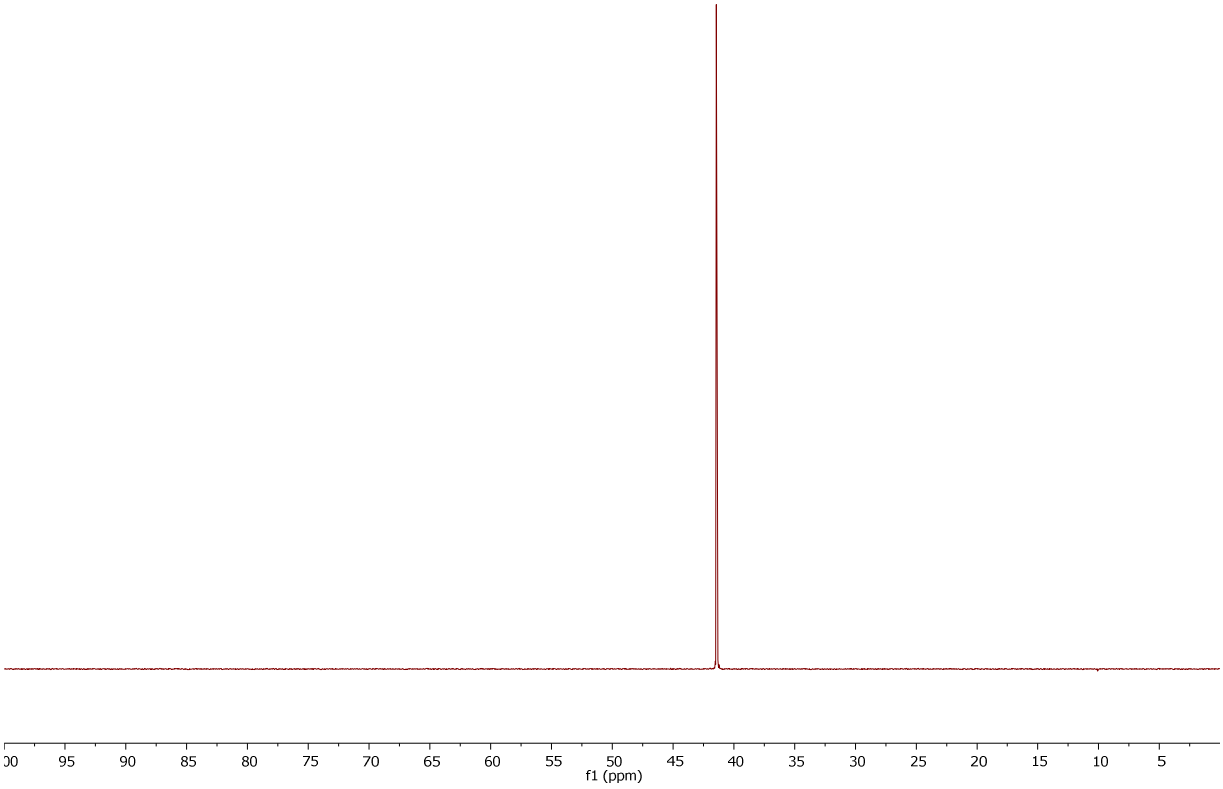

Figure S27. $^{31}P\{^{1}H\}$ NMR spectrum (162 MHz, $CDCl_3$) of **5b**

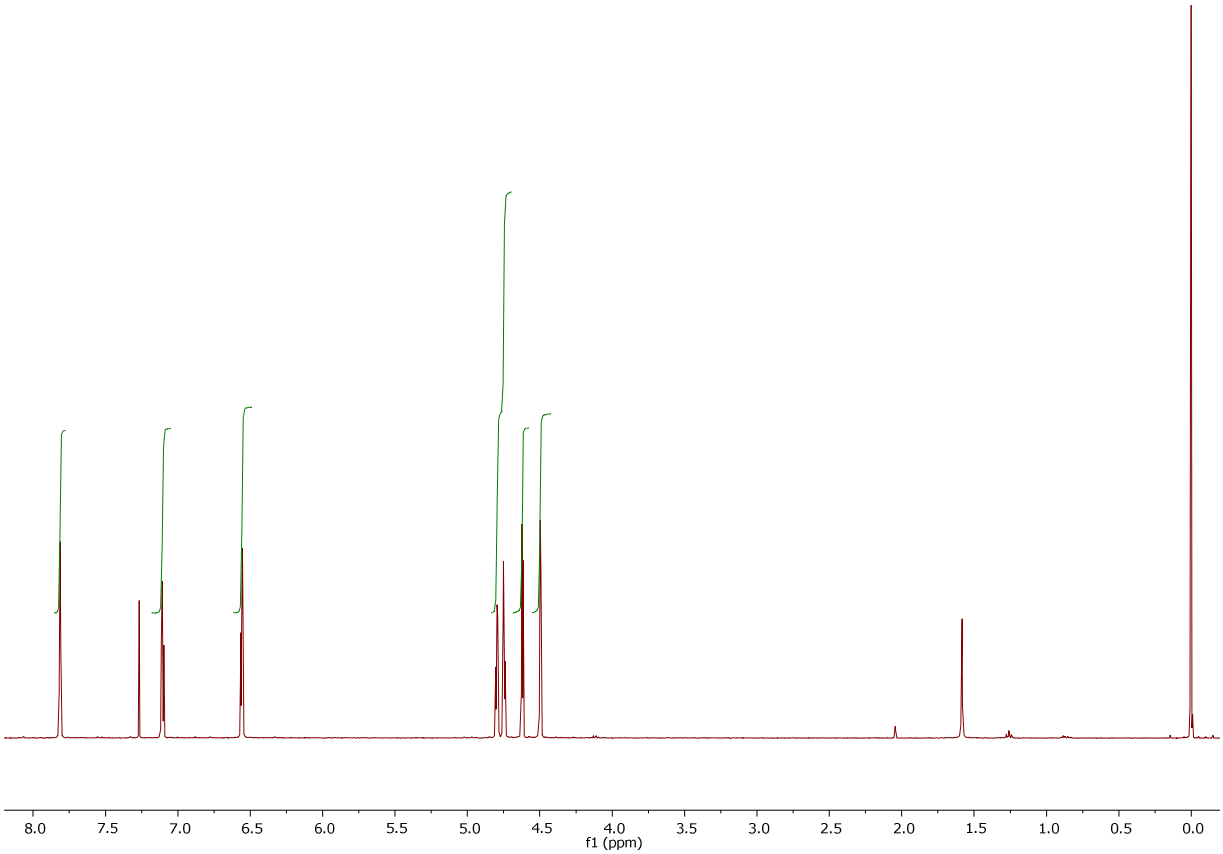

Figure S28. ^{1}H NMR spectrum (400 MHz, $CDCl_3$) of **5d**

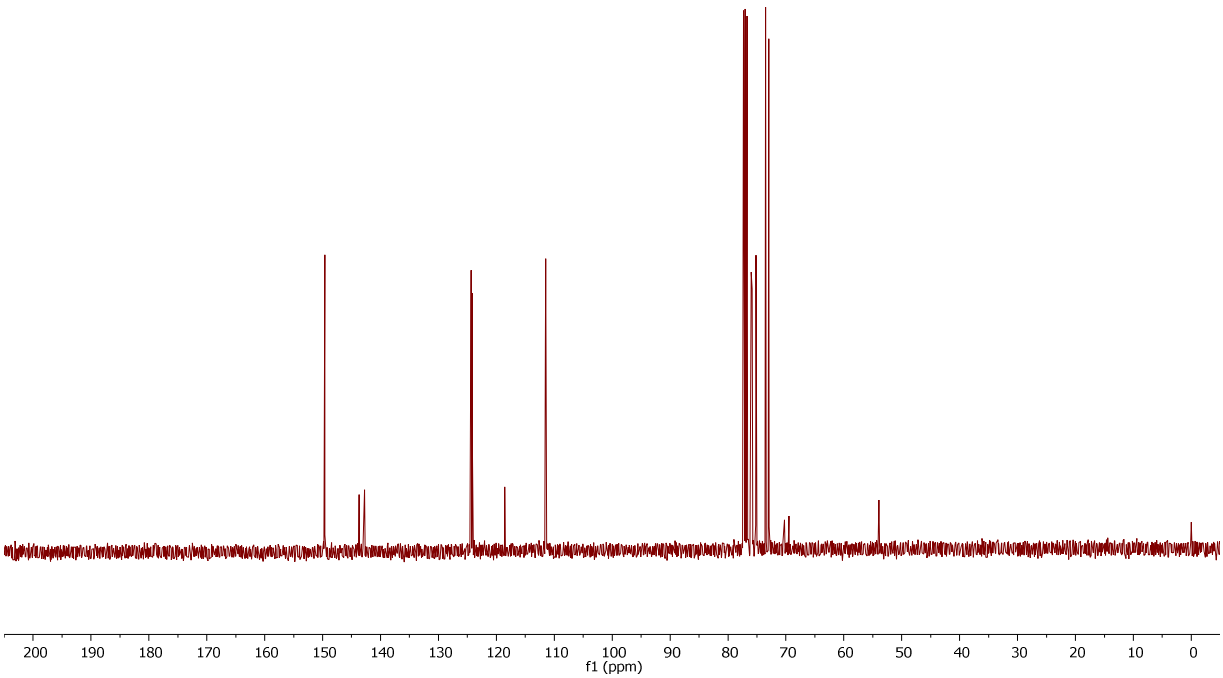

Figure S29. $^{13}C\{^{1}H\}$ NMR spectrum (101 MHz, $CDCl_3$) of **5d**

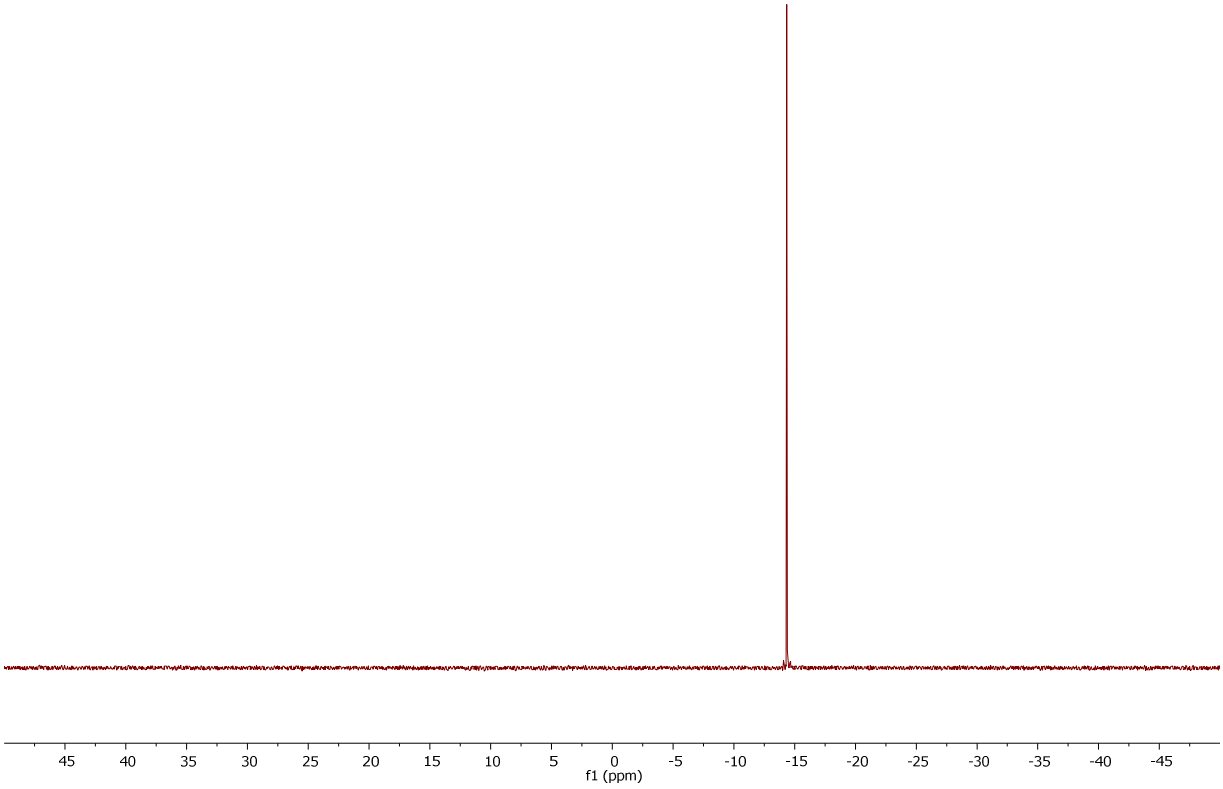

Figure S30. $^{31}P\{^{1}H\}$ NMR spectrum (162 MHz, $CDCl_3$) of **5d**

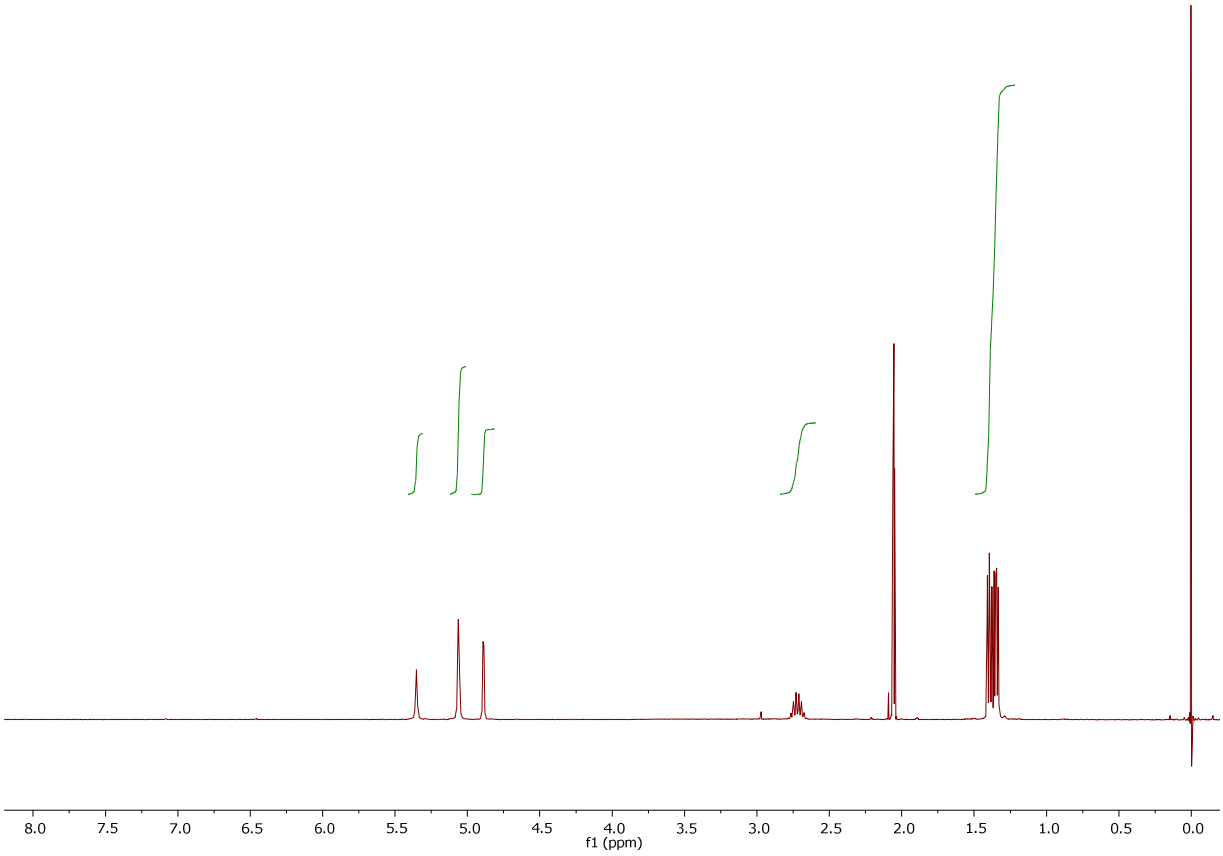

Figure S31. ^{1}H NMR spectrum (400 MHz, acetone-d_6) of **6a**

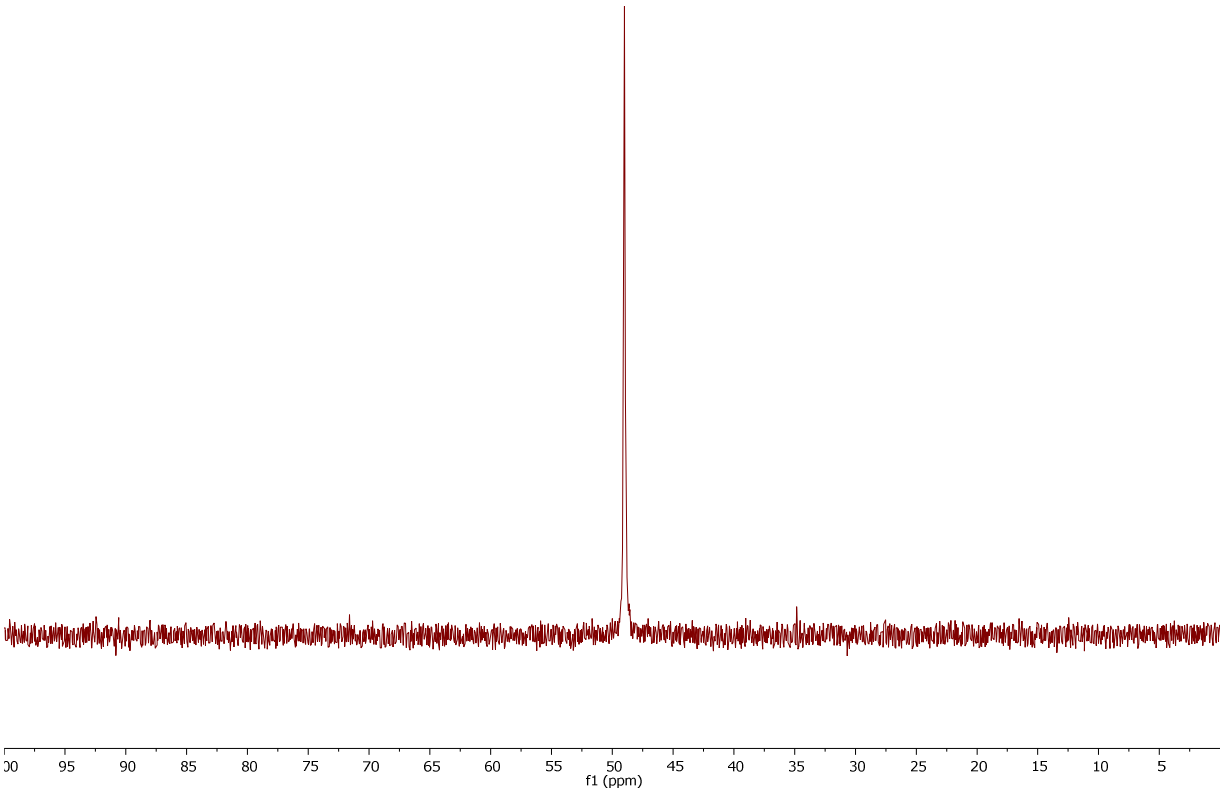

Figure S32. $^{31}P\{^{1}H\}$ NMR spectrum (162 MHz, acetone-d_6) of **6a**

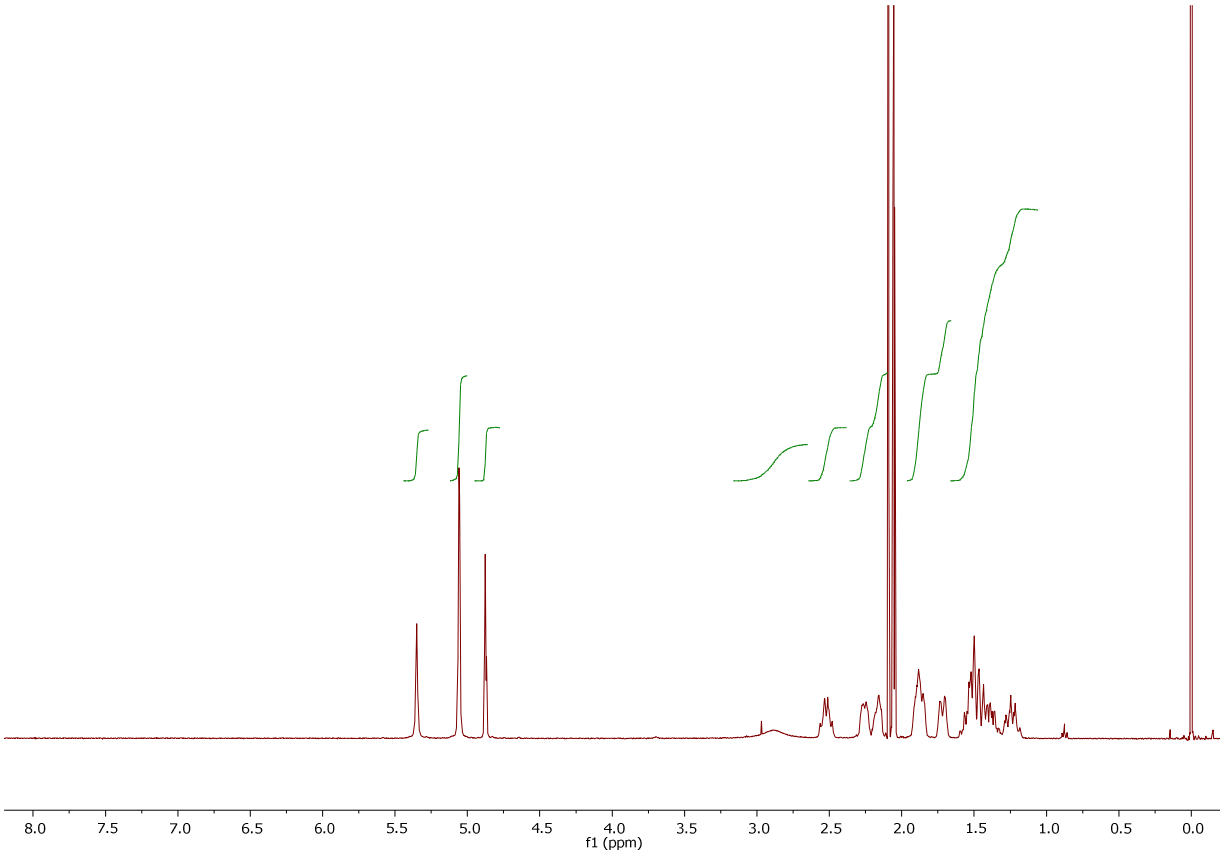

Figure S33. ^{1}H NMR spectrum (400 MHz, acetone-d_6) of **6b**

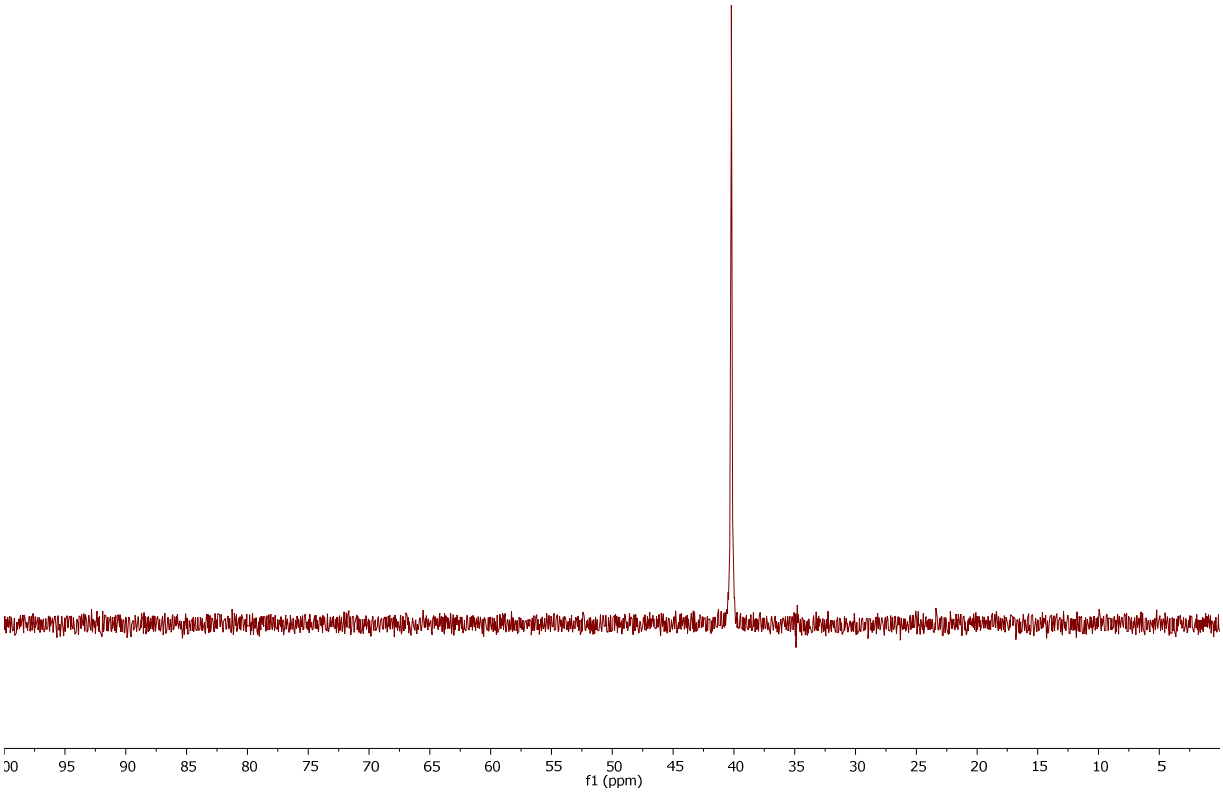

Figure S34. $^{31}P\{^{1}H\}$ NMR spectrum (162 MHz, acetone-d_6) of **6b**

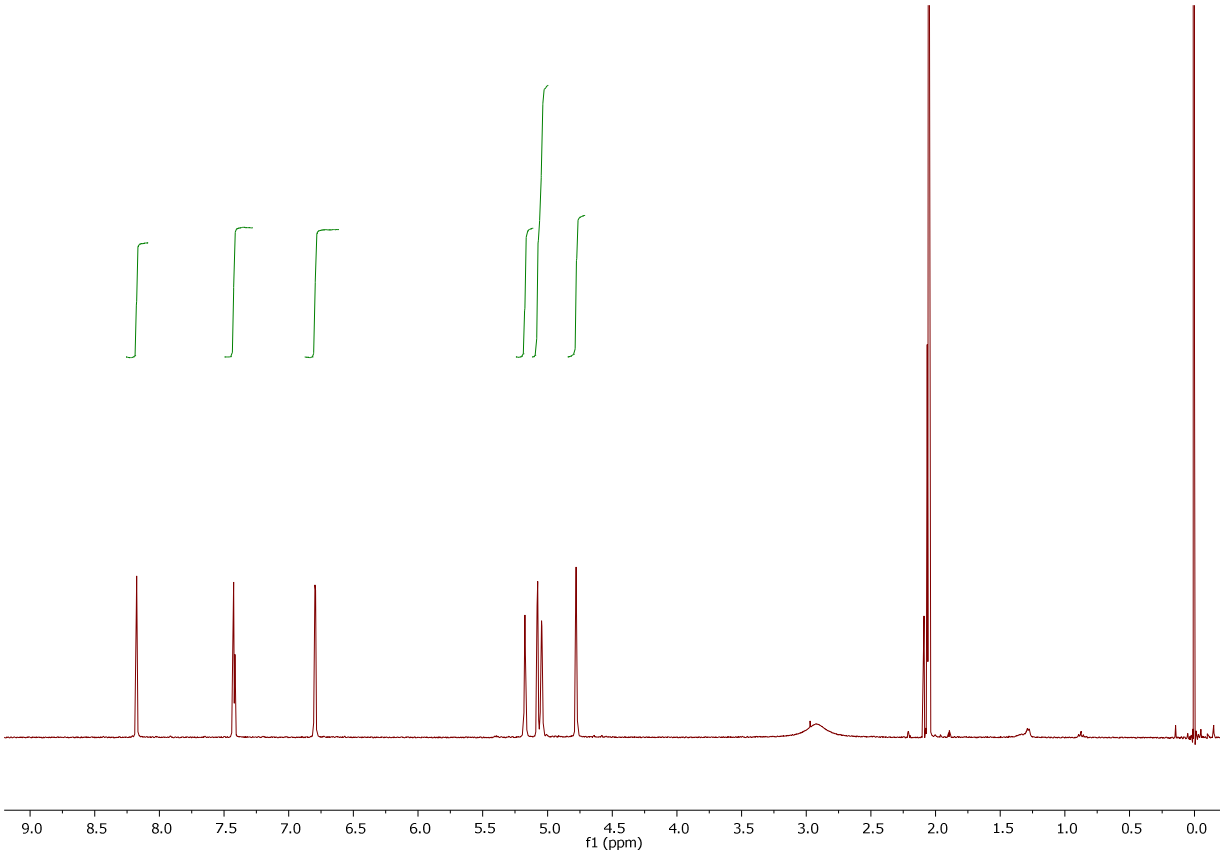

Figure S35. ^{1}H NMR spectrum (400 MHz, acetone-d_6) of **6d**

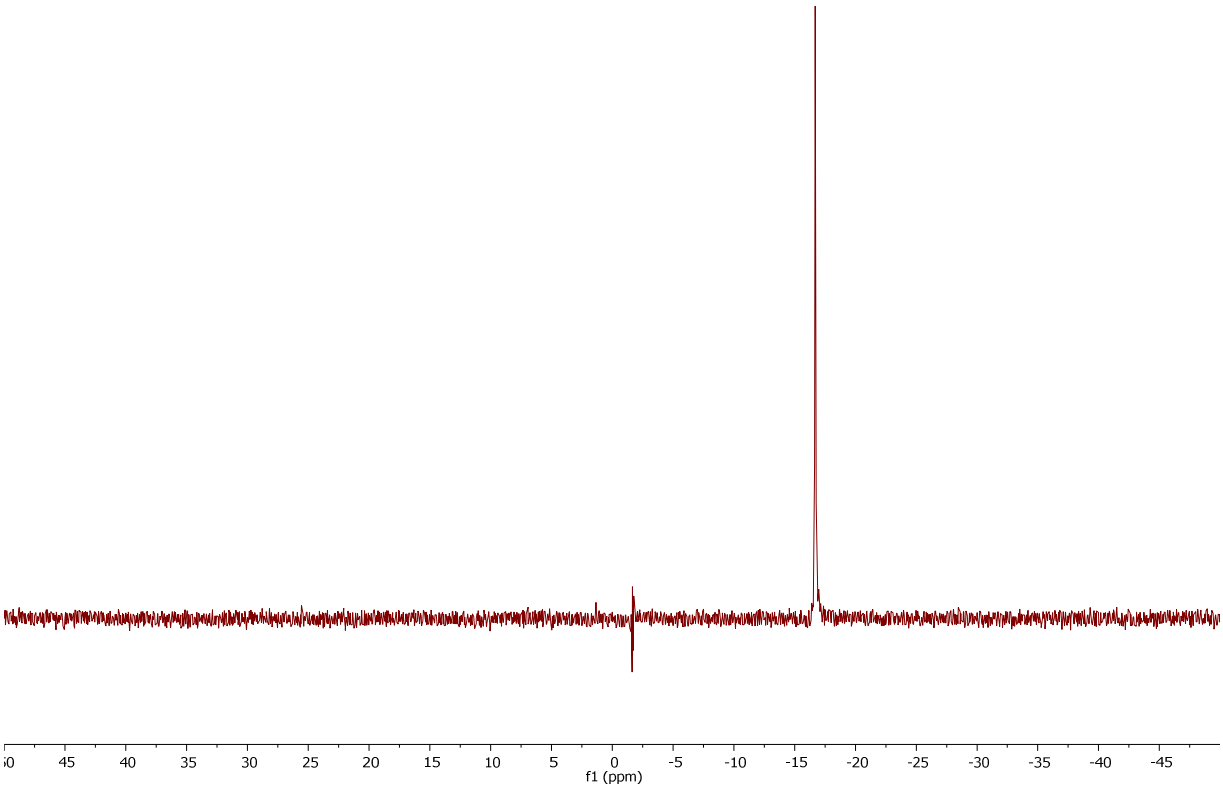

Figure S36. $^{31}P\{^{1}H\}$ NMR spectrum (162 MHz, acetone-d_6) of **6d**

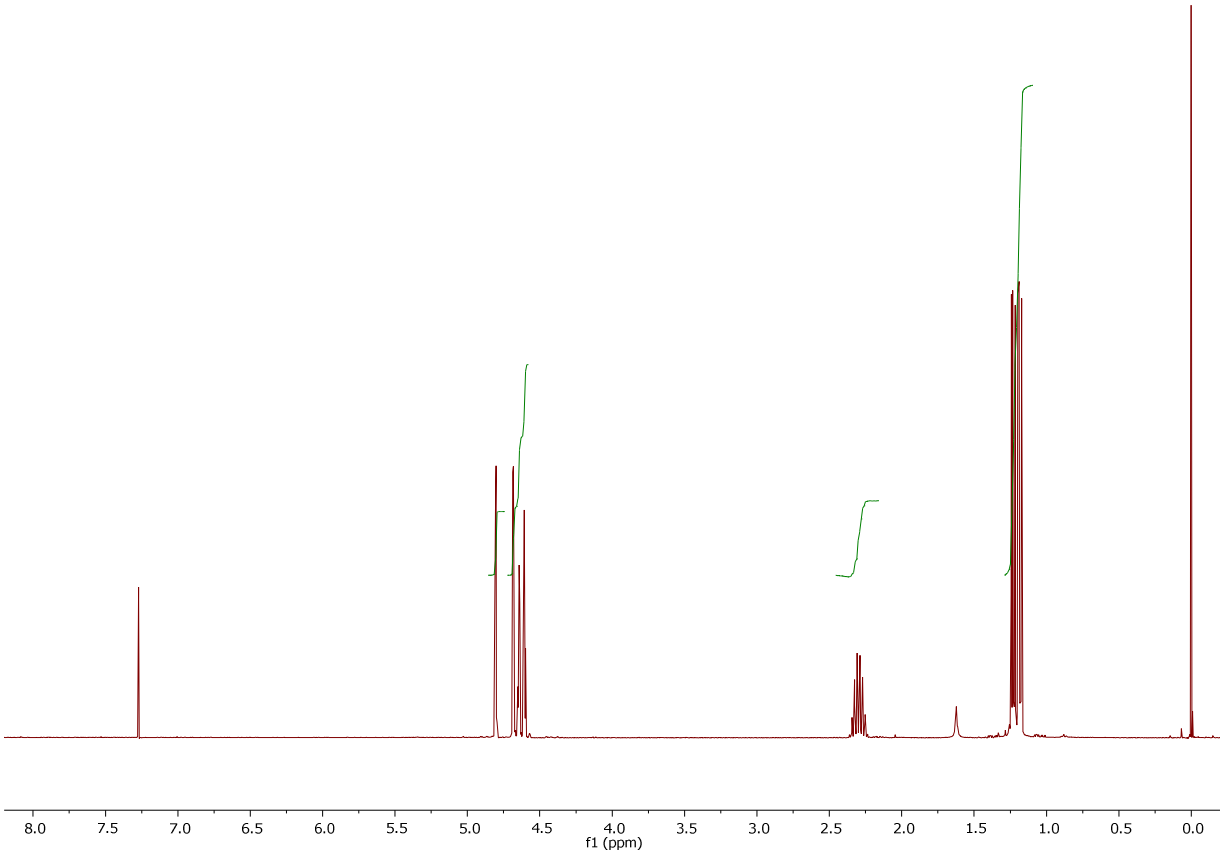

Figure S37. ^{1}H NMR spectrum (400 MHz, $CDCl_3$) of **7a**

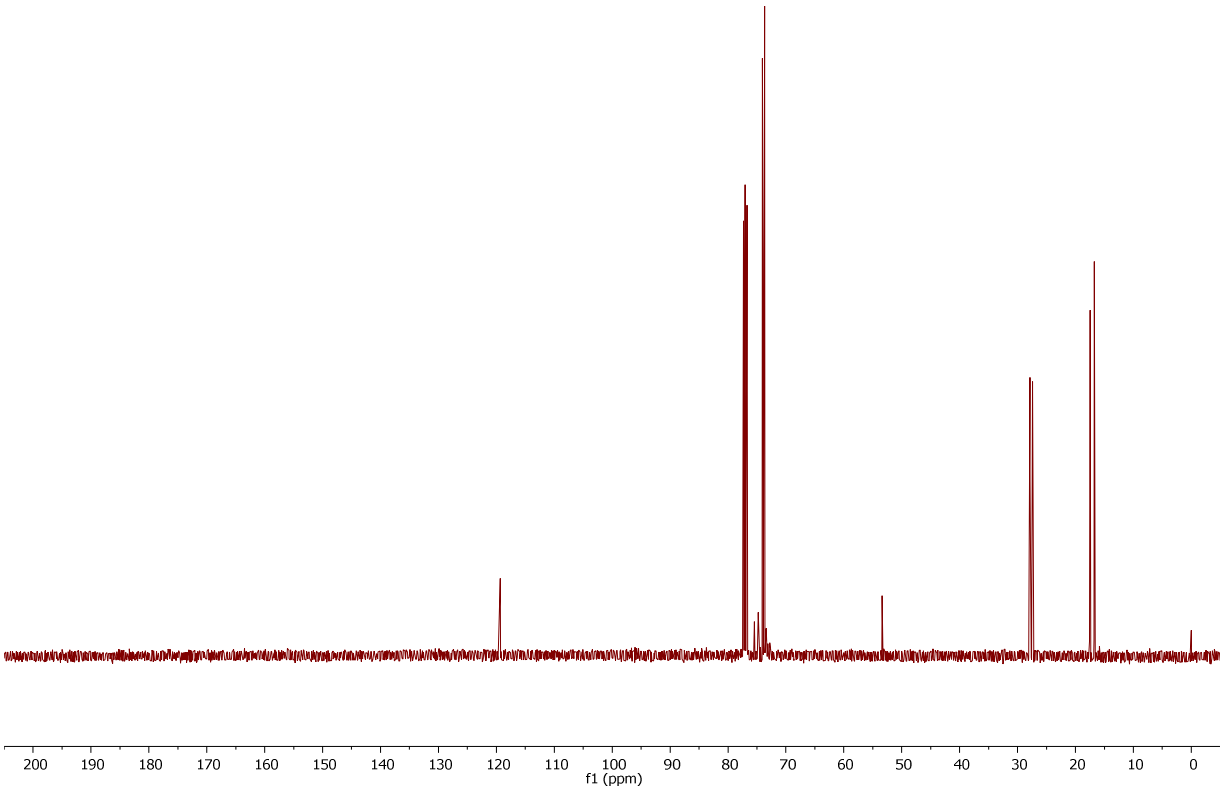

Figure S38. $^{13}C\{^{1}H\}$ NMR spectrum (101 MHz, $CDCl_3$) of **7a**

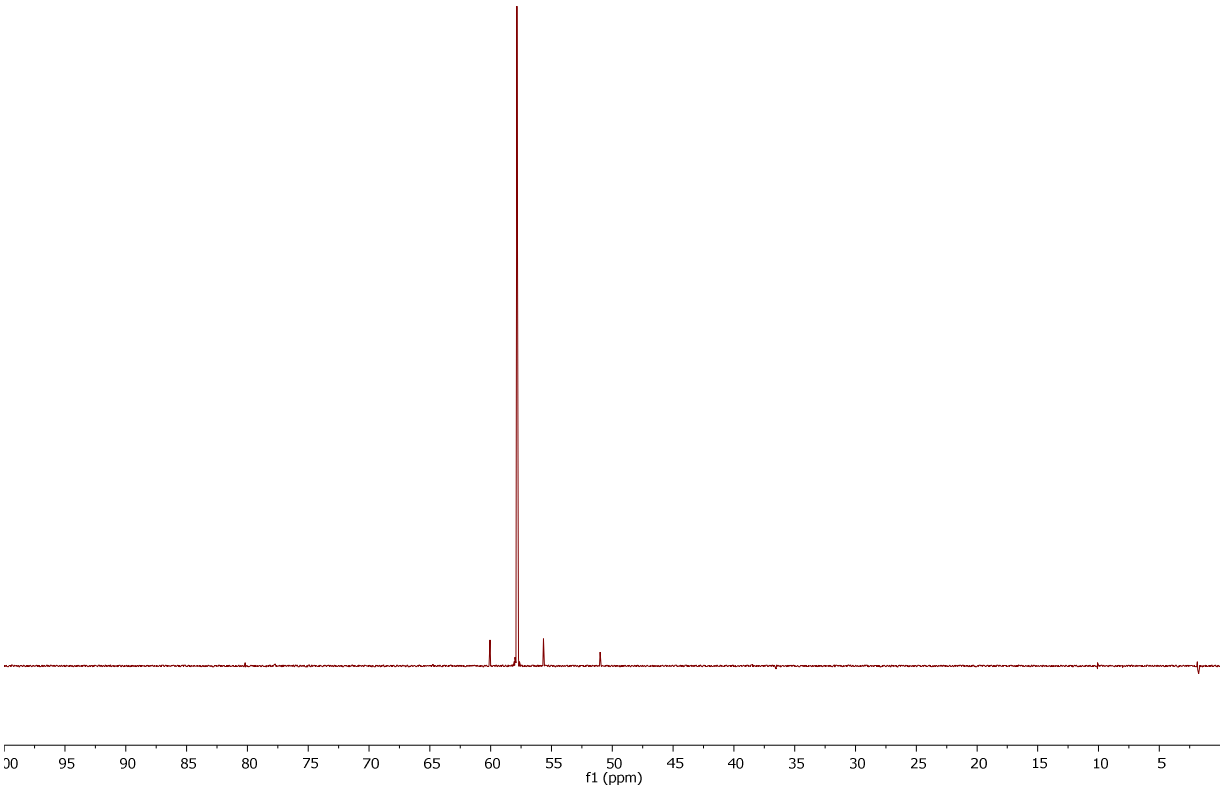

Figure S39. $^{31}P\{^{1}H\}$ NMR spectrum (162 MHz, $CDCl_3$) of **7a**

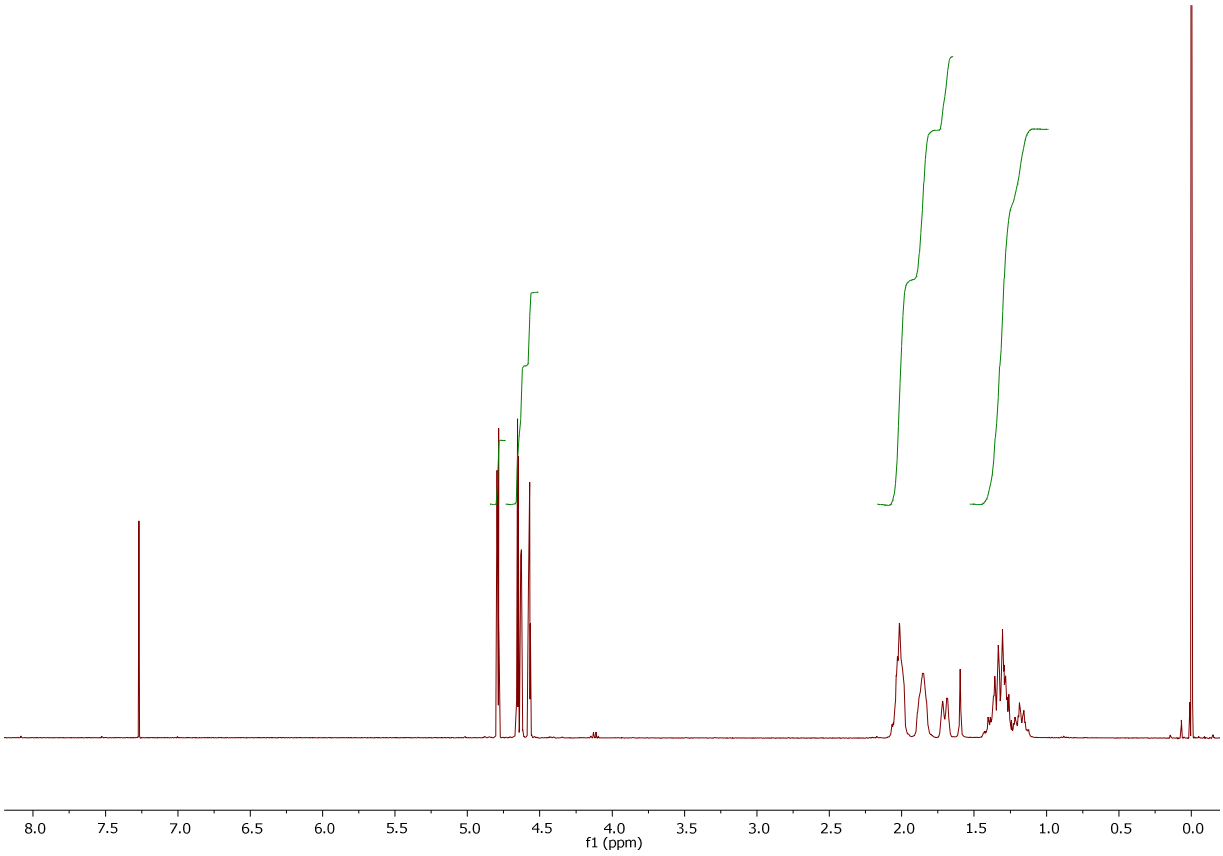

Figure S40. ^{1}H NMR spectrum (400 MHz, $CDCl_3$) of **7b**

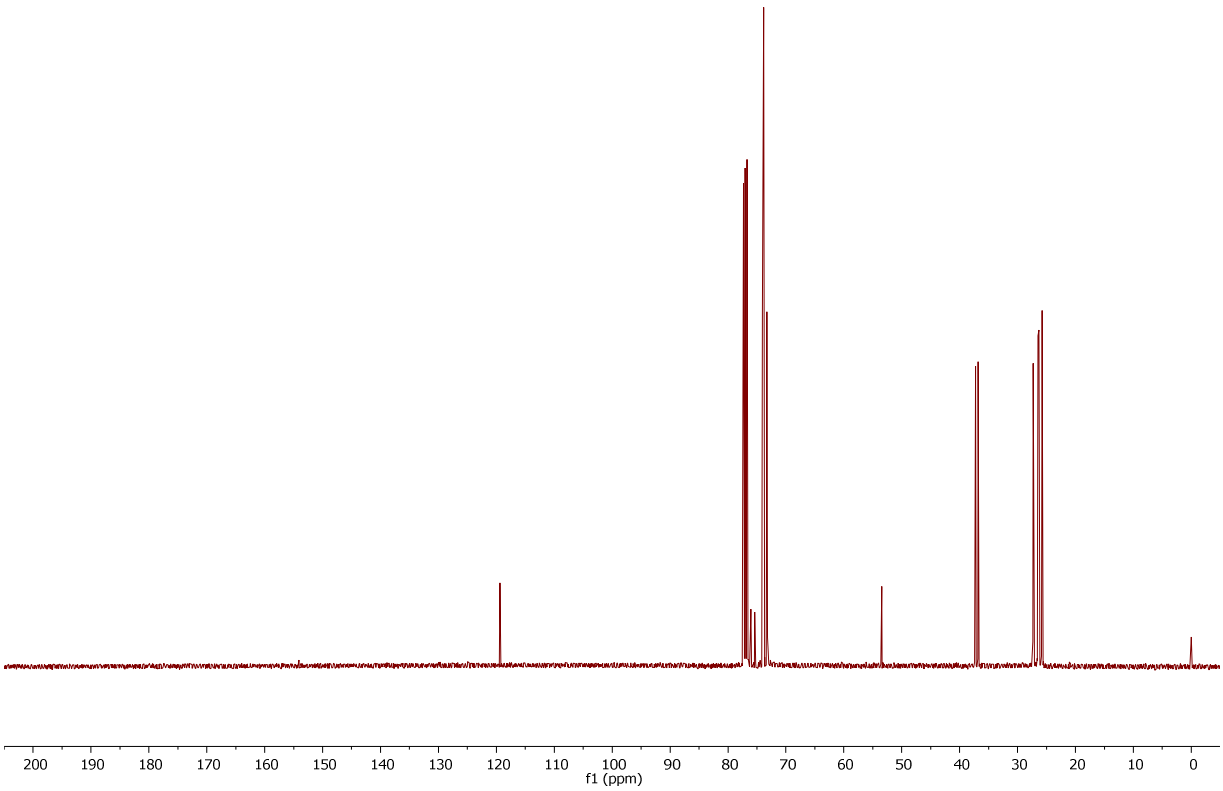

Figure S41. $^{13}C\{^{1}H\}$ NMR spectrum (101 MHz, $CDCl_3$) of **7b**

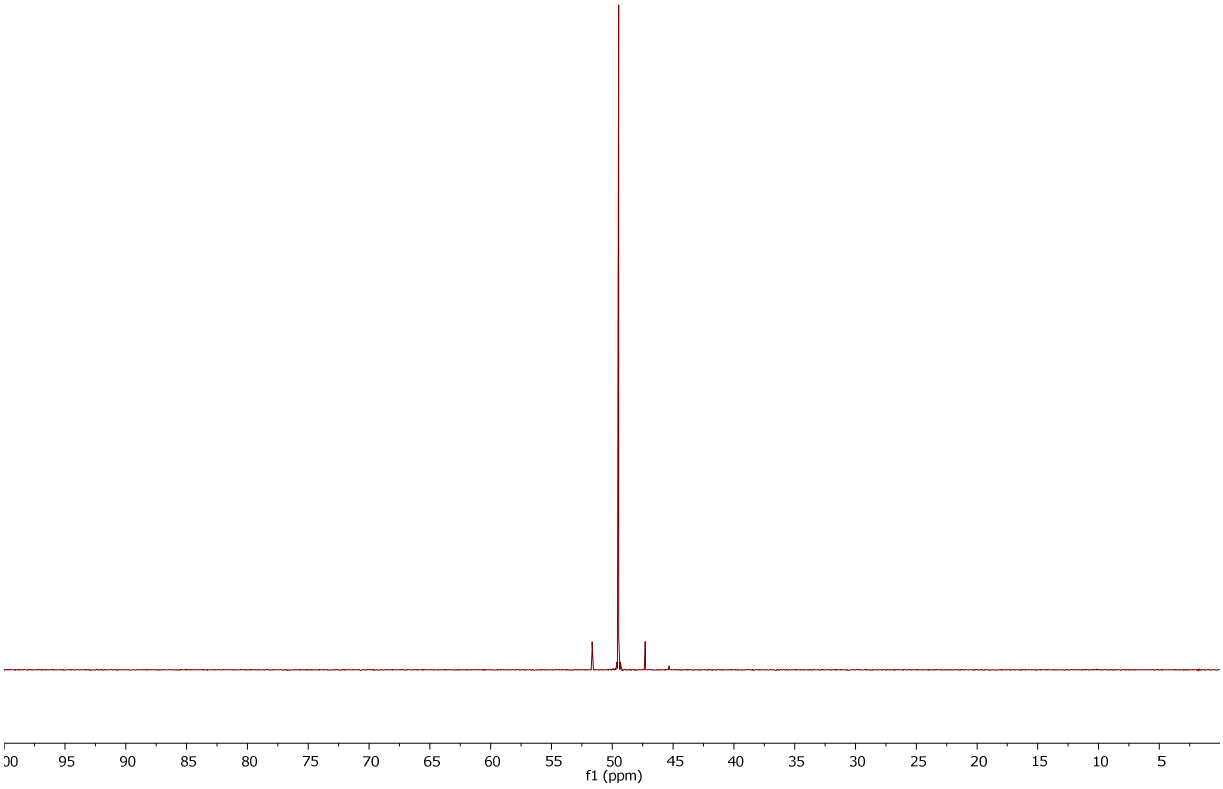

Figure S42. $^{31}P\{^{1}H\}$ NMR spectrum (162 MHz, $CDCl_3$) of **7b**

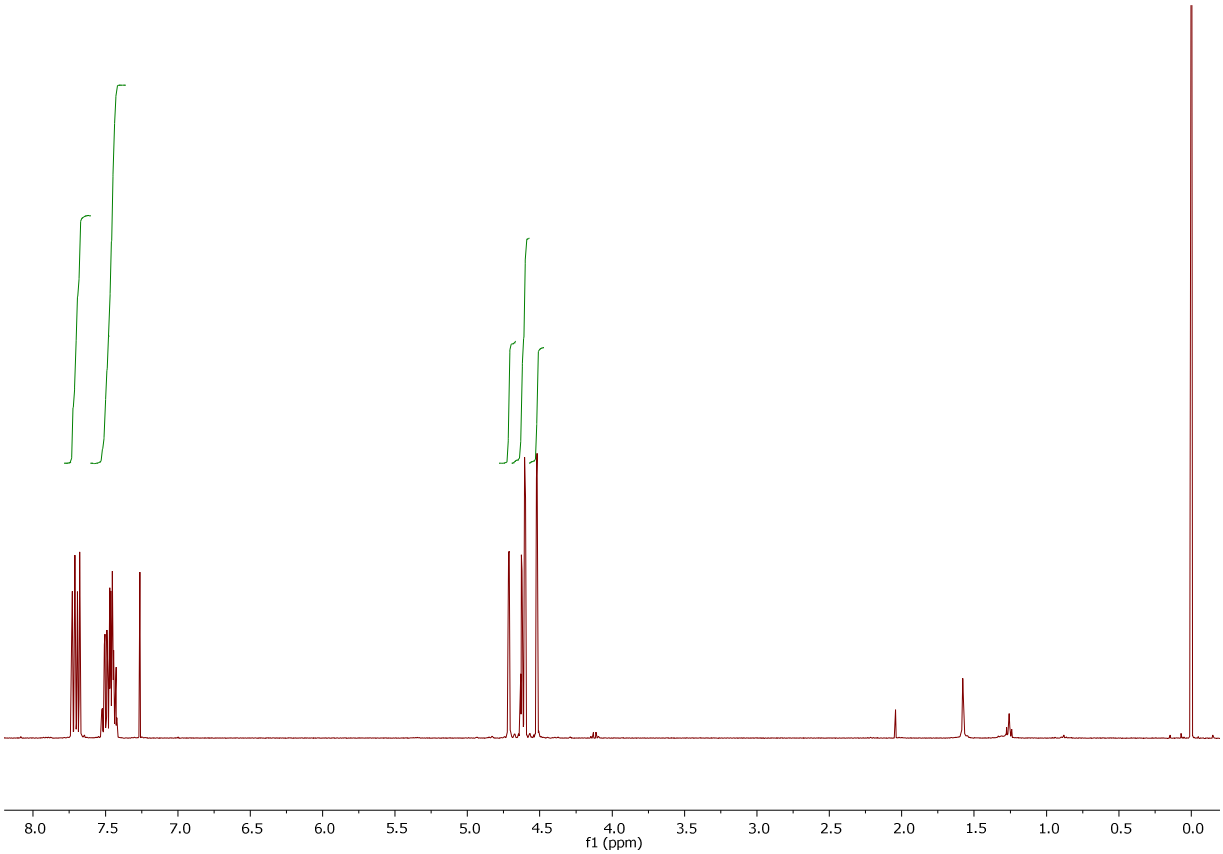

Figure S43. ^{1}H NMR spectrum (400 MHz, $CDCl_3$) of **7c**

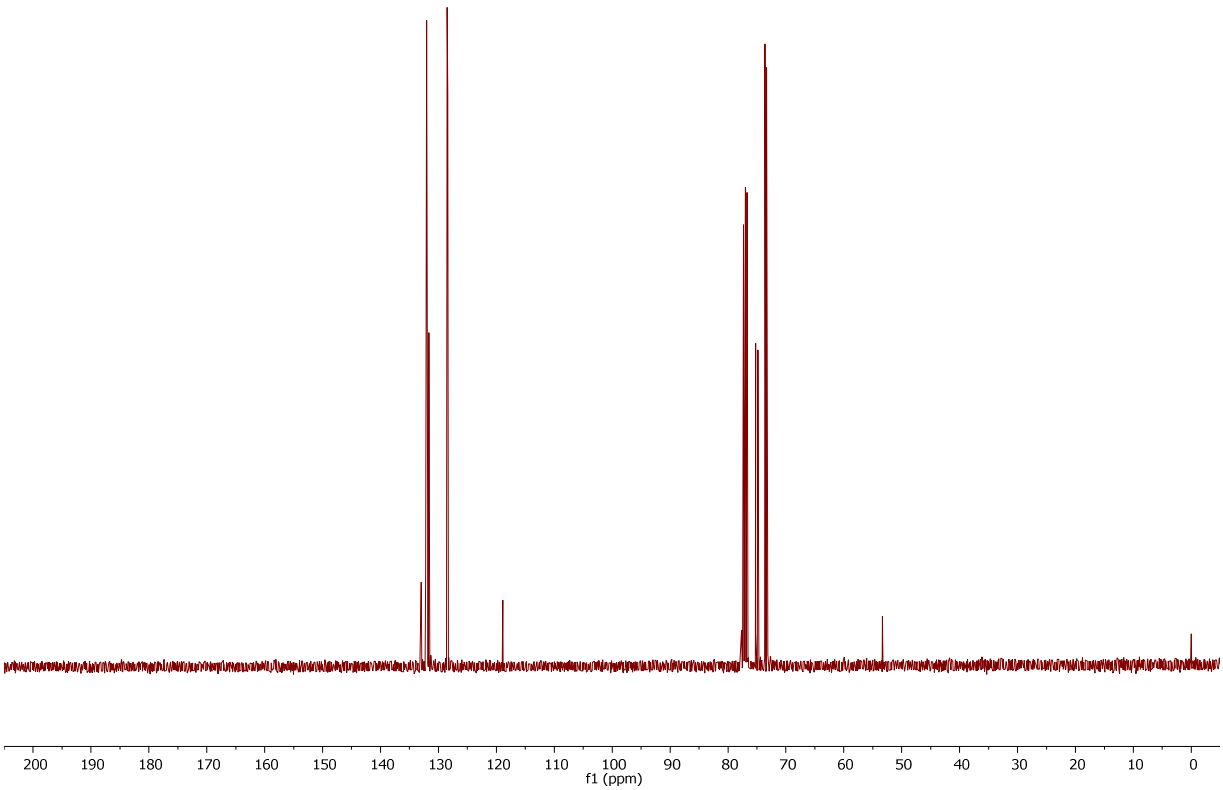

Figure S44. $^{13}C\{^{1}H\}$ NMR spectrum (101 MHz, $CDCl_3$) of **7c**

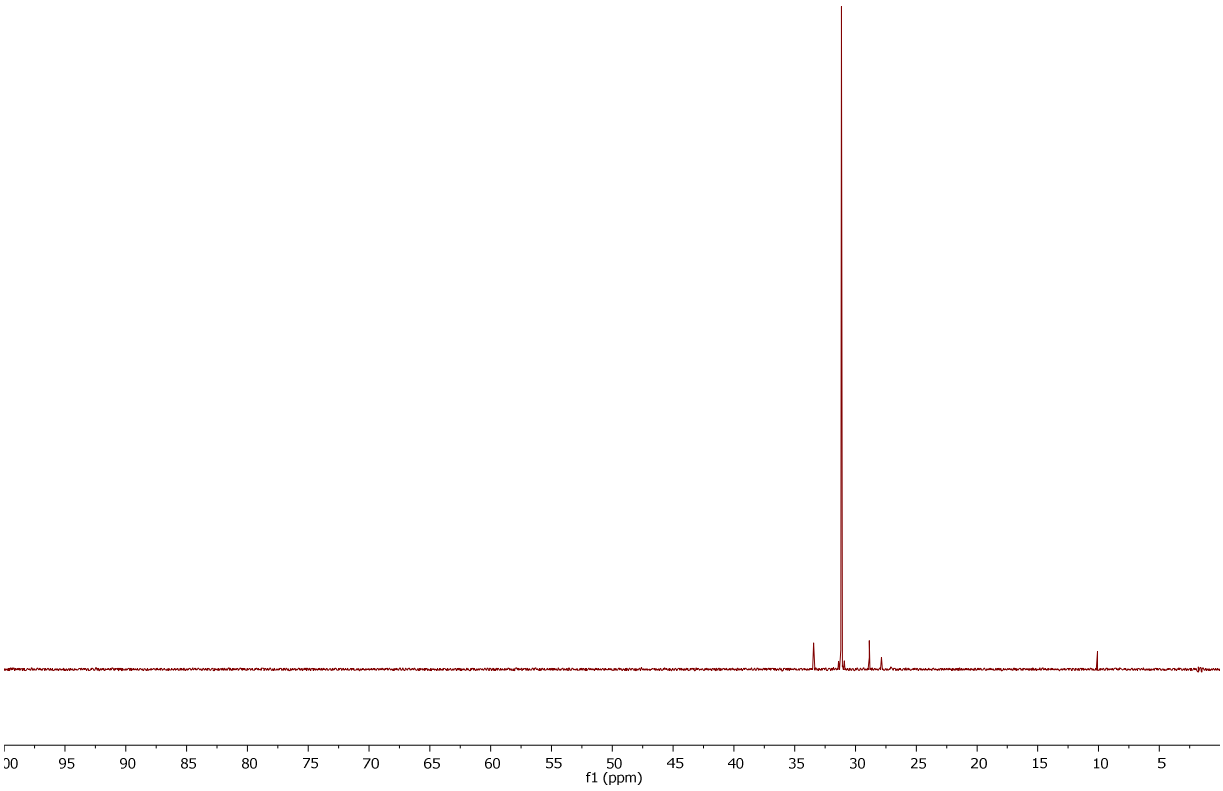

Figure S45. $^{31}P\{^{1}H\}$ NMR spectrum (162 MHz, $CDCl_3$) of **7c**

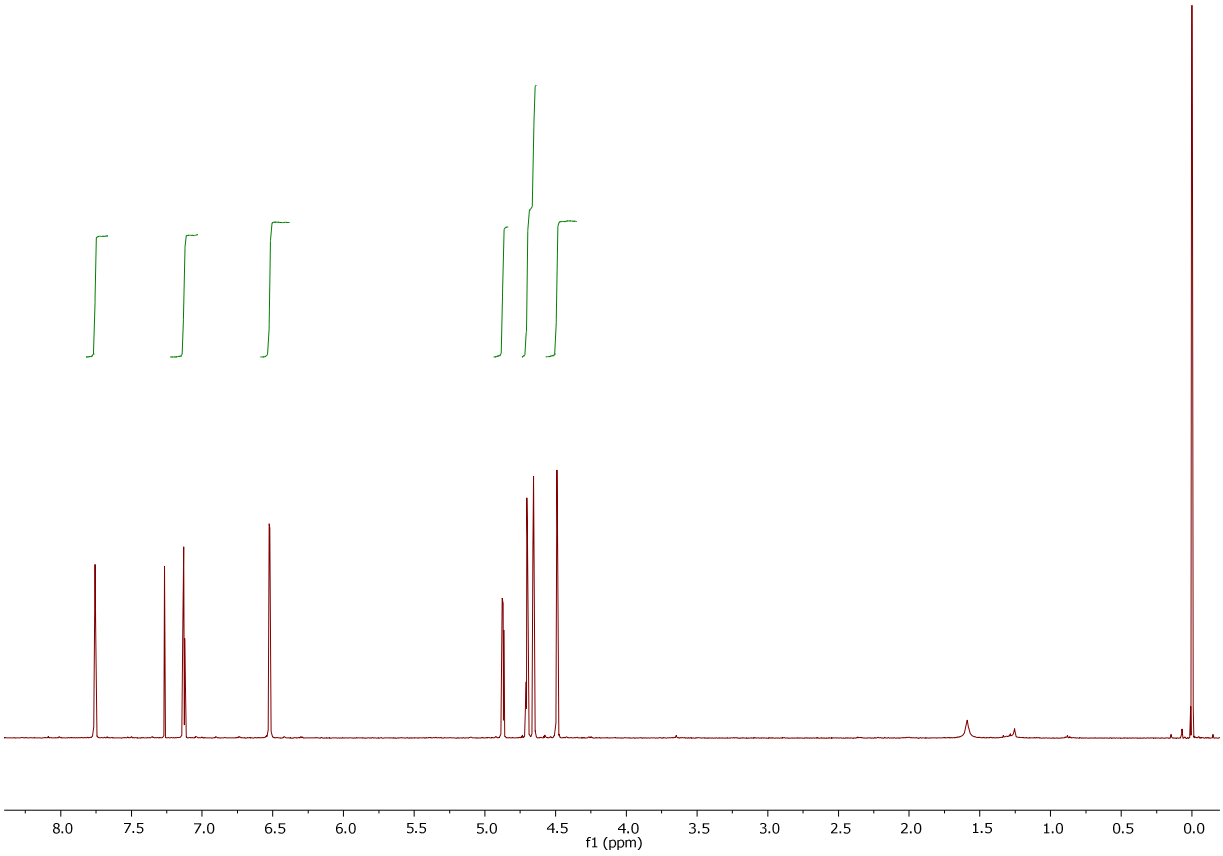

Figure S46. ^{1}H NMR spectrum (400 MHz, $CDCl_3$) of **7d**

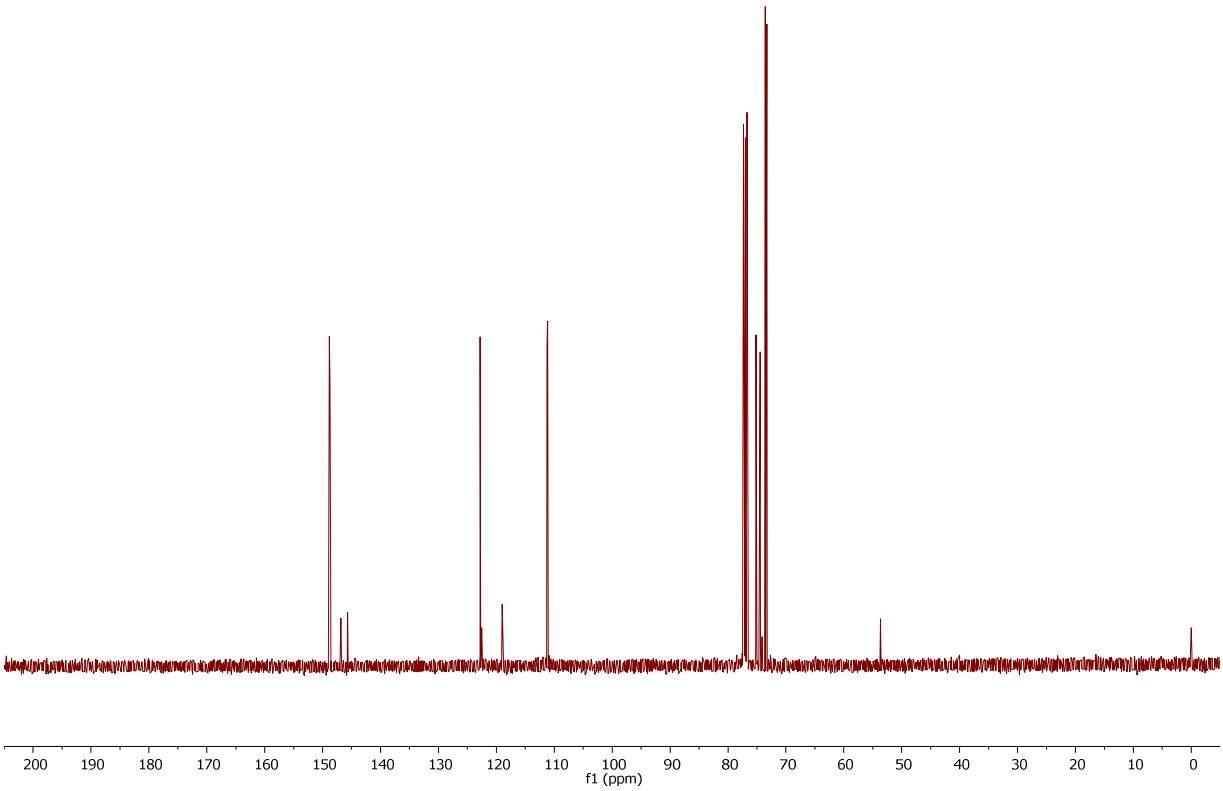

Figure S47. $^{13}C\{^{1}H\}$ NMR spectrum (101 MHz, $CDCl_3$) of **7d**

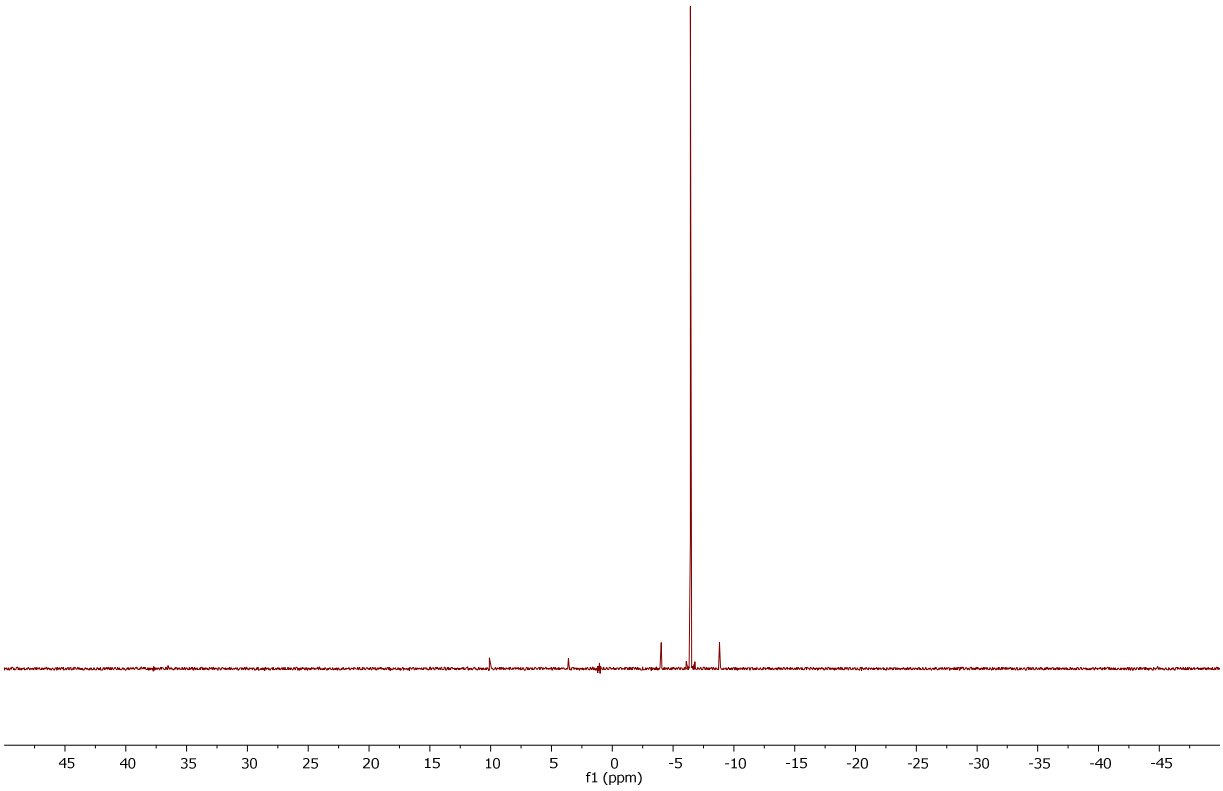

Figure S48. $^{31}P\{^{1}H\}$ NMR spectrum (162 MHz, $CDCl_3$) of **7d**

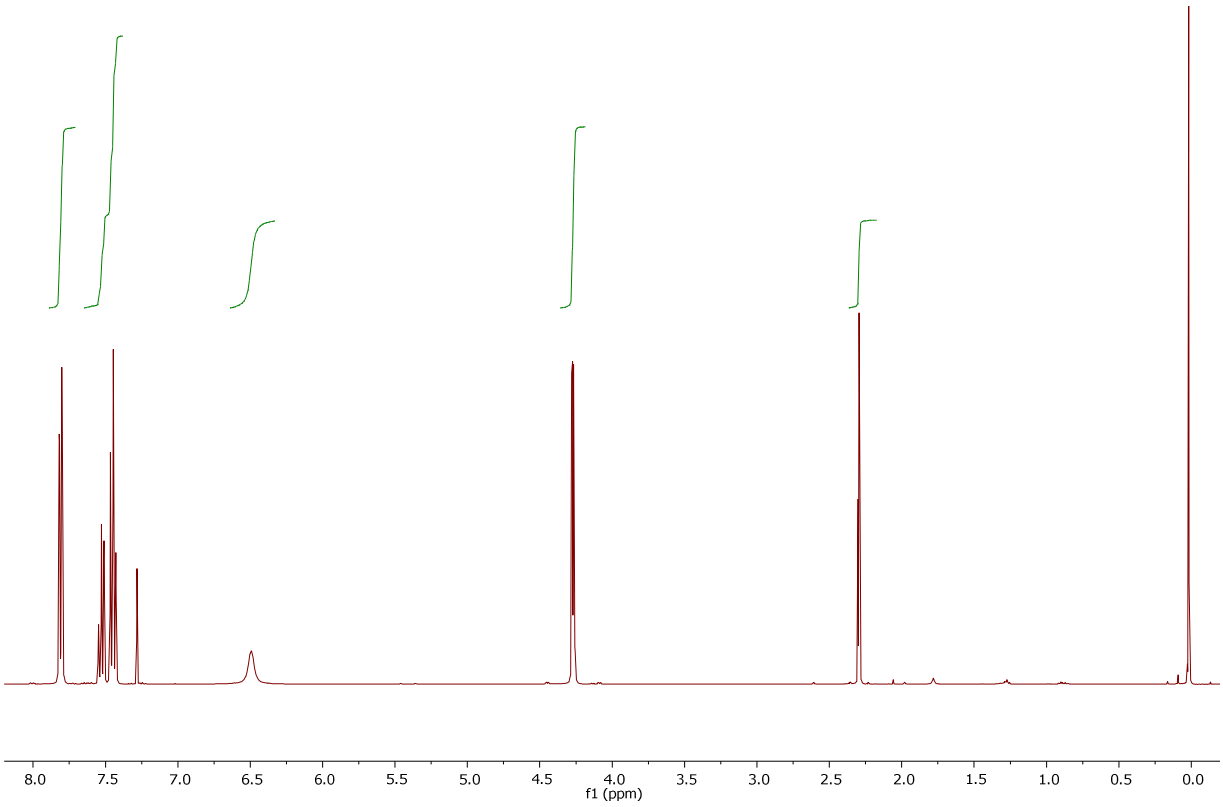

Figure S49. ^{1}H NMR spectrum (400 MHz, $CDCl_3$) of **8a**

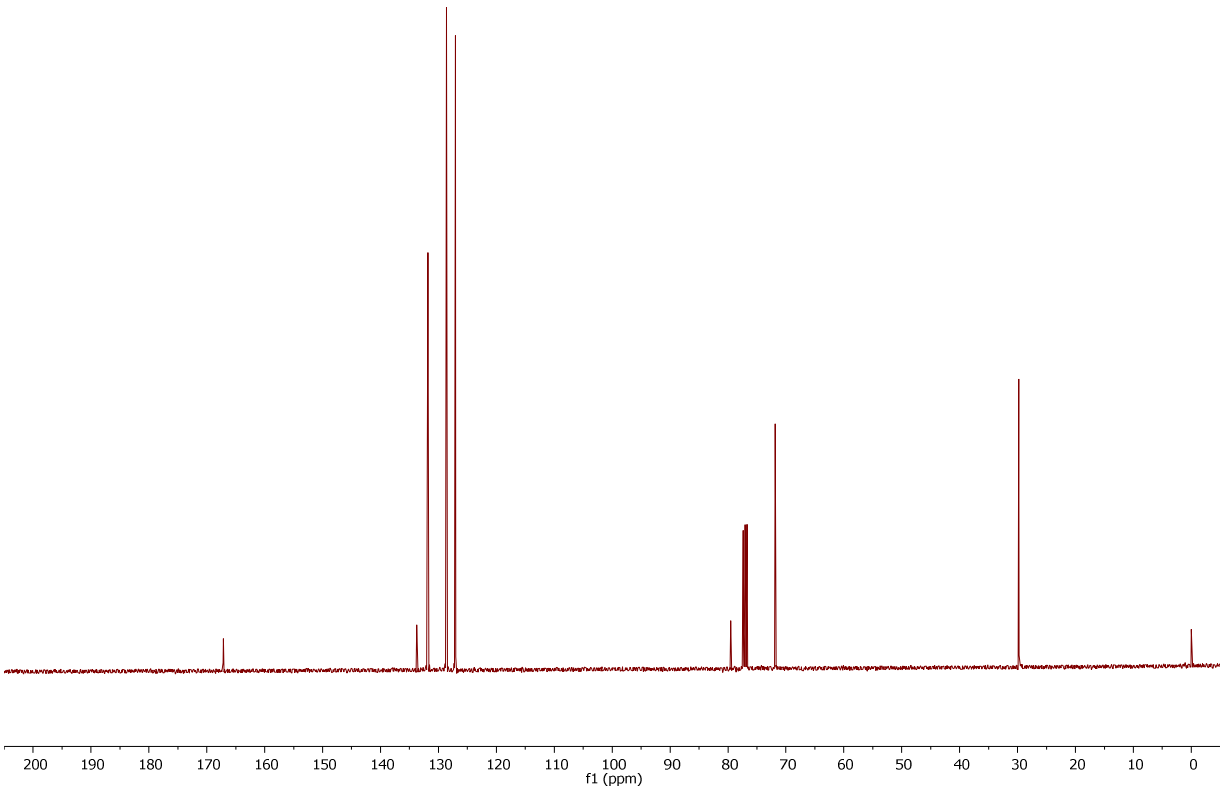

Figure S50. $^{13}C\{^{1}H\}$ NMR spectrum (101 MHz, $CDCl_3$) of **8a**

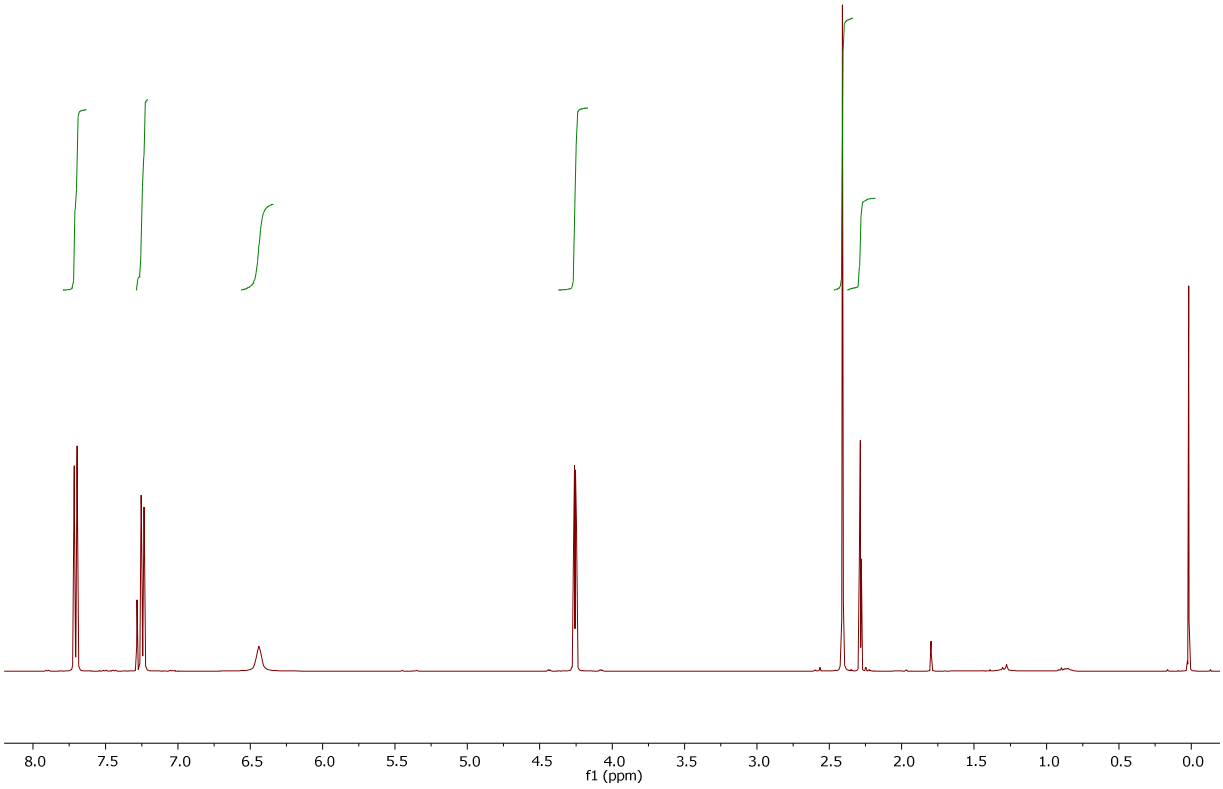

Figure S51. ^{1}H NMR spectrum (400 MHz, $CDCl_3$) of **8b**

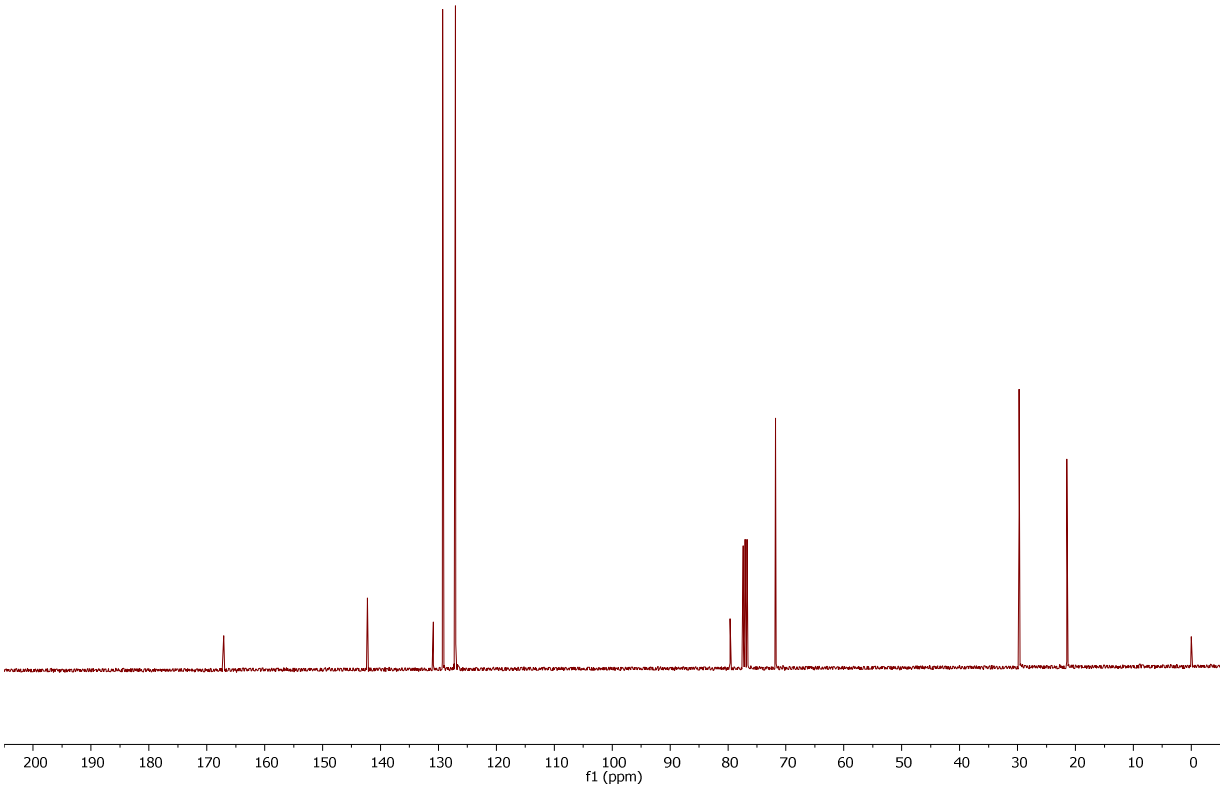

Figure S52. $^{13}C\{^{1}H\}$ NMR spectrum (101 MHz, $CDCl_3$) of **8b**

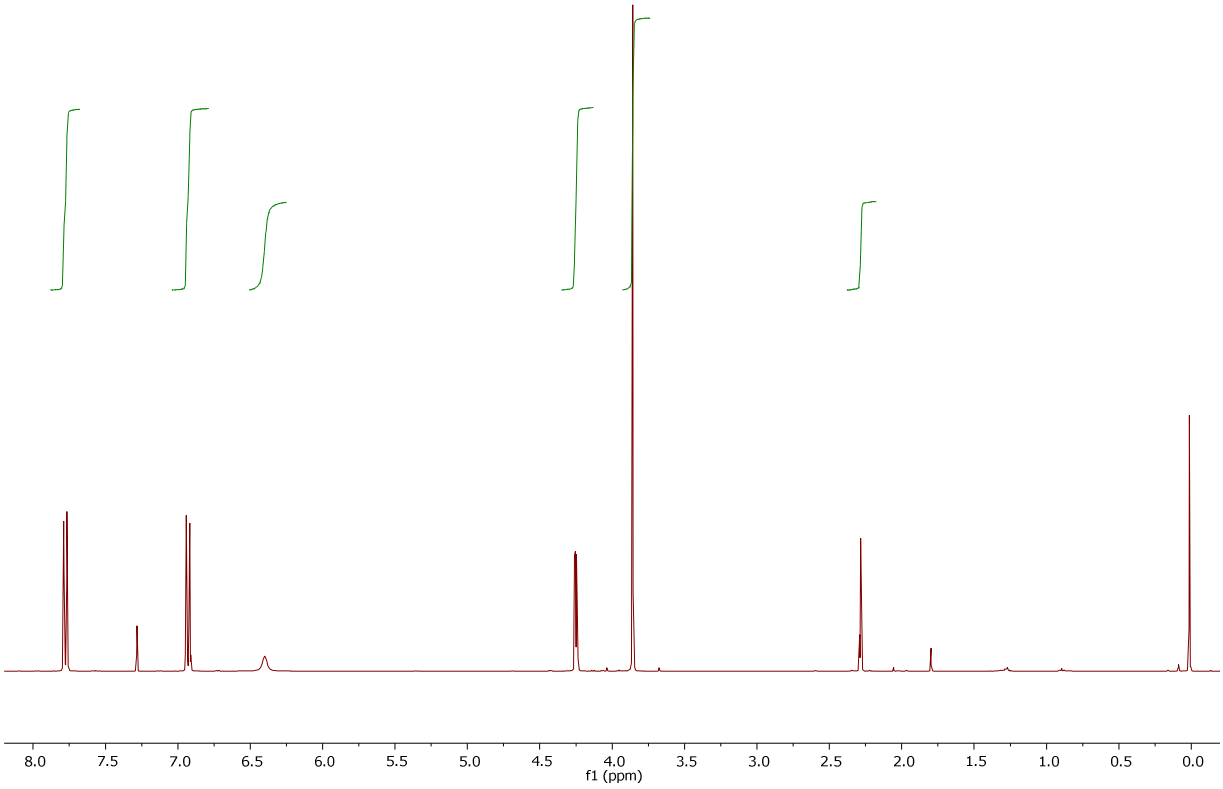

Figure S53. ^{1}H NMR spectrum (400 MHz, $CDCl_3$) of **8c**

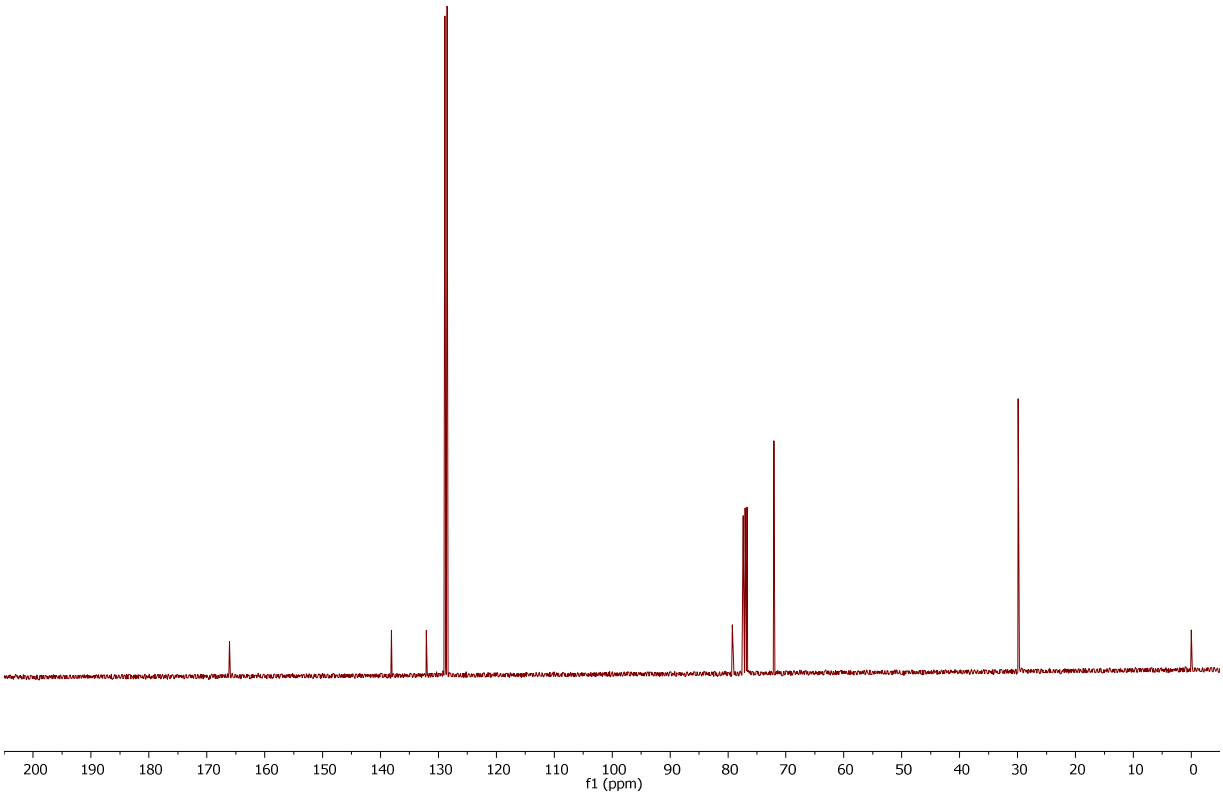

Figure S54. $^{13}C\{^{1}H\}$ NMR spectrum (101 MHz, $CDCl_3$) of **8c**

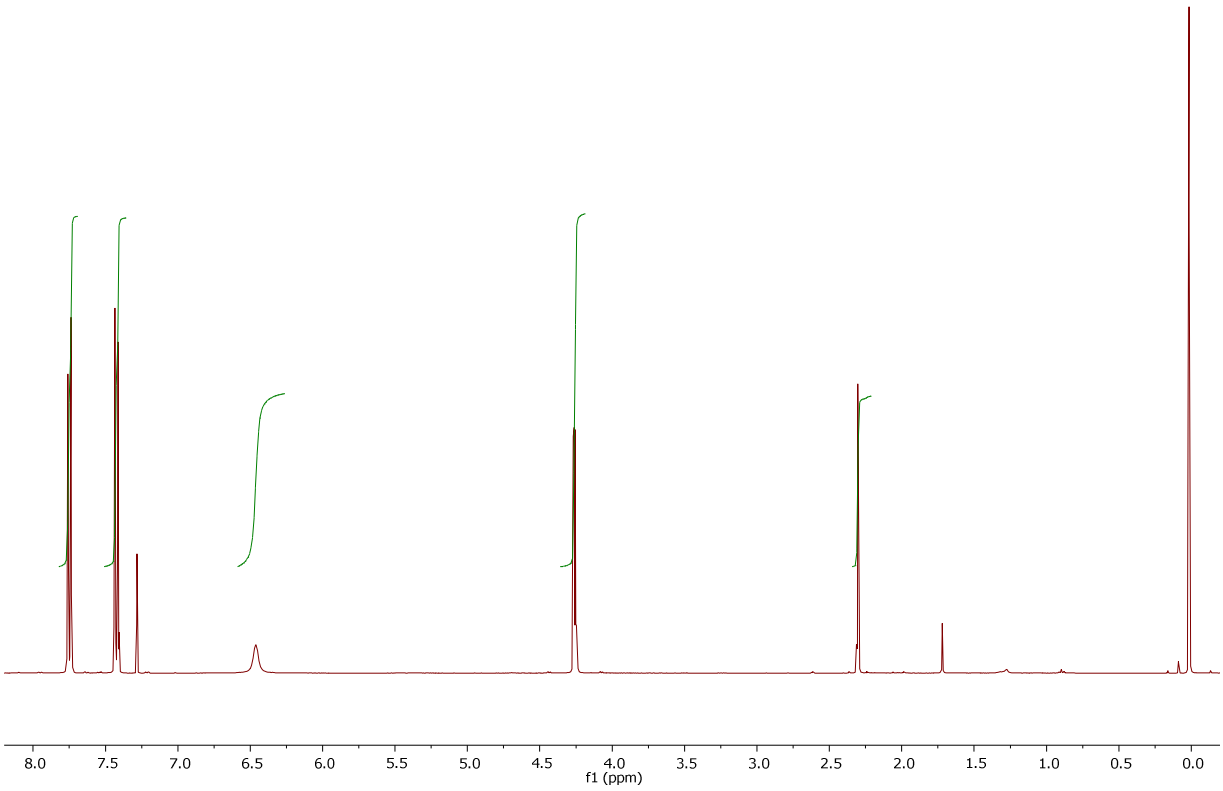

Figure S55. ^{1}H NMR spectrum (400 MHz, $CDCl_3$) of **8d**

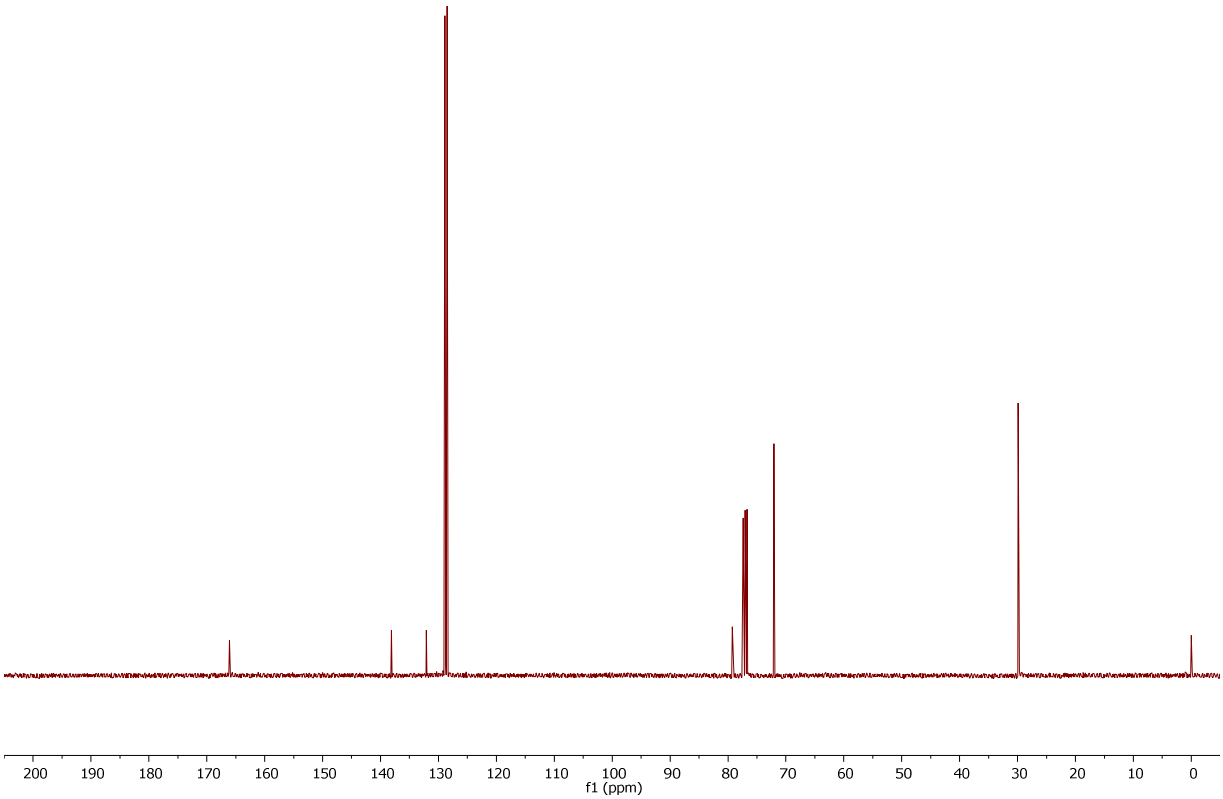

Figure S56. $^{13}C\{^{1}H\}$ NMR spectrum (101 MHz, $CDCl_3$) of **8d**

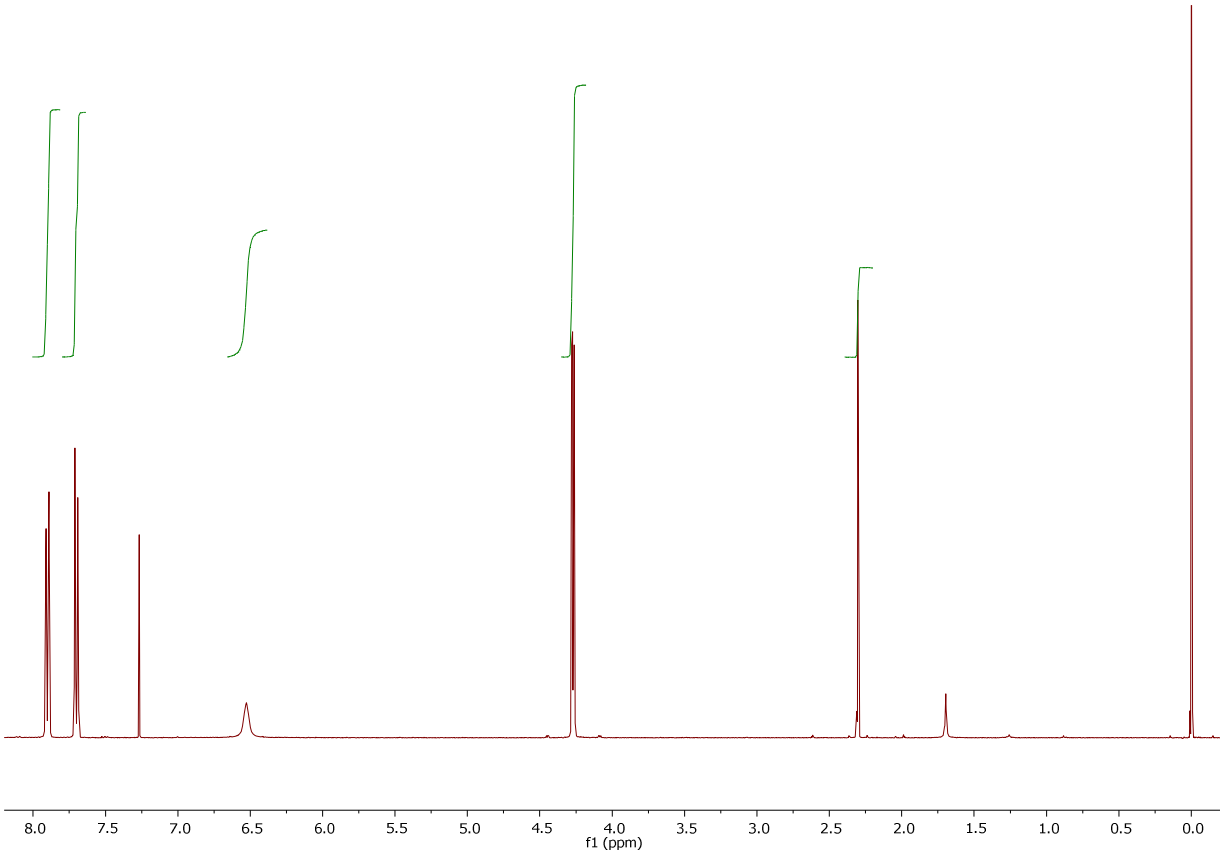

Figure S57. ^{1}H NMR spectrum (400 MHz, $CDCl_3$) of **8e**

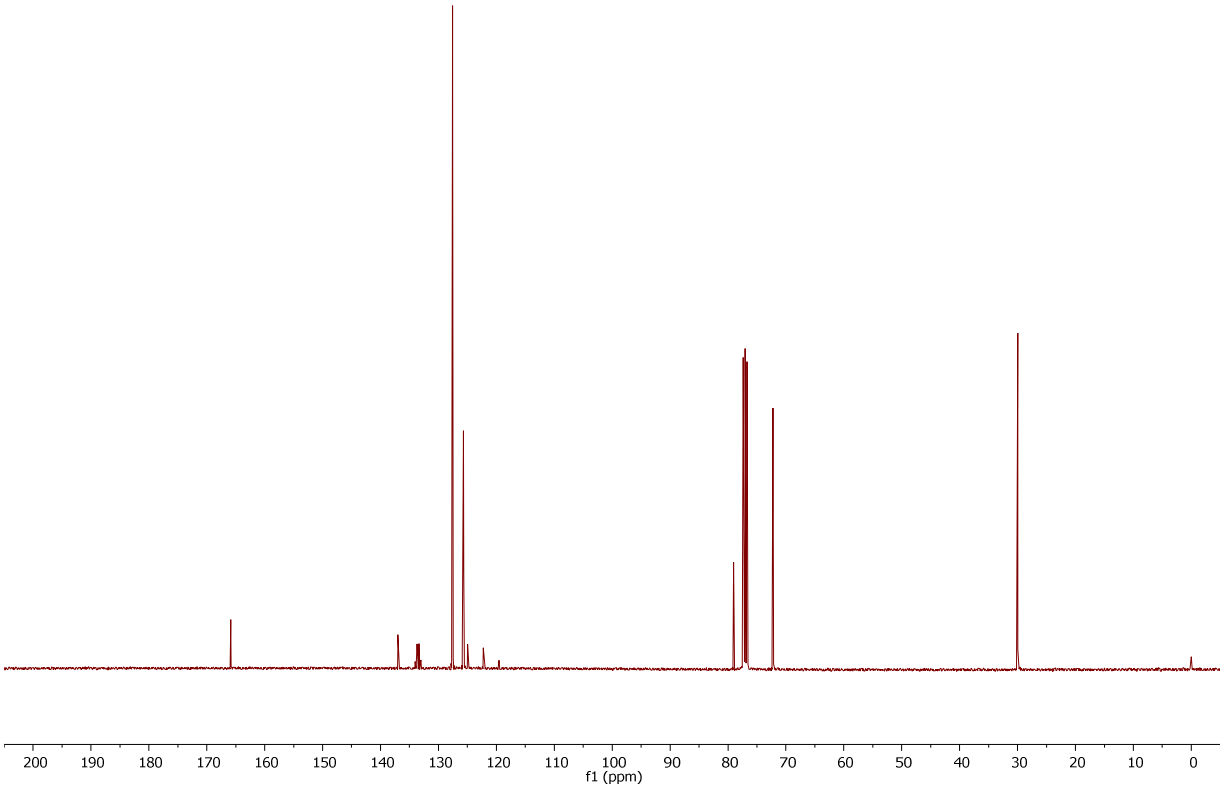

Figure S58. $^{13}C\{^{1}H\}$ NMR spectrum (101 MHz, $CDCl_3$) of **8e**

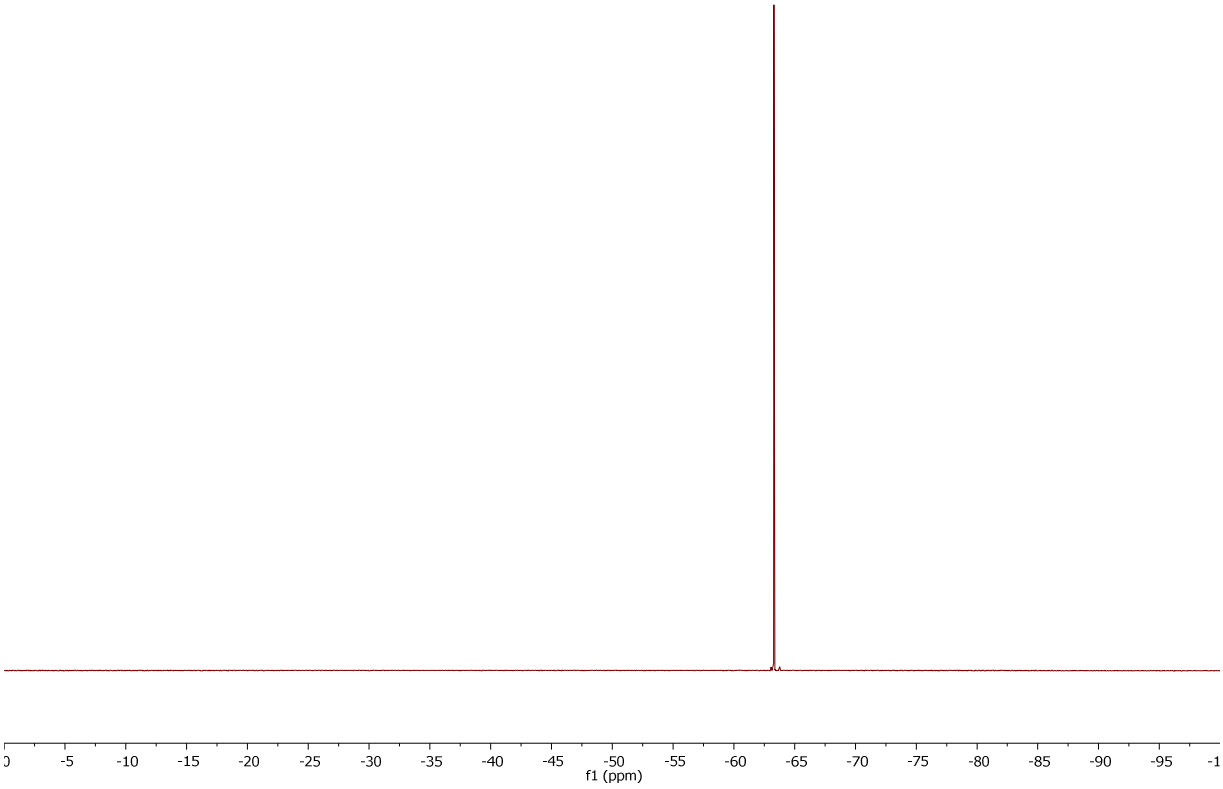

Figure S59. ^{19}F NMR spectrum (376 MHz, $CDCl_3$) of **8e**

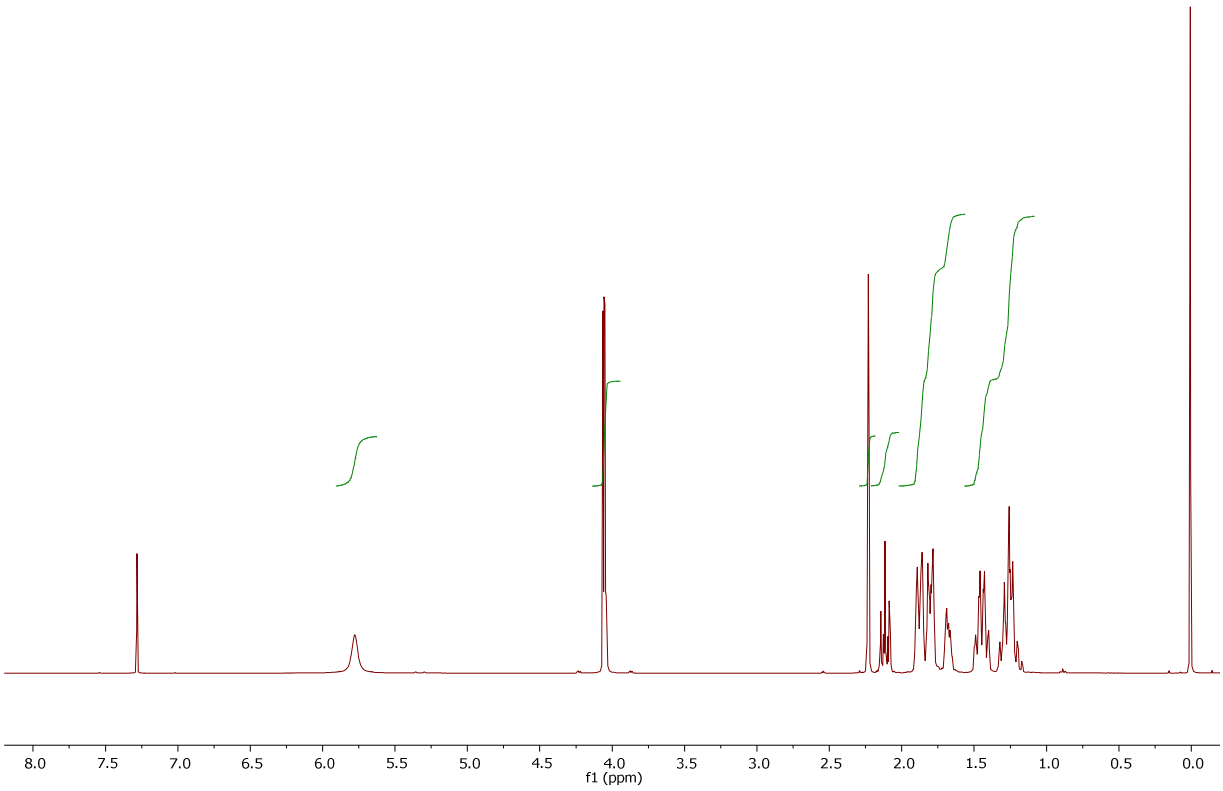

Figure 60. ^{1}H NMR spectrum (400 MHz, $CDCl_3$) of **8f**

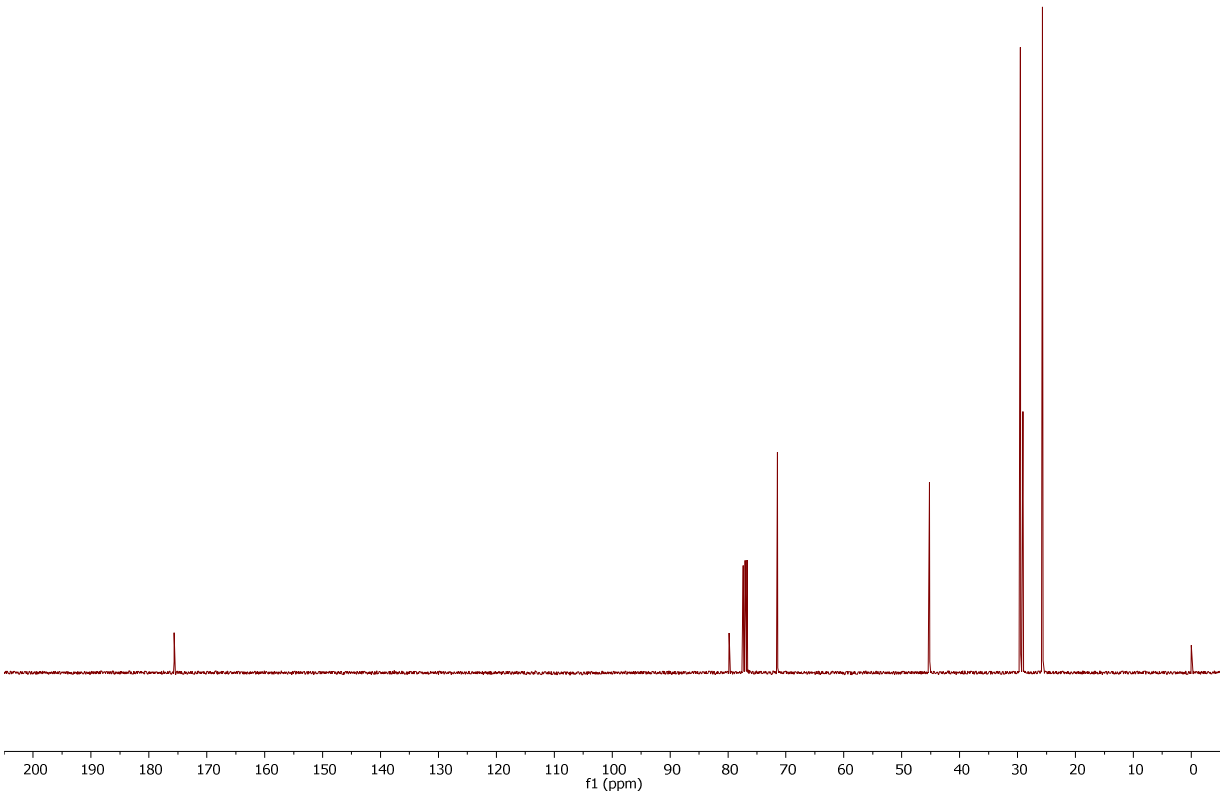

Figure S61. $^{13}C\{^{1}H\}$ NMR spectrum (101 MHz, $CDCl_3$) of **8f**

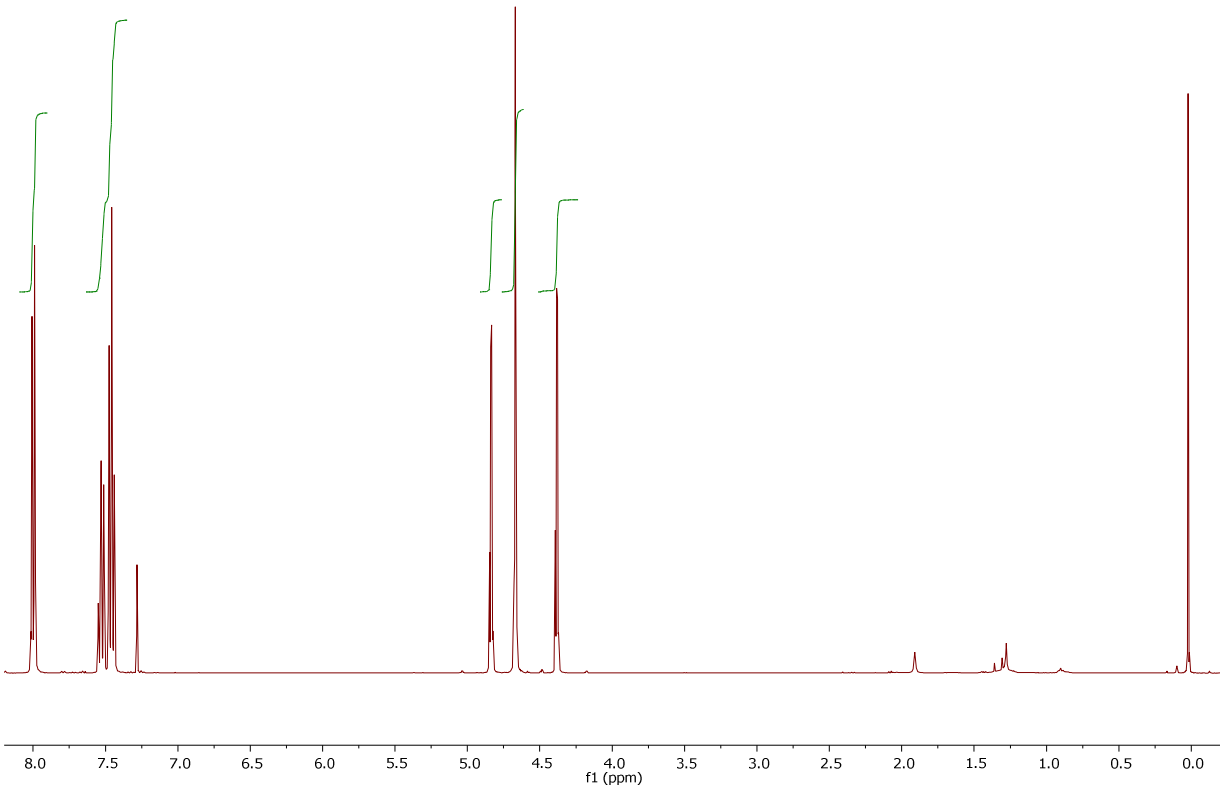

Figure S62. ^{1}H NMR spectrum (400 MHz, $CDCl_3$) of **9a**

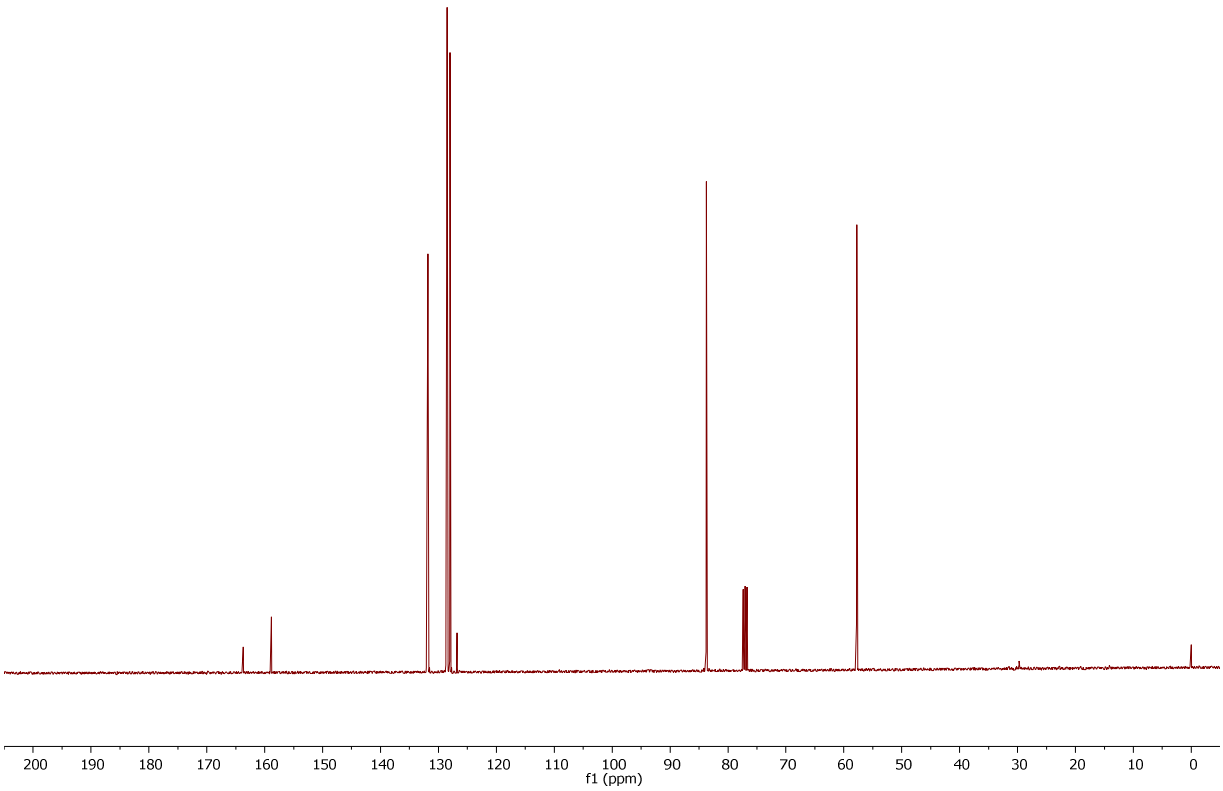

Figure S63. $^{13}C\{^{1}H\}$ NMR spectrum (101 MHz, $CDCl_3$) of **9a**

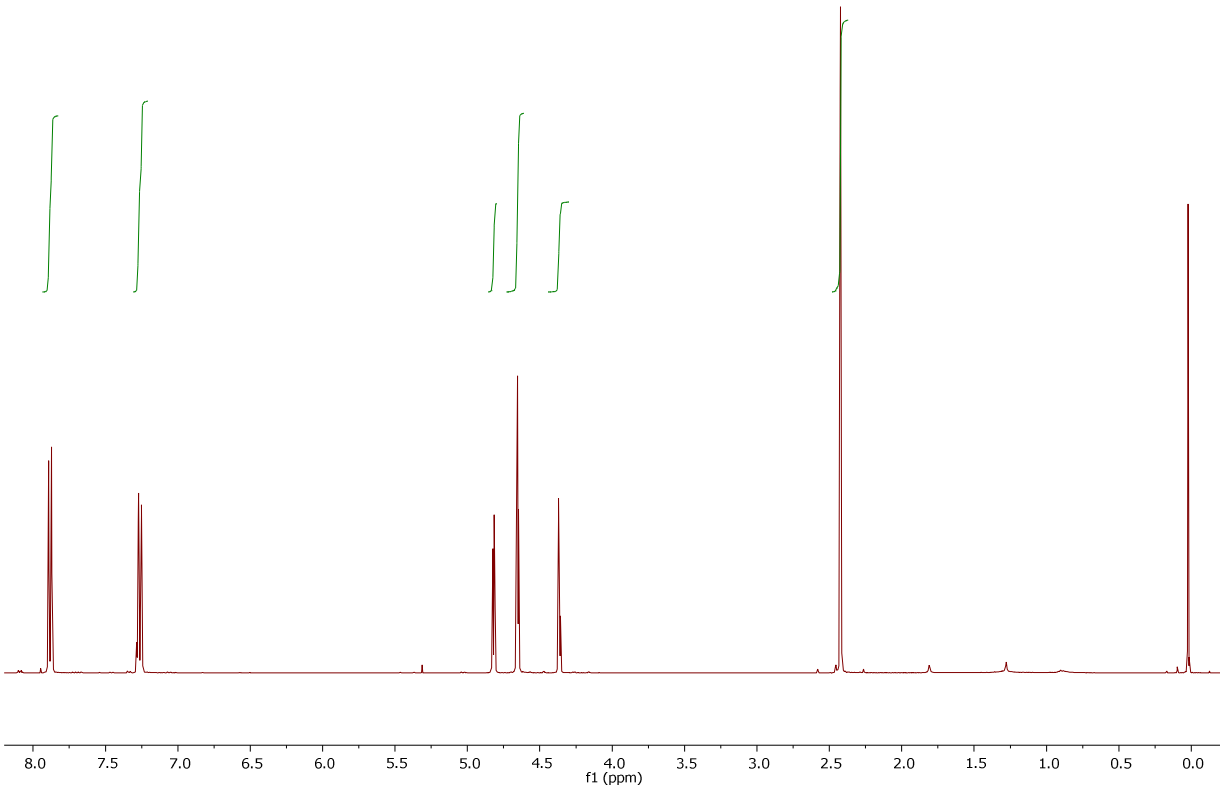

Figure S64. ^{1}H NMR spectrum (400 MHz, $CDCl_3$) of **9b**

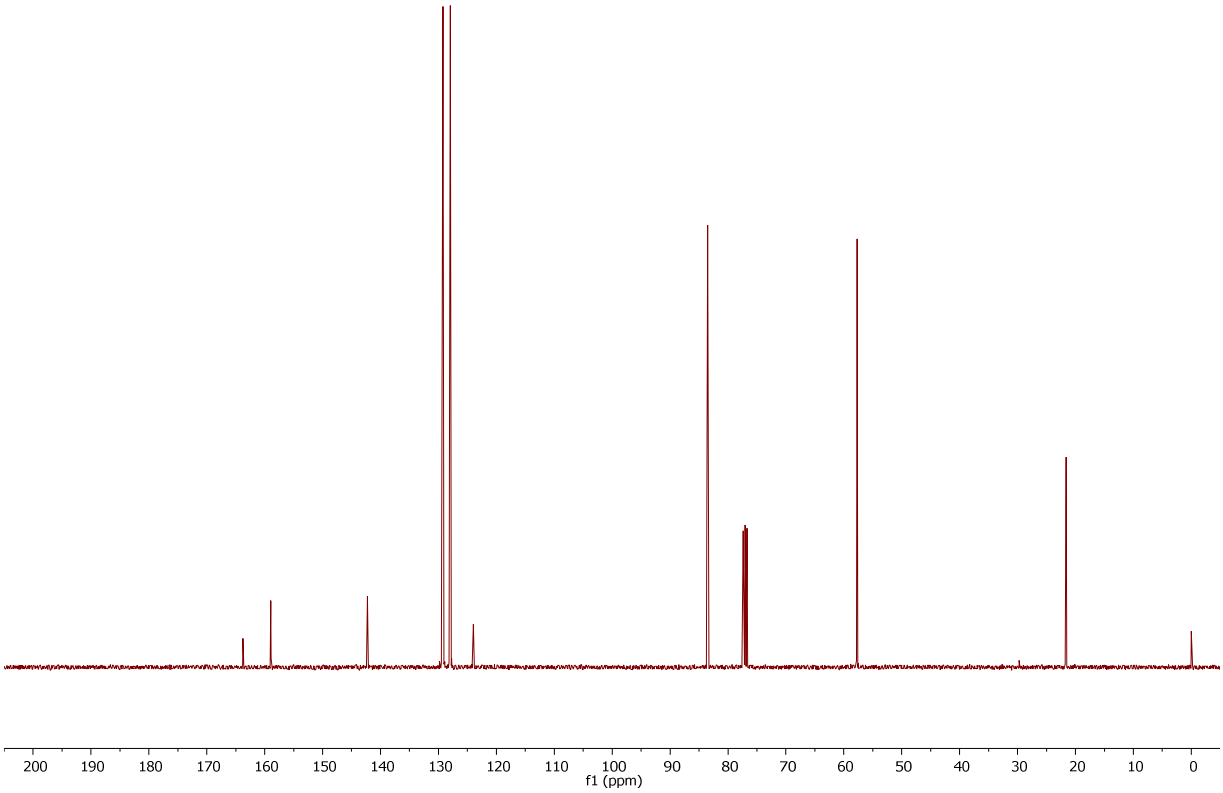

Figure 65. $^{13}C\{^{1}H\}$ NMR spectrum (101 MHz, $CDCl_3$) of **9b**

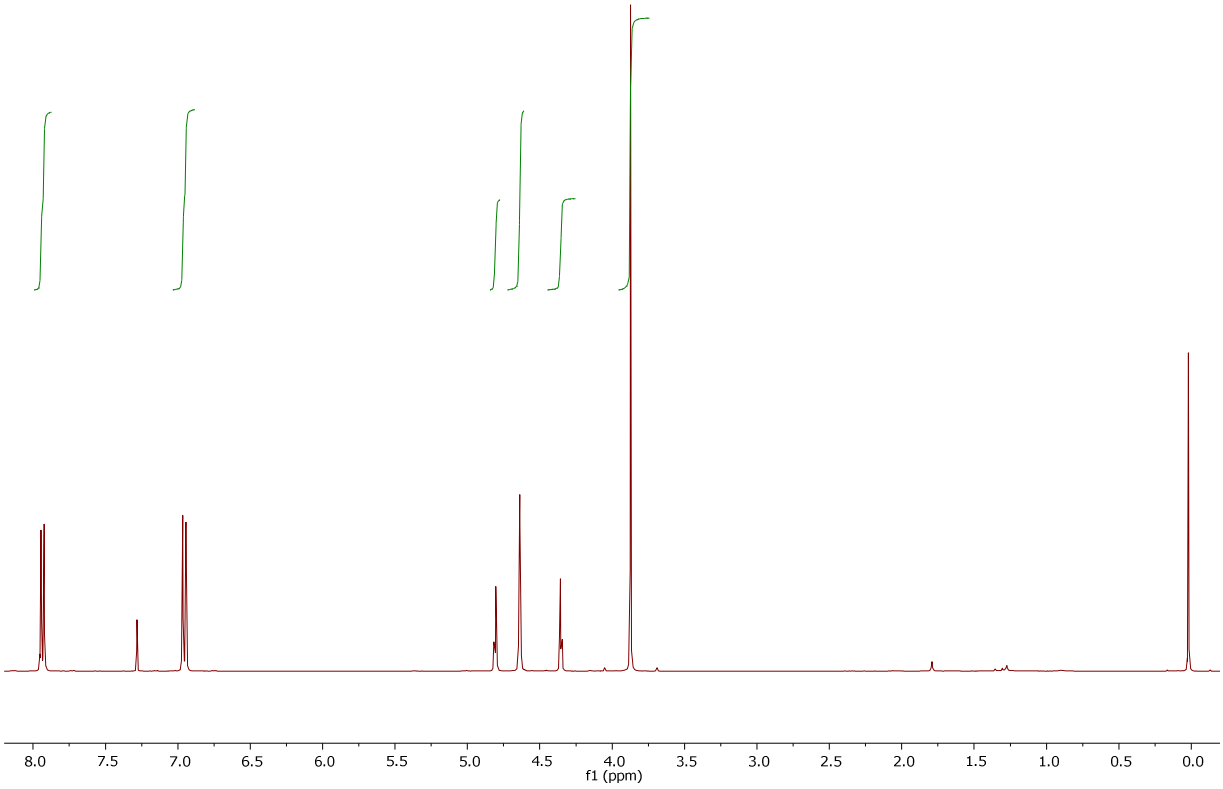

Figure S66. ^{1}H NMR spectrum (400 MHz, $CDCl_3$) of **9c**

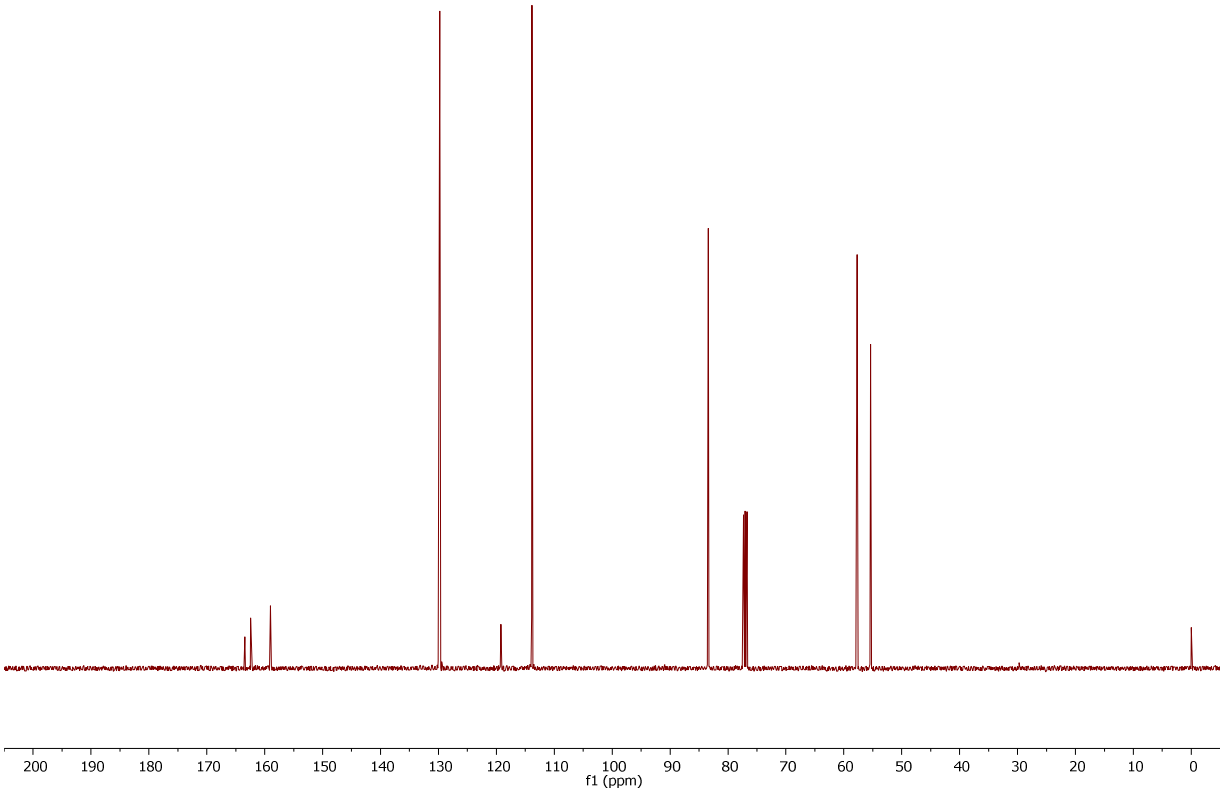

Figure S67. $^{13}C\{^{1}H\}$ NMR spectrum (101 MHz, $CDCl_3$) of **9c**

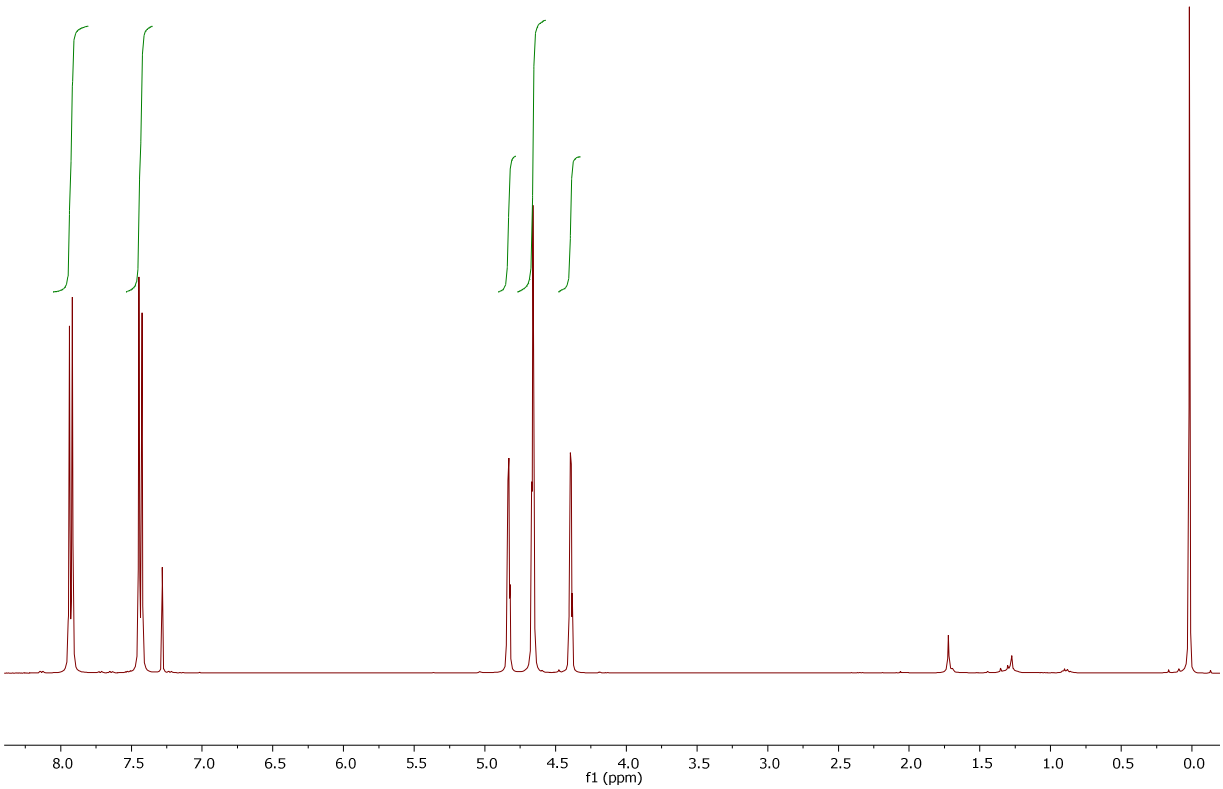

Figure S68. ^{1}H NMR spectrum (400 MHz, $CDCl_3$) of **9d**

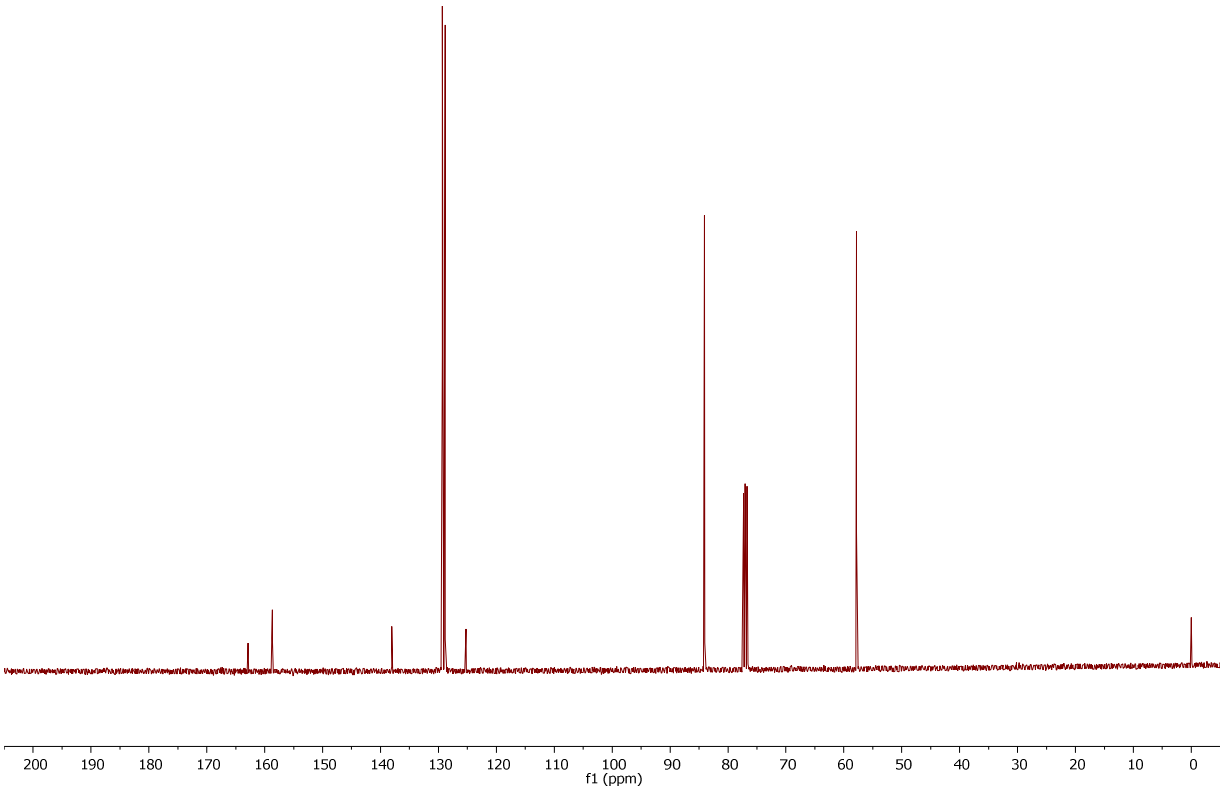

Figure S69. $^{13}C\{^{1}H\}$ NMR spectrum (101 MHz, $CDCl_3$) of **9d**

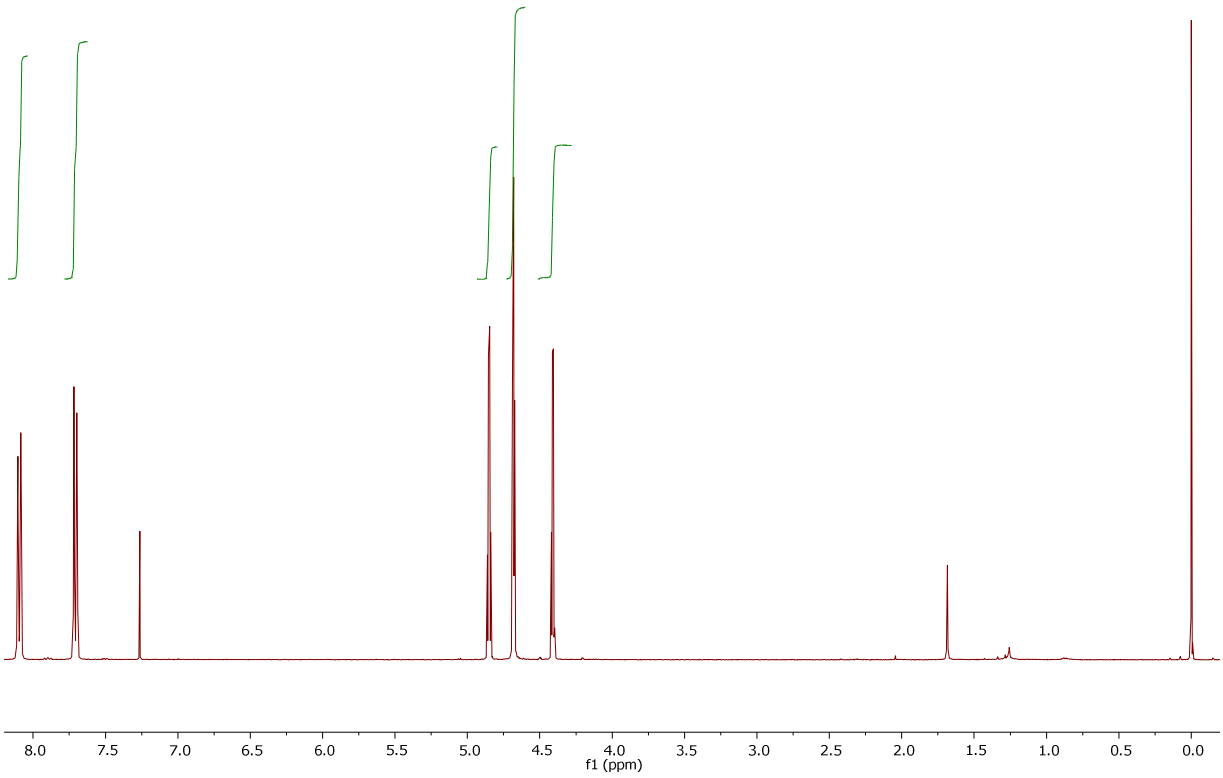

Figure S70. ^{1}H NMR spectrum (400 MHz, $CDCl_3$) of **9e**

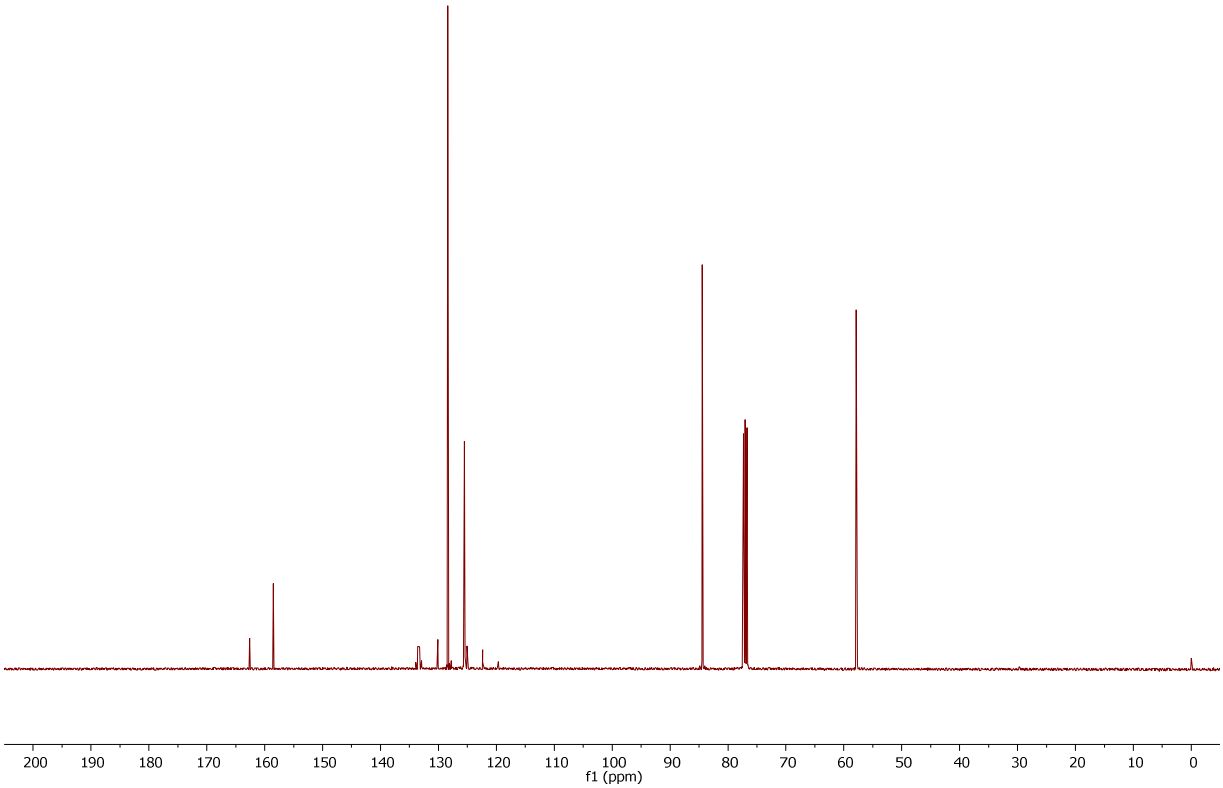

Figure S71. $^{13}C\{^{1}H\}$ NMR spectrum (101 MHz, $CDCl_3$) of **9e**

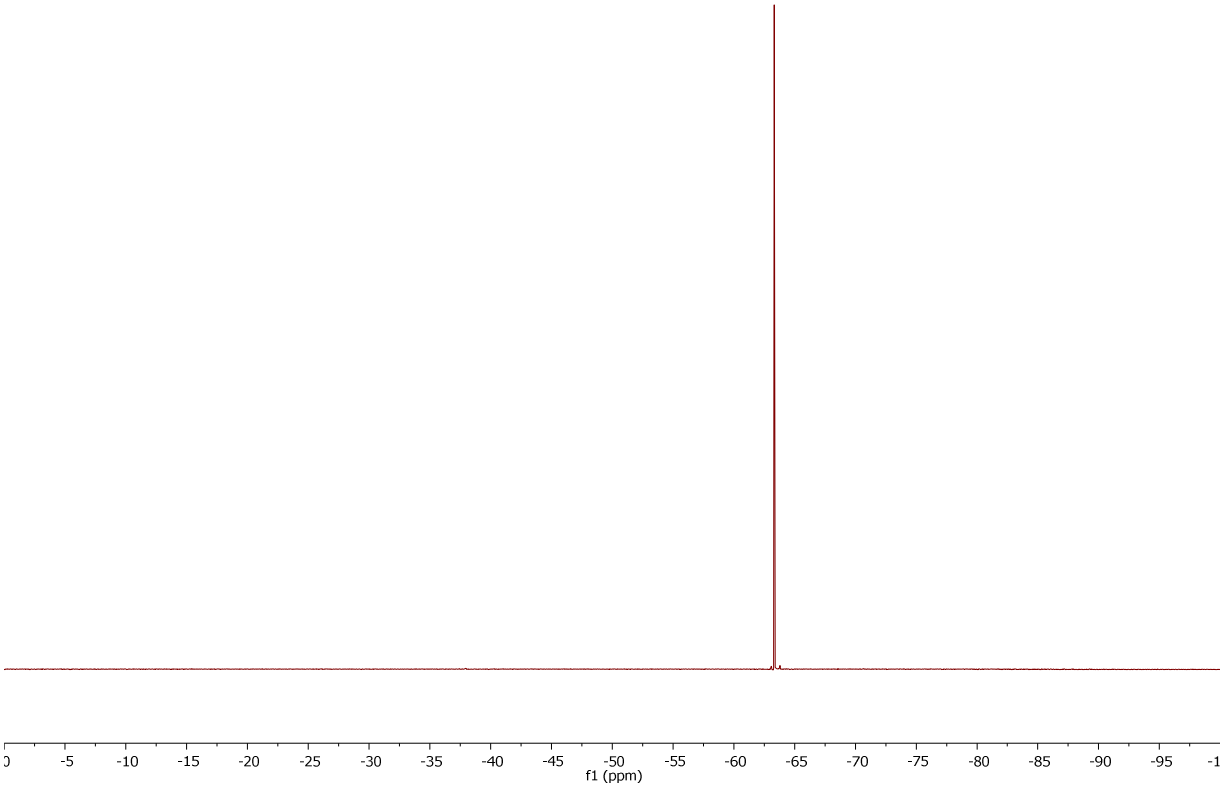

Figure S72. ^{19}F NMR spectrum (376 MHz, $CDCl_3$) of **9e**

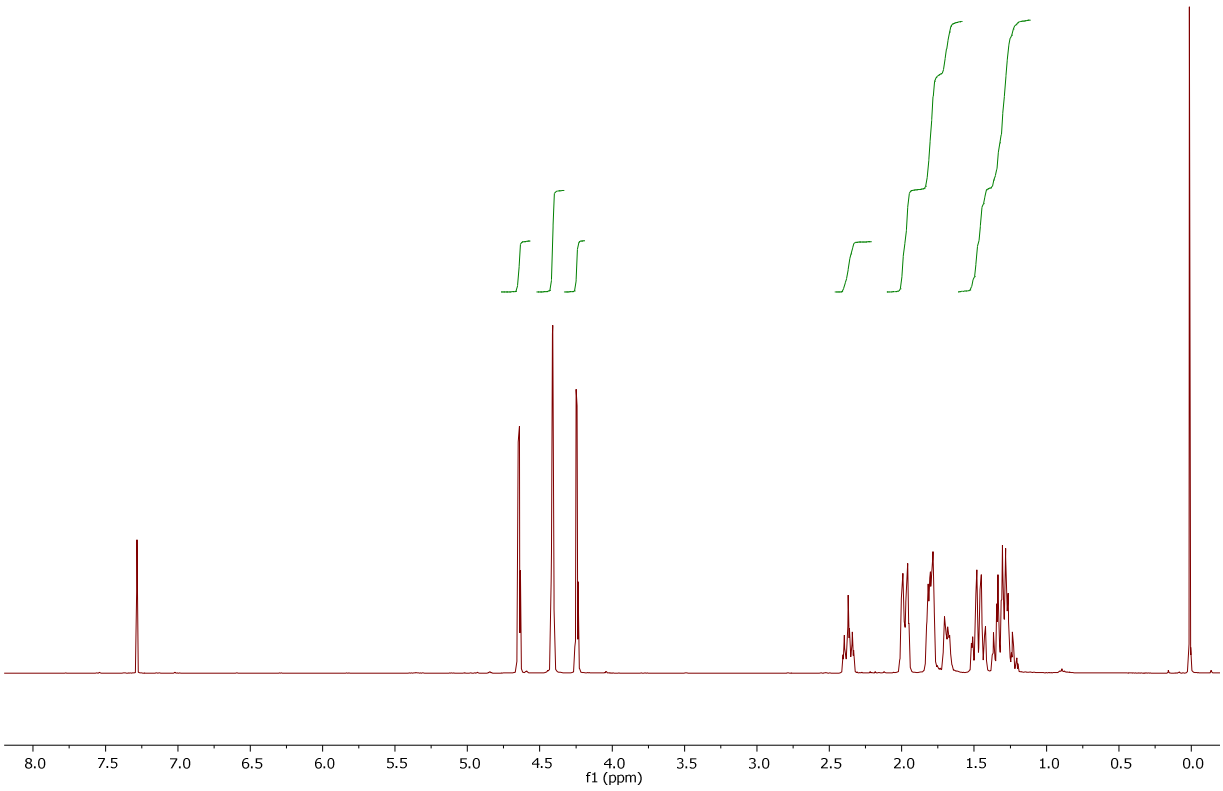

Figure S73. ^{1}H NMR spectrum (400 MHz, $CDCl_3$) of **9f**

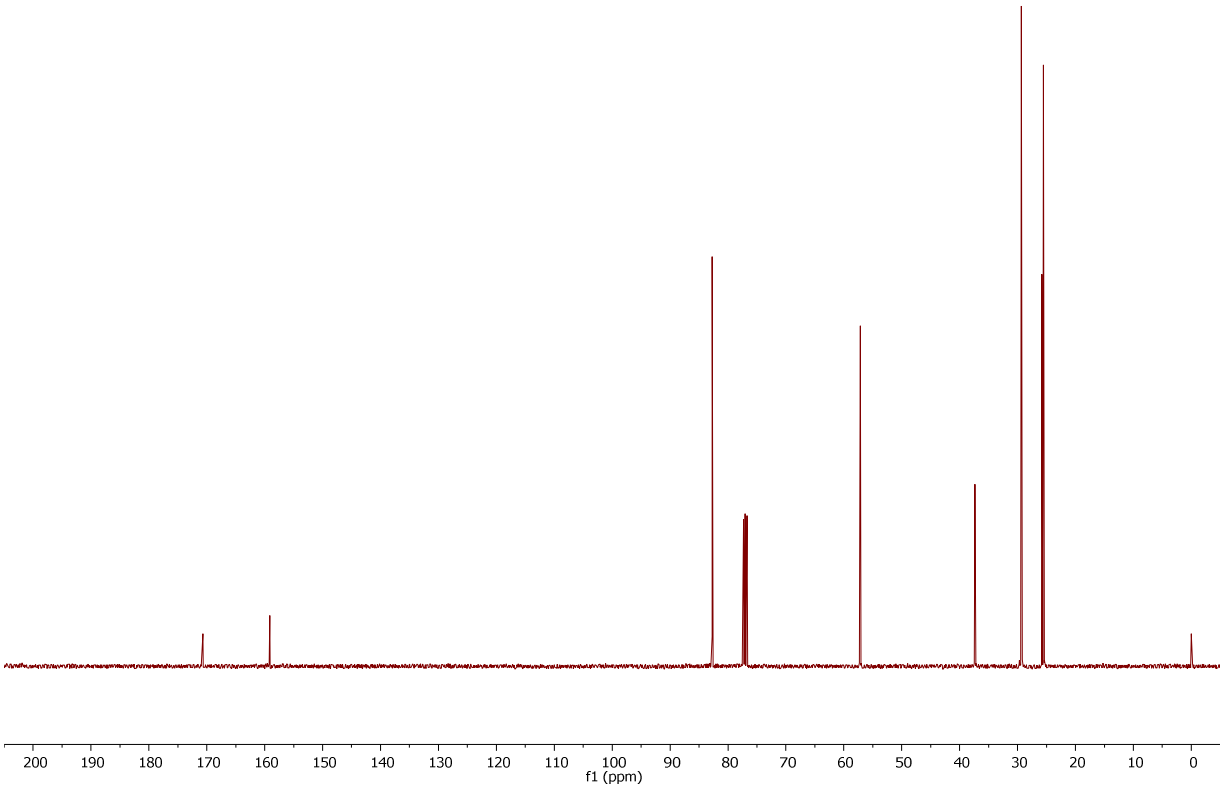

Figure S74. $^{13}C\{^{1}H\}$ NMR spectrum (101 MHz, $CDCl_3$) of **9f**